약학박사학위논문

지방간 발생에서 3-Phosphoglycerate Dehydrogenase 발현 억제에 의한 L-Serine 대사 이상의 역할

Role of Abnormal L-Serine Metabolism by Lowered Expression of 3-Phosphoglycerate Dehydrogenase in Fatty Liver Disease

2018년 2월

서울대학교 대학원
약학과 예방약학전공
심우철

Abstract

Role of Abnormal L-Serine Metabolism by Lowered Expression of 3-Phosphoglycerate Dehydrogenase in Fatty Liver Disease

Woo-Cheol Sim
Preventive Pharmacy, College of Pharmacy
Seoul National University

Fatty liver disease is early-stage liver disease that fat makes up more than 5% of the organ's weight. Fatty liver is a reversible state and benign, but without proper treatments, it can lead to liver dysfunction. In this study, we propose that 3-phosphoglycerate dehydrogenase (PHGDH), which is a rate-limiting enzyme in serine biosynthesis, can affect lipid metabolism by regulating L-serine pool in fatty liver disease.

Previous study showed that hepatic L-serine is decreased in chronically ethanol-fed rats. Based on the result, L-serine was treated in alcoholic fatty liver model and it reversed ethanol-induced fatty liver by metabolizing homocysteine via methionine synthase (MS) and cystathionine β-synthase (CβS). L-serine also increased intracellular NAD^+ and silent information regulator 1 (SIRT1) activity via lactate dehydrogenase (LDH). L-serine increased mitochondrial gene expression, mass and function by deacetylated PGC-1α.. Increased SIRT1 activity by L-serine ameliorated lipid accumulation and insulin resistance *in vitro*.

PHGDH and L-serine were found to be significantly lowered in chronic ethanol diet and high-fat diet fatty liver model. Free fatty acids and ethanol also decreased PHGDH expression *in vitro*.

Diminished synthesis of L-serine led to increase in abnormal sphingolipids and ceramides in PHGDH-KO MEF cells and alcoholic fatty liver model. GEO analysis of hepatitis patients revealed *phgdh* gene expression was diminished. Serum L-serine of fatty liver patients was also down-regulated and negatively correlated with MRI fat fraction, serum ALT and triglyceride (TG). Increased synthesis of L-serine by PHGDH gain of function reversed lipid accumulation in various cells by increasing intracellular NAD^+ and SIRT1 activity.

PHGDH is found to be positively regulated by nuclear factor like 2 (NRF2) at both transcriptional and translational levels. Fatty liver disease model showed the decreased expression of NRF2 and increased NRF2 activity reversed free fatty acid-induced decrease in PHGDH expression.

In conclusion, PHGDH plays an important role in regulating lipid metabolism by synthesizing L-serine in the liver. This study showed that PHGDH can be used as a therapeutic target for hepatosteatosis and L-serine has a potential for curing fatty liver disease.

Key words : L-Serine, Homocysteine, 3-Phosphoglycerate dehydrogenase, SIRT1, Lipid metabolism, Fatty liver

Student Number : 2011-21733

Contents

I. Introduction

1.1. Fatty liver

Fatty liver diseases are classified into two categories. First, alcoholic fatty liver disease (ALD) is developed by heavy alcohol intake (Feinman and lieber, 1999) and secondly, nonalcoholic fatty liver disease (NAFLD) is induced by excessive calorie intake, virus, chemicals and so on (Ahn et al., 2008; Li et al., 2012). Because intracellular lipid itself is not that toxic to hepatocyte, patients have little symptoms and liver functions are mostly normal. But without proper therapy, lipid accumulation is ongoing and reversible fatty liver can develop into irreversible steatohepatitis, liver fibrosis and finally liver failure (Figure 1 and Table 1) (Sorensen et al., 1984; Teli et al., 1995; Jonathan et al., 2011; Falck-Ytter et al., 2001).

The molecular mechanisms that contribute to fatty liver include increased de novo fatty acid synthesis by sterol regulatory element binding protein (SREBP)-1, decreased fatty acid oxidation by peroxisome proliferator-activated receptor-α (PPAR-α), up-regulated fatty acid uptake by CD36 and fatty acid transport protein (FATP) and disabled VLDL lipoprotein secretion by phosphatidylethanolamine methyltransferase (PEMT) (Figure 2) (Purohit V et al., 2009; ,Jonathan et al., 2011).

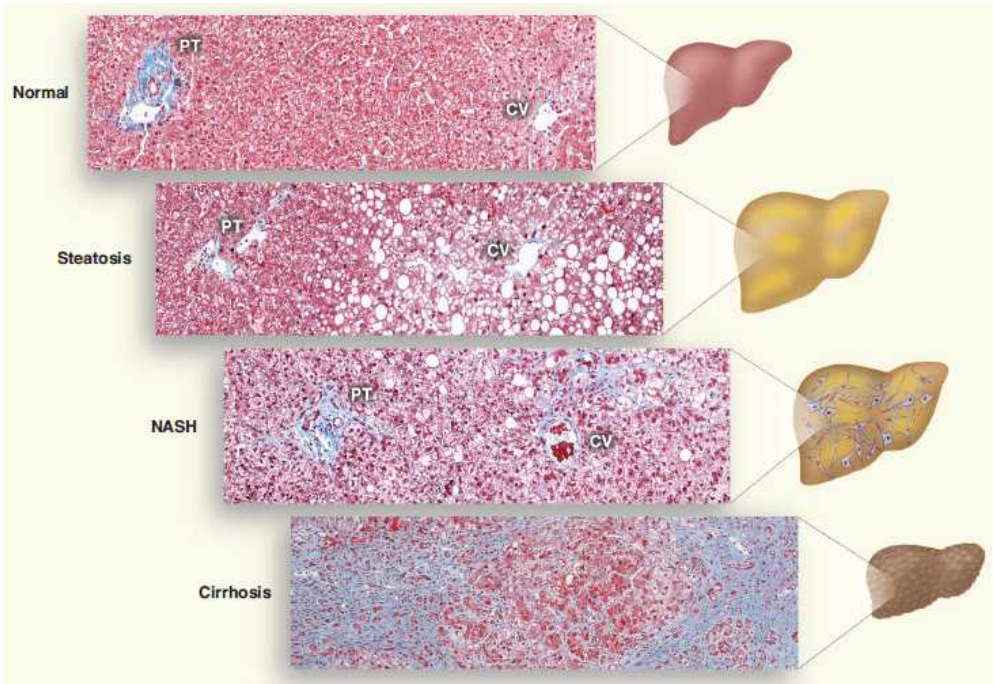

Figure 1. Histological sections illustrating normal liver, steatosis, NASH, and cirrhosis (Jonathan et al., 2011).

Table 1. NAFLD patients with sequential biopsies (Falck-Ytter et al., 2001)

	Length of Follow-up (Years)	n/Total*	Subsequent Histology			
					Progressed to	
			Improved	No Change	Fibrosis	Cirrhosis
Lee† (1989)	1.2–6.9	12/38	0/12	7/12	3/12	2/12
Powell† (1990)	1–9	12/41	1/12	5/12	4/12	2/12
Bacon (1994)	4–7	2/33	0/2	1/2	0/2	1/2
		26/112	1/26 (4%)	13/26 (50%)	7/26 (27%)	5/26 (19%)

*Represents the number of patients out of the total group who had sequential biopsies.
†In both the studies of Lee and Powell, one of the 13 patients with follow-up histology available had cirrhosis at index biopsy. Therefore, only the 12 patients without cirrhosis at index biopsy are included in this analysis.

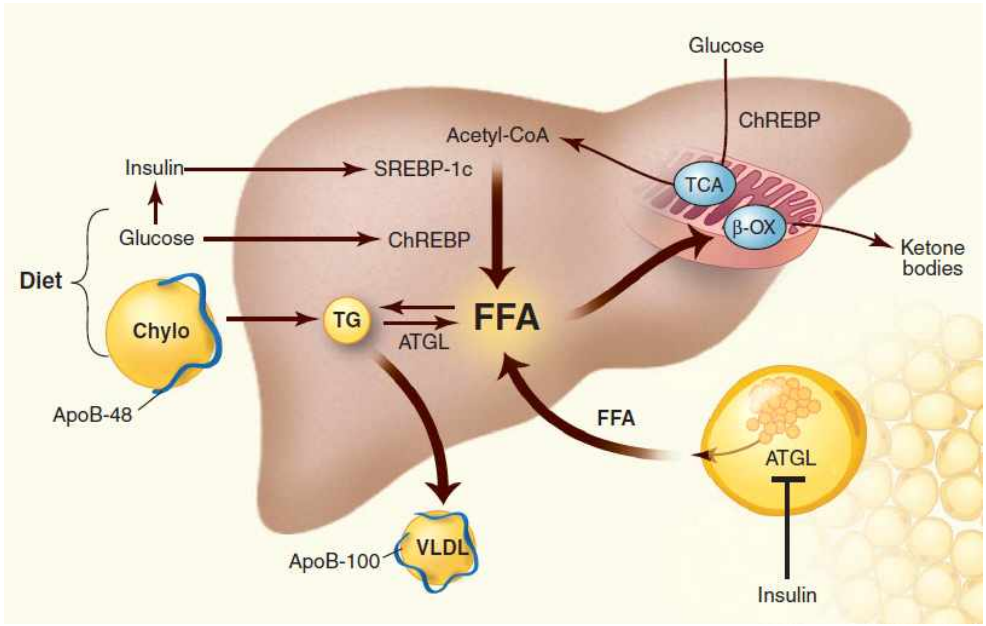

Figure 2. Metabolism of TG in the liver (Jonathan et al., 2011).

1.2. L-serine

L-serine is classified as a non-essential amino acid, but displays a diverse role in several biological processes (Figure 3) (Ming et al., 2016). L-serine is a major contributor to the one-carbon groups for the purine and pyrimidine nucleotide synthesis. L-serine is also converted to D-serine, which is a neuro-modulator acting as a N-methyl-D-aspartate (NMDA) receptor co-agonist by D/L-serine racemase (Matsui et al., 1995). L-serine also can condense with palmitoyl CoA by serine palmitoyltransferase (SPT) to produce sphinganine, which is a precursor of ceramides (Hanada, 2003). L-serine also participates in homocysteine metabolism producing glutathione by supplying glycine and cysteine which are the two products of L-serine metabolism or by reacting with homocysteine. L-serine is required either as a methyl group donor for MS or as a substrate for CβS (Sim et al., 2015).

Our previous study found that L-serine is decreased in chronic ethanol model induced by Lieber-DeCarli ethanol diet (Table 2). Based on this result, we performed further study.

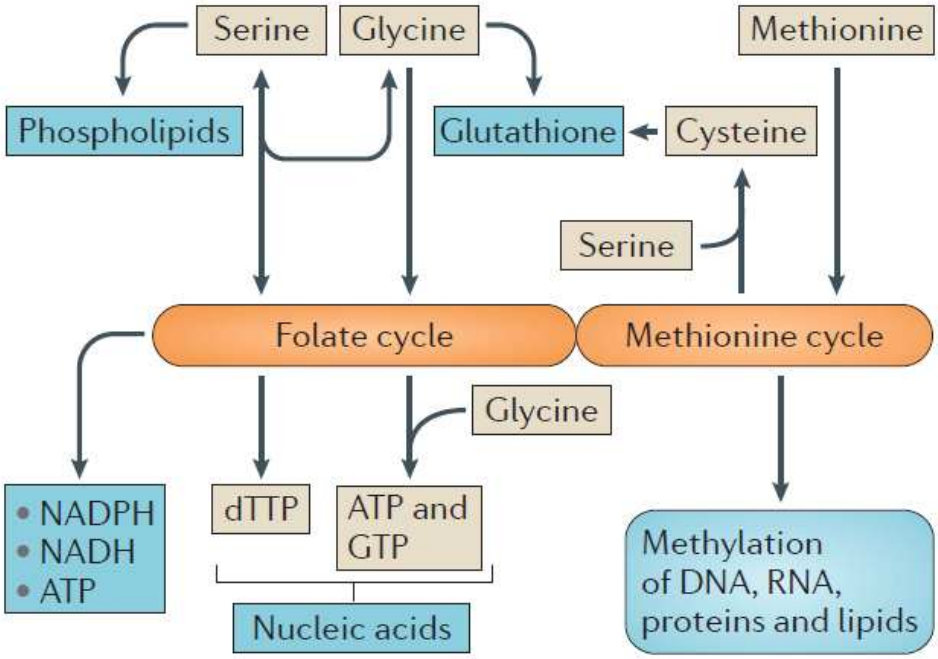

Figure 3. Overview of serine metabolism (Ming et al., 2016).

L-serine donates one-carbon units to the folate cycle while producing glycine. The folate cycle is essential for de novo synthesis of adenosine, guanosine and thymidylate, and can contribute to mitochondrial NADH, NADPH and ATP regeneration. The methionine cycle also provides precursors, such as cysteine for the synthesis of glutathione.

Table 2. Amino acid analysis in the livers from chronically ethanol fed rats.

Amino acid (μmol/g liver)	Control	Ethanol (4 week)	Change
Aspartate	26.4 ± 5.0	30.6 ± 9.6	-
Glutamate	42.3 ± 8.7	39.1 ± 10.3	-
Asparagine	1.5 ± 0.2	1.8 ± 0.3	-
Serine	8.4 ± 1.5	5.9 ± 2.1	- Δ 30%
Glutamine	88.6 ± 4.5	94.1 ± 16.9	-
Histidine	11.1 ± 1.5	11.2 ± 1.2	-
Glycine	15.8 ± 1.9	17.1 ± 3.8	-
Threonine	10.2 ± 1.3	10.9 ± 4.7	-
Alanine	29.8 ± 9.3	27.8 ± 11.4	-
Tyrosine	2.8 ± 0.4	3.7 ± 0.4	Δ 32%
Valine	4.2 ± 0.5	5.7 ± 0.8	Δ 36%
Methionine	0.39 ± 0.04	0.62 ± 0.10	Δ 59%
Tryptophan	0.69 ± 0.06	0.81 ± 0.08	Δ 17%
Phenylalanine	1.6 ± 0.2	2.1 ± 0.3	Δ 31%
Isoleucine	2.0 ± 0.2	2.5 ± 0.3	Δ 25%
Leucine	3.6 ± 0.4	5.0 ± 0.6	Δ 39%
Lysine	8.3 ± 1.9	9.5 ± 2.3	-
Proline	3.4 ± 0.9	4.5 ± 1.3	-

1.3. Homocysteine toxicity and role of homocysteine in fatty liver

Homocysteine is a sulfur-containing toxic metabolite produced by methionine metabolism and is known to be associated with the pathogenesis of the fatty liver disease (Hajer et al., 2007; Gulsen et al., 2005; Bjorck et al., 2006). Hyperhomocysteinemia has been identified as an independent risk factor for coronary artery disease (Clarke et al., 1991).

Homocysteine represents its toxicity through various mechanisms. Pathophysiological levels of homocysteine increased expression and secretion of interleukin-8 (IL-8) and monocyte chemoattractant protein-1 (MCP-1) and induced inflammatory response (Poddar et al., 2001; Wang et al., 2000; Wang and O, 2001).

Homocysteine can damage the function of proteins by making stable disulfide bonds with cysteine residues (Jacobsen et al., 2005) and homocysteine incorporation into protein via *S*-homocysteinylation may leads to impairment of protein function (Undas et al., 2001; Majors et al., 2002; Lim et al., 2003; Sass et al., 2003; Roda et al., 2003).

Homocysteine also induces endoplasmic reticulum (ER) stress, which is a consequence of unfolded protein response (Kaufman, 1999), associated gene expression including glucose-regulated protein 78 (GRP78). Homocysteine can also activate protein kinase RNA-like ER kinase (PERK) (Nonaka et al., 2001; Werstuck et al., 2001). Geoff et al. reported that homocysteine-induced ER stress can dysregulate the triglyceride synthesis pathway resulting in fatty liver (Werstuck et al., 2001).

Mice fed homocysteine or a high-methionine, and low-folate diet have increased homocysteine concentrations and increased incidence of liver

disease, characterized by hepatic steatosis (Ji et al., 2008). Chronic ethanol consumption increases homocysteine accumulation in the liver, which is closely linked to the development of various liver diseases. Moreover, patients with chronic liver disease, as well as alcoholics, develop substantially increased serum homocysteine concentrations regardless of the stage of steatosis, from mild fibrosis to severe cirrhosis (Table 2) (Remková et al., 2009; Cylwik et al., 2009).

Chronic ethanol ingestion induces a deficiency in many nutrients, including folate, choline, vitamin B, betaine and methionine (Kharbanda, 2009). Homocysteine-lowering intervention using folate, betaine, vitamin B reversed homocysteine concentrations and/or liver injuries by normalizing homocysteine metabolism (Verhoef et al., 2004; Ji et al., 2003; Sumiyoshi et al., 2010).

Table 2. Serum folate and homocysteine levels in alcoholics (Cylwik et al., 2009).

Group	Folate (nmol/L)		Homocysteine (μmol/L)	
	Median	Range	Median	Range
Healthy controls	17.9	9.7–42.4	10.58	7.58–14.96
Total alcoholic group	12.9	4.7–35.1	16.85	8.80–68.35
	p^c=0.001		p^c<0.001	
Alcoholics with normal liver enzymes	12.5	4.7–34.9	16.40	8.80–68.35
	p^c=0.002		p^c<0.001	
Alcoholics with elevated liver enzymes	14.0	5.0–35.1	17.89	10.92–48.95
	p^c=0.023		p^c<0.001	
	p^b=0.477		p^b=0.916	
Alcoholics with normal homocysteine	15.3	5.0–34.9	—	
	p^c=0.110			
Alcoholics with elevated homocysteine	11.3	4.8–35.1	—	
	p^c<0.001			
	p^b=0.058			
Alcoholics with normal folate	—		15.63	8.80–40.82
			p^c<0.001	
Alcoholics with low folate	—		17.89	9.11–68.35
			p^c<0.001	
			p^b=0.047	

The differences between alcoholic subgroups and between alcoholics and controls estimated by Mann-Whitney *U*-test. p^b, between supplementary alcoholic subgroups (i.e. alcoholics with normal homocysteine vs alcoholics with elevated homocysteine), p^c, alcoholics vs controls.
Normal liver enzymes: ALT and AST in the range 5–50 U/L, and GGT 10–75 U/L, elevated liver enzymes: ALT and AST higher than 50 U/L, and GGT than 75 U/L. Normal homocysteine: in the range 5.46–16.20 μmol/L, elevated homocysteine: above 16.20 μmol/L. Normal folate: in the range 10.92–43.03 nmol/L, low folate: below 10.92 nmol/L.

1.4. Homocysteine metabolism

The intake of dietary proteins produce various amino acids including methionine. Methionine can be metabolized into S-adenosylmethionine (SAM) by Methionine S-adenosyltransferase (MAT). SAM acts as a methyl donor which is used in amino acid, protein, phospholipids, DNA methylation (Mato et al., 1994). In this reaction, SAM is converted to SAH and metabolized SAH is metabolized into homocysteine by S-adenosylhomocysteine hydrolase.

Liver is a major organ that metabolizes homocysteine. Methionine synthase (MS), betaine homocysteine methyltransferase (BHMT) or cystathionine β-synthase (CβS) change homocysteine into methionine or cysteine (Figure 4) (Verhoef et al., 2004). First, BHMT metabolizes homocysteine into methionine by methylating homocysteine using betaine (Finkelstein, 1990). Secondly, MS metabolizes homocysteine into methionine using 5-methyltetrahydrofolate (5-methylTHF) as a methyl donor and vitamin B_{12} as a cofactor (Seljub J, 1999). Thirdly, homocysteine is metabolized by trans-sulfuration pathway. CβS converts homocysteine into cystathionine by using L-serine and vitamin B_6 as a cofactor. Cystathionine is hydrolyzed into cysteine by cystathionine γ-lyase. Cysteine is then synthesized into glutathione (GSH) or sulfate or secreted as a urea (Mudd, S.H. et al., 1995).

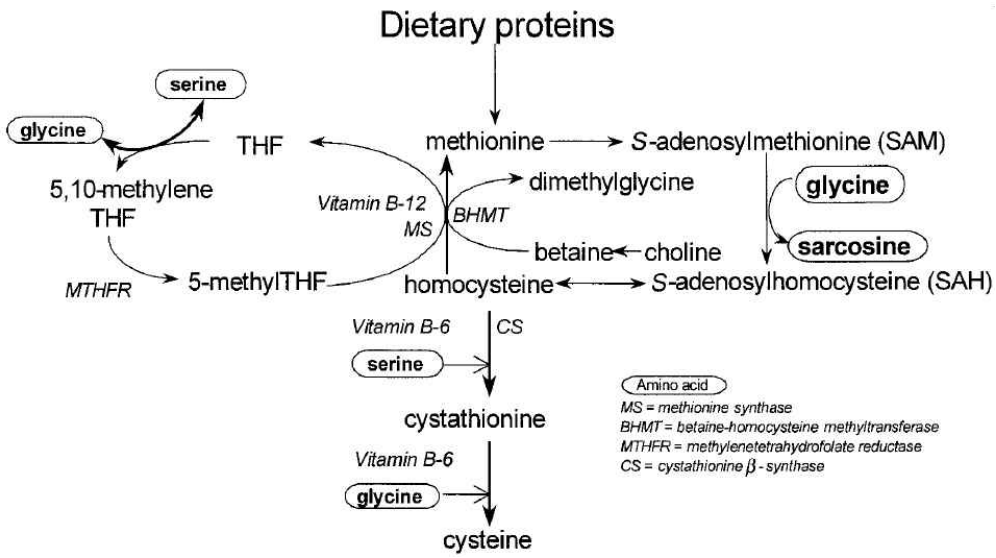

Figure 4. Schematic representation of homocysteine metabolism (Verhoef et al., 2004)

1.5. SIRT1

Mammalian silent information regulators (SIRT) have seven isoforms which belong to the SIRT family. These members have various subcellular localization and distribution in organs (Nogueiras et al., 2012). SIRT1 is most well known member of SIRT family and acts as a NAD^+-dependent deacetylase.

SIRT1 is known as one of a key metabolic sensor which regulates various proteins including transcription factors by its deacetylating activity (Li, 2013; Chaudhary and Pfluger, 2009; Xie et al., 2013; Simmons et al., 2015; Guclu et al.). SIRT1 gain of function has been known to affect vascular function, mitochondria biogenesis, neurodegenerative disease, diabetes mellitus and lipid metabolism (Delmas et al., 2005; Lagouge et al., 2006; Marambaud et al., 2005; Milne et al., 2007; Li et al., 2007).

SIRT1 is widely distributed in metabolic tissues including adipose tissue, liver, skeletal muscle, brain and kidney. In these tissues, SIRT1 expression is up-regulated by calorie restriction (Figure 5) (Cohen et al., 2004; Heilbronn et al., 2005; Nisoli et al., 2005; Picard et al., 2004).

In the muscle tissues, resveratrol improved mitochondrial function and enhanced oxidative capacity in muscle by activating SIRT1 and its target protein, PGC-1α (Lagouge et al., 2006; Milne et al., 2007).

In the liver, the role of SIRT1 in fatty liver disease was first identified by liver-specific SIRT1 knockout (KO) models (Purushotham et al., 2009; Wang et al., 2010). SIRT1 KO mice showed higher lipid deposition in liver and serum compared with control mice. SIRT1 overexpressing transgenic mouse improved high-fat diet-induced glucose tolerance, hepatic steatosis, and inflammation compared with control mouse (Pfluger et al., 2008). Resveratrol and caloric restriction

also prevented hepatic steatosis by regulating SIRT1 pathway in high-fat diet-fed animals (Ding et al., 2017; Baur et al., 2006; Lagouge et al., 2006). In this study, SIRT1 is focused as PHGDH mediated regulation of lipid metabolism.

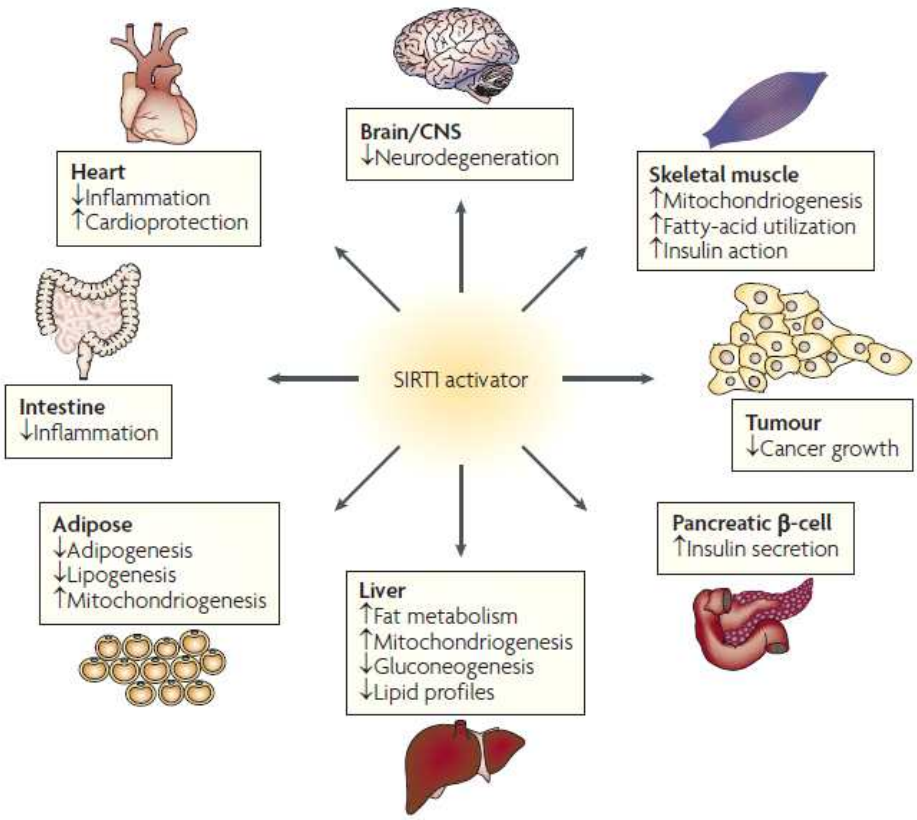

Figure 5. Multiple target organs in which SIRT1 activation can potentially have effects to treat diseases (Lavu et al., 2008).

1.6. De novo Serine Synthesis

L-serine can be synthesized by glycolytic metabolite, 3-phosphoglycerate. 3-phosphoglycerate dehydrogenase (PHGDH) catalyzes first rate-limiting step in de novo serine synthesis. PHGDH converts 3-phosphoglycerate into 3-phosphohydroxypyruvate using NAD^+ as a cofactor (Ravez et al., 2017). Then, 3-Phosphohydroxypyruvate is metabolized into phosphoserine by phosphoserine aminotransferase 1 (PSAT-1) and then L-serine is produced by phosphoserine phosphatase (PSPH). SHMT mediates serine to glycine conversion (Figure 6).

Although L-serine can be absorbed by dietary intake, L-serine from biosynthesis plays important roles in many situations. Nigdelioglu et al. reported that transforming growth factor (TGF)-β promotes de novo serine synthesis for collagen production. Whether there is serine and glycine in culture media or not, only de novo synthesis of glycine from L-serine is sufficient for the production of collagen. Snell et al, first showed that enzymic imbalance in serine metabolism in rat hepatomas (Snell et al., 1986) and several studies reported that PHGDH expression is up-regulated in melanoma and breast cancer cells (Beroukhim et al., 2010; Locasale et al., 2011; Possemato et al., 2011).

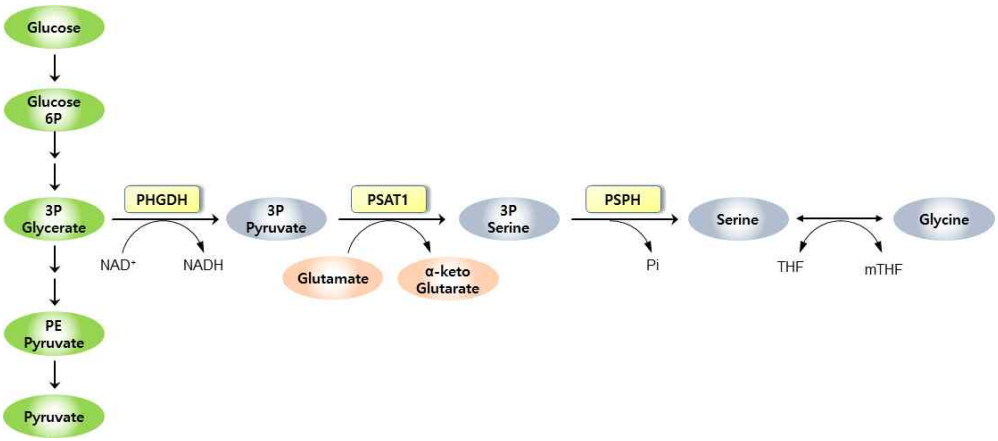

Figure 6. Schematic representation of *de novo* serine synthesis pathway and glycolysis.

1.7. Regulation of PHGDH

PHGDH expression has been known to be regulated by various molecules including human epidermal growth factor receptor 2 (HER2), specificity protein 1 (Sp1), nuclear transcription factor Y (NF-Y), G9A, p53, and erythroid 2-related factor 2 (NRF2).

First, HER2, receptor tyrosine kinase, overexpression increased PHGDH expression in MCF10A cells by using differential analysis of time series gene expression (Bollig et al., 2011).

Second, human PHGDH promoter activity was reported to be positively regulated by the action of transcription factors Sp1 and NF-Y (Jun et al., 2008). Epigenetic study showed that histone H3 lysine 9 (H3K9) methyltransferase G9A is required for maintaining the serine-glycine biosynthetic pathway enzyme genes in an active state marked by H3K9 monomethylation and for the transcriptional activation in response to serine deprivation (Ding et al., 2013).

Third, Ou et al. reported that PHGDH is a target of p53 in human melanoma cells (Ou et al., 2015). Upon serine starvation, p53 suppressed PHGDH expression and inhibited de novo serine biosynthesis and p53-mediated cell death is enhanced dramatically in response to Nutlin-3 treatment.

Fourth, the transcription factor NRF2 is a key regulator in response to oxidative stress (Kansanen et al., 2012). Frequently deregulated NRF2 in non-small cell lung cancer (NSCLC) controls the expression of the key serine/glycine biosynthetic enzyme genes PHGDH, PSAT1, and SHMT2 via activating transcription factor 4 (ATF4) to support macromolecule production (DeNicola et al., 2015).

1.8. The aim of study

The overall goal of this study is to identify the effect of the L-serine on improving fatty liver and the role of PHGDH in lipid metabolism by regulating the synthesis of L-serine.

First, L-serine was significantly reduced in Lieber-DeCarli ethanol in vivo model in previous study and it is assumed that L-serine can reverse the fatty liver. In this study, the effect of L-serine on alcoholic fatty liver disease was identified and the mechanism of L-serine on fatty liver was also studied focusing on homocysteine metabolism.

Second, L-serine mediated regulation of fatty liver disease was studied. We assumed that NAD^+ can be produced by L-serine by the action of lactate dehydrogenase and measured intracellular NAD^+ and the activity of SIRT1, NAD^+ using deacetylation enzyme.

Third, the reason why L-serine is decreased in various fatty liver diseases model was investigated. L-serine can not only be uptaken by dietary sources but also be synthesized by de novo L-serine synthesis pathway using glycolytic intermediate, 3-phosphoglycerate. The expression of enzymes involved in this pathway was measured and the rate-limiting enzyme, PHGDH, was identified as a key factor for L-serine mediated lipid metabolism.

Fourth, the regulation of PHGDH is investigated. One of the various regulators, NRF2 is studied by focusing on its expression and protein stability.

II. Materials and Methods

2.1. L-serine effect on alcoholic fatty liver

2.1.1. Cell culture

AML12 was obtained from the American Type Culture Collection (ATCC, Rockville, MD) and cultured following ATCC guidelines. Briefly, cells were cultured with growth medium which is DMEM/F12 (Gibco BRL, Grand island, NY) with 0.005 mg/mL insulin, 0.005 mg/mL transferrin, 5 ng/mL selenium (Insulin-Transferrin-Selenium, Gibco BRL), and 40 ng/mL dexamethasone (Sigma, St. Louis, MO) containing 10% heat inactivated fetal bovine serum (FBS; Gibco BRL), 50 units/mL of penicillin, and 50 units/mL of streptomycin (Antibiotic-antimycotic; Gibco BRL).

2.1.2. Nile red assay

AML12 cells were plated into black 96-well plates at a density of 10^4 cells per well and incubated overnight. Ethanol was treated for 48 hr with or without L-serine at indicated concentrations. After 48 hr, cells were fixed in paraformaldehyde containing Hoechst 33258 for 10 minutes at room temperature. Then paraformaldehyde was removed and cells were washed with Dulbacco's modified phosphate-buffered saline (DPBS) twice. DPBS containing nile red solution was added and incubated for 10 minutes and washed with DPBS. Fluorescence was measured using a microplated fluorescence reader at the excitation/emission wavelengths of 470/580 nm. Data were normalized by Hoechst 33258 determined at the excitation/emission wavelengths of

365/488 nm.

2.1.3. Animal experiments

Animals used in the study were purchased from Japan SLC, Inc., housed in an air-conditioned room (24℃) with a 12-h light/dark cycle, and acclimatized over 1 wk to a nonpurified diet. The experiments using animals were carried out in accordance with animal experiment guidelines with the approval of the Institutional Animal Care and Use Committee of Seoul National University.

2.1.3.1. Binge ethanol study

Male C57BL/6 mice (20 g) were randomly divided into 4 groups: control (C), binge ethanol + vehicle (EV), binge ethanol + 20 mg/kg L-serine (ES20), and binge ethanol + 200 mg/kg L-serine (ES200). They were fed the nonpurified diet throughout the experiments. Three mice in each group were gavaged with 5 g/kg of ethanol or isocaloric dextran-maltose 3 times every 12 h. L-Serine dissolved in tap water was administered twice by oral gavage 30 min before the last 2 ethanol doses, and the mice were killed by cardiac puncture after Zoletil (10 mg/kg tiletamine, 10 mg/kg zolazepam, ip; Virbac) anesthesia 24 h after the last dose. The binge ethanol study was performed twice independently .

2.1.3.2. Chronic ethanol feeding study

Male Wistar rats (250 g) were divided into 3 groups: C, ethanol diet (E), and ethanol diet + 1% L-serine (ES). The rats were fed a standard Lieber-DeCarli ethanol diet (36% ethanol-derived calories;

Dyets) for 4 wk ; pair-fed control rats were administered dextran-maltose to match the alcohol-derived calories in the ethanol diet. For pair-feeding, 2 rats were housed in a single cage. The food intake of each cage in the E group was determined daily between 09:00 and 10:00 h, and the same amount of the food was then given on the following day to the C and ES groups. Pair-feeding was conducted throughout the study. The ethanol diet was supplemented either with or without 1% (wt:vol) L-serine for the last 2 wk.

2.1.4. Histopathologic evaluation

For Oil Red O staining, frozen liver tissues were cut into 7-mm sections and affixed to microscope slides. Sections were stained with Oil Red O solution buffer and counter-stained with Harris hematoxylin.

2.1.5. Serum biochemistry

Serum alanine aminotransferase (ALT), aspartate aminotransferase (AST), TGs, and cholesterol were monitored by standard clinical chemistry assays on a Tokyo Boeki Prestige 24I Chemistry Analyzer (Tokyo Boeki Machinery Limited). Serum and cellular total homocysteine concentrations were quantified by using an Axis Homocysteine EIA Reagent kit (Axis-Shield) following the manufacturers' protocol with SpectraMax 340 (Molecular Devices).

2.1.6. TG analysis

Liver and cellular TGs were determined by a modified Folch method by using a Serum Triglyceride Determination kit (Sigma) following the manufacturers protocol.

2.1.7. Determination of sulfur amino acids and metabolites

Liver homogenates were diluted, and denatured protein was removed by centrifugation at 10,000 g for 10 min; the supernatant was used to measure hepatic homocysteine, SAM, SAH, cysteine and GSH. An HPLC method was used to determine SAM and SAH, and total homocysteine, total cysteine, and total GSH were quantified by the 7-benzo-2-oxa-1,3-diazole-4-sulfonic acid (SBD-F) method. For hepatic methionine and cystathionine analysis, liver homogenates were diluted in ice-cold methanol. They were then derivatized with O-phthalaldehyde/2-mercaptoethanol and quantified by using an HPLC (SCL-10A; Shimadzu) system with a fluorescence detector (RF-10AXL, Ex 385 nm and Em 515 nm; Shimadzu).

2.1.8. RNA interference

AML12 cells were seeded with 2 x 10^5 cells per well in 6-well plates in medium containing 10% FBS for 24 h. The cells were transiently transfected with *Ms*, *Cbs*, and *Bhmt* small interfering RNA (siRNA; Santa Cruz Biotechnology) by using the Fugene HD Transfection Reagent (Promega) as recommended by the manufacturers protocol. After 48 h, the cells were collected for homocysteine and TG measurement.

2.1.9. Statistical analysis

All results are presented as means ± SDs. Data were evaluated by student's t-test or one-way ANOVA followed by Tukey's multiple comparison procedure or Dunnett's post-test. All data were analyzed

by GraphPad Prism 5 (GraphPad Software).

2.2. L-serine effect on SIRT1 activity

2.2.1. Cell culture

C2C12 mouse skeletal muscle cell and AML12 was obtained from the American Type Culture Collection (ATCC) and PHGDH KO-MEF cells were kindly obtained from Dr. Furuya Shigeki from Kyushu university. Cells were cultured following ATCC guidelines. C2C12 myoblasts were maintained in DMEM (Gibco BRL) containing 10% FBS and 50and AML12 cells were cultured with DMEM/F12 containing 0.005 mg/mL insulin, 0.005 mg/mL transferrin, 5 ng/mL selenium (Insulin-Transferrin-Selenium, Gibco BRL), and 40 ng/mL dexamethasone (Sigma) containing 10% FBS and 50 units/mL of penicillin and streptomycin (Antibiotic-antimycotic; Gibco BRL). To differentiate myoblast, cells were allowed to reach 90% confluence, and the media were replaced with 2% horse serum containing DMEM for 6 days. PHGDH KO-MEF cells were cultured with DMEM (Gibco BRL) containing 10% heat inactivated fetal bovine serum (FBS) and antibiotic-antimycotic.

2.2.2. NAD^+/NADH measurement

Intracellular NAD^+ and NAD were determined using NAD+/NADH Quantitation Colorimetric Kit (Biovision, Milpitas, CA) according to the manufacturer's protocols. Briefly, cells were homogenized in 200 μL acid or alkali extraction buffer to measure NAD^+ or NADH. After extraction, samples were neutralized using the opposite buffer and the

intracellular NAD and NADH were determined by enzymatic cycling reactions. The level of nucleotides were normalized by cellular protein concentrations.

2.2.3. PGC-1α deacetylation assay

To determine PGC-1α acetylation level, immunoprecipitation (IP) was performed using specific antibodies against acetyl-lysine (Cell signaling Technology) for overnight and subjected to bind protein G agarose bead (Thermo Fisher Scientific, Waltham, MA). Immunoprecipitated beads were washed with IP buffer three times and mixed with sample buffer. After centrifugation, supernatant was used for western blot analysis and PGC-1 antibody was conjugated. After overnight incubation, HRP-conjugated secondary anti-rabbit antibody were added for 2 hr and protein level was determined.

2.2.4. RNA interference

Differentiated C2C12 myotubes were transiently transfected with *Ldh* small interfering RNA (siRNA; Cell signaling) by using Lipofectamine® RNAiMax Reagent (Thermo Fischer Scientific) as recommended by the manufacturers protocol.

2.2.5. Quantitative Real-time Polymerase Chain Reaction (qRT-PCR)

For qRT-PCR, total RNA was prepared from animal livers or C2C12 myotubes using Easy-Blue™ Total RNA Extraction Kit (Intron Biotechnology, Seoul, Korea). After RNA extraction, cDNA was produced using QuantiTect Reverse Transcription Kit (Qiagen, Hilden,

Germany). The resulting cDNA was amplified by qRT-PCR using iTaq™ Universal SYBR® Green Supermix Kit (Bio-rad, Hercules, CA) in a Stepone™ Real-Time PCR System (Applied Biosystems. Seoul, Korea).

2.2.6. Mitotracker Red staining

C2C12 myotubes differentiated in 96 black well plates are stained by MitoTracker® red dye. Cells were added warmed staining media containing MitoTracker® Red CMXRos probe (Invitrogen, Carlsbad, CA) for 30 minutes. Then, cells were washed with fresh growth media and incubated with 4% formaldehyde containing Hoechst33258 (Invitrogen) for 10 minutes. After fixation, cells were rinsed twice with DPBS and analyzed by fluorescence detection.

2.2.7. Mitochondrial DNA quantification

Genomic DNA was extracted by QIAamp® DNA Mini Kit (Qiagen) from C2C12 myocytes. To quantify mtDNA, cytochrome b primers was used and to quantify nuclear DNA, 18s rRNA primers were used.

2.2.8. ATP measurements

C2C12 myotubes differentiated in a 96 white well plate and after 24 hr L-serine treatment, the plate was incubated at room temperature for 30 minutes and added with CellTiter-Glo® in 100 μL per well. After mixing contents, luminescence was detected by Centro LB960 luminometer.

2.2.9. Oxygen consumption ratio (OCR) measurements

OCR was measured using Extracellular Flux Analyzers XFp (Agilent Technologies, Santa Clara, CA). C2C12 differentiated in XFp cell culture miniplates were treated with L-serine, fatty acids, and resveratrol were washed twice with assay media and incubated in a CO2 free incubator at 37℃ 30 minutes prior to the assay. After incubation, the culture plate and drug catridge were injected according to the XFp analyzers.

2.2.10. Nile red assay

After treatment, C2C12 myotubes were fixed in paraformaldehyde containing Hoechst 33258 for 10 minutes at room temperature. Then paraformaldehyde was removed and cells were washed with Dulbacco's modified phosphate-buffered saline (DPBS) twice. DPBS containing nile red solution was added and incubated for 10 minutes and washed with DPBS. Fluorescence was measured using a microplated fluorexcence reader at the excitation/emission wavelengths of 470/580 nm. Data was normalized by Hoechst 33258 determined at the excitation/emission wavelengths of 365/488 nm.

2.2.11. Western blot analysis

Western blotting was basically performed by established procedures using specific antibodies against pAkt, Akt, GLUT4, APTase and β-Actin (Cell signaling Technology, Beverly, MA) and HRP-conjugated secondary anti-rabbit or anti-mouse antibody (Cell Signaling Technology).

2.2.12. Membrane fraction

To confirm GLUT4 membrane translocation, subcellular fractionation was performed according to Li et al (Braz J Med Biol Res, 2015). Cells were washed with cold DPBS twice and suspended in cold sample preparation buffer, sonicated, and centrifuged at 100,000 g for 1 hr at 4 ℃. Supernatant was removed and remained pellet was resuspended in 0.5% Triton X added homogenization buffer and incubated on ice for 1 hr. After centrifuge, the supernatant was kept as the plasma membrane fraction.

2.2.13. Statistical analysis

All results are presented as means ± SDs. Data were evaluated by student's t-test or one-way ANOVA followed by Tukey's multiple comparison procedure or Dunnett's post-test. All data were analyzed by GraphPad Prism 5 (GraphPad Software).

2.3. Down-regulation of PHGDH in fatty liver disease.

2.3.1. Animal experiments

Animals used in the study were purchased from Japan SLC, Inc. housed in an air-conditioned room (24℃) with a 12-h light/dark cycle, and acclimatized over 1 wk to a nonpurified diet. The experiments using animals were carried out in accordance with animal experiment guidelines with the approval of the Institutional Animal Care and Use Committee of Seoul National University.

2.3.1.1. Chronic ethanol feeding study

Male Wistar rats (250 g) were fed a standard Lieber-DeCarli ethanol diet (36% ethanol-derived calories; Dyets) for 4 wk ; pair-fed control rats were administered dextran-maltose to match the alcohol-derived calories in the ethanol diet. For pair-feeding, 2 rats were housed in a single cage. The food intake of each cage in the ethanol group was determined daily between 09:00 and 10:00 h, and the same amount of the food was then given on the following day to the C and ES groups. Pair-feeding was conducted throughout the study.

2.3.1.2. High-fat diet study

Male C57BL/6 mice were purchased from SLC Inc. (Hamamatsu, Japan) and housed in an air-conditioned room (24 °C) with a 12 h light/dark cycle. Mice were fed with lard-based high fat diet (60% of calories derived from fat; Research Diets, Inc., NJ, USA) for 6 weeks. Pair-feeding was conducted throughout the study.

2.3.1.3. Methionine-choline deficient (MCD) diet study

Male C57BL/6 mice were purchased from SLC Inc. (Hamamatsu, Japan) and housed in an air-conditioned room (24 °C) with a 12 h light/dark cycle. Mice were fed with methionine choline deficient diet (Research Diets, Inc., NJ, USA) for 4 weeks. pair-fed control mice were administered dextran-maltose to match the alcohol-derived calories in the ethanol diet.Pair-feeding was conducted throughout the study.

2.3.2. Quantitative Real-time Polymerase Chain Reaction (qRT-PCR)

For qRT-PCR, total RNA was prepared from animal livers or C2C12 myotubes using Easy-Blue™ Total RNA Extraction Kit (Intron Biotechnology). After RNA extraction, cDNA was produced using QuantiTect Reverse Transcription Kit (Qiagen). The resulting cDNA was amplified by qRT-PCR using iTaq™ Universal SYBR® Green Supermix Kit (Bio-rad) in a Stepone™ Real-Time PCR System (Applied Biosystems. Seoul, Korea).

2.3.3. Primary hepatocyte isolation

Primary hepatocytes were isolated by a two-step collagenase perfusion as dexcribed previously (LeCluyse et al., 1996). Briefly, after anesthesia, abdominal cavitiy of mouse was opened and portal vein was cannulated with catheter and perfused with Hank's balanced salt solution (HBSS; Gibco BRL). As soon as the liver is swelling, inferior vena cava was cut. When the blood from the liver is completely removed, $CaCl_2$ solution containing collagenase was perfused. After collagen perfusion, the liver was extracted and hepatocytes were suspended in digestion media. The suspension was sieved and centrifuged and cell pellet was washed twice with culture media. Cell viability was determined by trypan blue exclusion and cells were used when 90-95% cell viability was confirmed. Cells were incubated in a 37°C incubator in an atmosphere of 5 % CO_2 in air.

2.3.4. Western blot analysis

Western blotting was basically performed by established procedures

using specific antibodies against PHGDH and β-Actin (Cell signaling Technology, Beverly, MA) and HRP-conjugated secondary anti-rabbit or anti-mouse antibody (Cell Signaling Technology).

2.3.5. Clinical data from fatty liver disease patients

Serum from twenty control group and sixty-eight fatty liver disease patients were provided by Dr. Dae Won Jun from Hanyang University college of medicine and serum amino acid analysis was performed by Sang Kyum Kim from Chungnam National University. Data were provided by nd analyzed with GraphPad Prism 5 (GraphPad Software).

2.3.6. Cell culture

AML12 was obtained from the American Type Culture Collection (ATCC) and PHGDH KO-MEF cells were kindly obtained from Dr. Furuya Shigeki from Kyushu university. Cells were cultured following ATCC guidelines. Briefly, AML12 cells were cultured with DMEM/F12 containing 0.005 mg/mL insulin, 0.005 mg/mL transferrin, 5 ng/mL selenium (Insulin-Transferrin-Selenium, Gibco BRL), and 40 ng/mL dexamethasone (Sigma) containing 10% heat inactivated fetal bovine serum (FBS; Gibco BRL), 50 units/mL of penicillin, and 50 units/mL of penicillin and streptomycin (Antibiotic-antimycotic; Gibco BRL). PHGDH KO-MEF cells were cultured with DMEM (Gibco BRL) containing 10% heat inactivated fetal bovine serum (FBS) and antibiotic-antimycotic.

2.3.7. NAD^+/NADH measurement

Intracellular NAD^+ and NAD were determined using NAD^+/NADH Quantitation Colorimetric Kit (Biovision, Milpitas, CA) according to the manufacturer's protocols. Briefly, cells were homogenized in 200 μL acid or alkali extraction buffer to measure NAD^+ or NADH. After extraction, samples were neutralized using the opposite buffer and the intracellular NAD^+ and NADH were determined by enzymatic cycling reactions. The level of nucleotides were normalized by cellular protein concentrations.

2.3.8. PGC-1α deacetylation assay

To determine PGC-1α acetylation level, immunoprecipitation (IP) was performed using specific antibodies against acetyl-lysine (Cell signaling Technology) for overnight and subjected to bind protein G agarose bead (Thermo Fisher Scientific). Immunoprecipitated beads were washed with IP buffer three times and mixed with sample buffer. After centrifugation, supernatant was used for western blot analysis and PGC-1 antibody was conjugated. After overnight incubation, HRP-conjugated secondary anti-rabbit antibody were added for 2 hr and protein level was determined.

2.3.9. Nile red assay and TG analysis

Cells were plated into black 96-well plates and after treatment, cells were fixed in paraformaldehyde containing Hoechst 33258 for 10 minutes at room temperature. Then paraformaldehyde was removed and cells were washed with DPBS twice. DPBS containing nile red solution was added and incubated for 10 minutes and washed with DPBS. Fluorescence was measured using a microplated fluorexcence

reader at the excitation/emission wavelengths of 470/580 nm. Data was normalized by Hoechst 33258 determined at the excitation/emission wavelengths of 365/488 nm.

Cellular TGs were determined by a modified Folch method by using a Serum Triglyceride Determination kit (Sigma) following the manufacturers protocol.

2.3.10. Transient transfection and RNA interference

Cells were transfected with PHGDH expression vector using Lipofectamine 2000 (Invitrogen) as recommended by the manufacturer's protocol. For RNA interference, cells were seeded with 2 x 10^5 cells per well in 6 well plates in medium containing 10% FBS for 24 h. The cells were transiently transfected with *Phgdh* siRNA (Cell signaling) by using Lipofectamine® RNAiMax Reagent (Thermo Fischer Scientific) as recommended by the manufacturers protocol.

2.3.11. Statistical analysis

All results are presented as means ± SDs. Data were evaluated by student's t-test or one-way ANOVA followed by Tukey's multiple comparison procedure or Dunnett's post-test. All data were analyzed by GraphPad Prism 5 (GraphPad Software).

2.4. The mechanism of regulating PHGDH

2.4.1. Bisulfite conversion

DNA was prepared by QIAamp® DNA Mini Kit (Qiagen) from cells

and tissues. Bisulfite conversion of DNA was performed using EpiTect Bisulfite Conversion Kit by manufacturer's protocol. Briefly, DNA was prepared with bisulfite reaction mixture through denaturation procedure. Bisulfited DNA was centrifuged and washed with washing buffer and eluted with DNA spin column and elution buffer. Eluted bisulfite converted DNA was amplified by specific primers.

2.4.2. Histone H3 and H4 acetylation assay

For the measurement of global histone H3 and H4 acetylation from cells and tissues, histone H3 and H4 acetylation assay kit (Abcam) was used by manufcaturer's protocols. Briefly, cell lysis and tissue disaggregation were performed by lysis buffer. By incubating extraction buffer/glycerol solution, extracted histone was coated onto assay wells. After washing, capture antibody and detection antibody was added. By treating developing solution, color was developed and absorbance was measured.

2.4.3. Western blot analysis

Western blotting was basically performed by established procedures using specific antibodies against PHGDH, Ace-H3K9, NRF2 and β-Actin (Cell signaling Technology, Beverly, MA) and HRP-conjugated secondary anti-rabbit or anti-mouse antibody (Cell Signaling Technology).

2.4.4. Statistical analysis

All results are presented as means ± SDs. Data were evaluated by student's t-test or one-way ANOVA followed by Tukey's multiple

comparison procedure or Dunnett's post-test. All data were analyzed by GraphPad Prism 5 (GraphPad Software).

III. Results

3.1. L-serine reverses alcoholic fatty liver

3.1.1. L-serine decreased ethanol-induced lipid accumulation

Previous study revealed that hepatic L-serine was significantly decreased in alcoholic liver disease model. First, L-serine was treated with ethanol in AML12 cells to identify the effect of L-serine on lipid accumulation. Ethanol treatment increased intracellular lipid about 2 fold and L-serine reversed lipid staining concentration-dependently (Figure 7).

To confirm the effects of L-serine in vivo, mouse ethanol binge model was used. Oil red O staining revealed that 3 times of ethanol gavage caused fatty liver and L-serine decreased lipid accumulation. 200 mg/kg of L-serine decreased ALT, which is a biomarker of liver dysfunction and hepatic TG (Figure 8). Next, the effect of L-serine was identified in chronic ethanol model. Rats were fed with Lieber-DeCarli ethanol diet to induce fatty liver and L-serine was treated last 2 weeks of ethanol diet. Lieber-DeCarli ethanol diet significantly increased lipid droplets and serum ALT. L-serine decreased these effects dose-dependently (Figure 9).

The decreased concentrations of SAM and GSH observed in the ethanol group were completely recovered in the L-serine treated rat group. As a result, the SAM:SAH ratio was also restored in the L-serine group (Table 3).

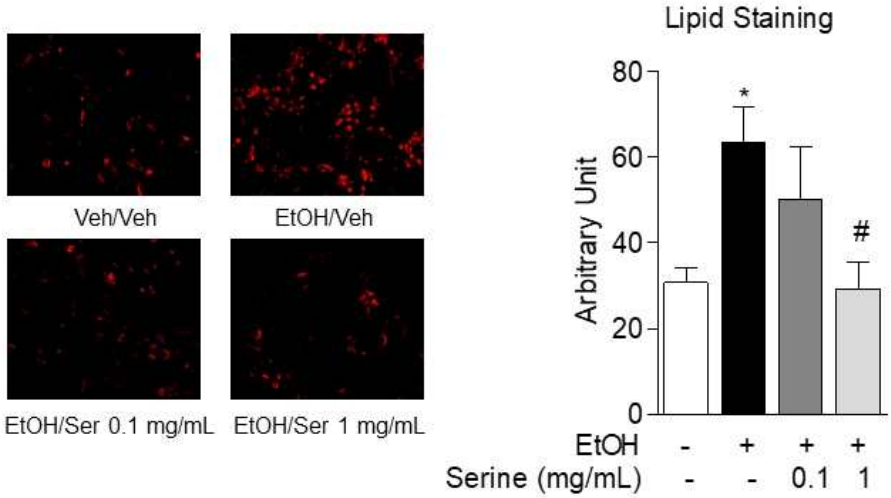

Figure 7. Nile red staining of ethanol-treated AML12 cells.

AML12 cells were treated with 100 mM ethanol with or without indicated concentrations of L-serine for 48 hr. Microscopic images of cells were shown in left panel. Right panel shows the quantification of nile red staining. Values in graph are means ± SDs, n = 3 of three independent experiments. Within each graph, * represents significance (*; $P < 0.05$) relative to the control group; # represents significance (#; $P < 0.05$) relative to the ethanol group. Statistical analysis was performed by using one-way ANOVA with Tukey's multiple-comparison procedure.

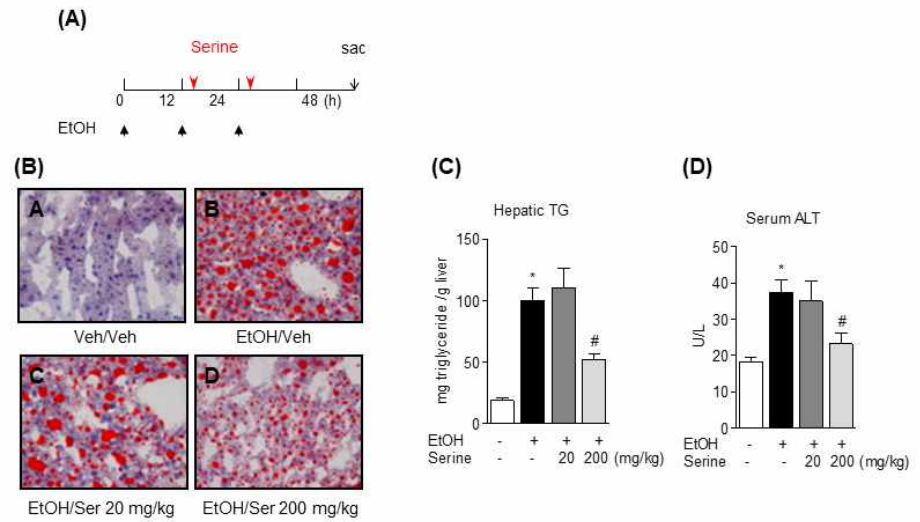

Figure 8. L-serine ameliorates binge ethanol induced fatty liver.

Binge ethanol feeding was performed as described in Materials and Methods section. Graphical protocol was described in (A). Below are Oil red O staining of the livers (B), hepatic TG (C) and serum ALT (D) in the binge ethanol study. Values in panels C-D are means ± SDs, n = 3 mice per group. Within each graph, * represents significance (*; $P < 0.05$) relative to the control group; # represents significance (#; $P < 0.05$) relative to the ethanol group. Statistical analysis was performed by using one-way ANOVA with Tukey's multiple-comparison procedure.

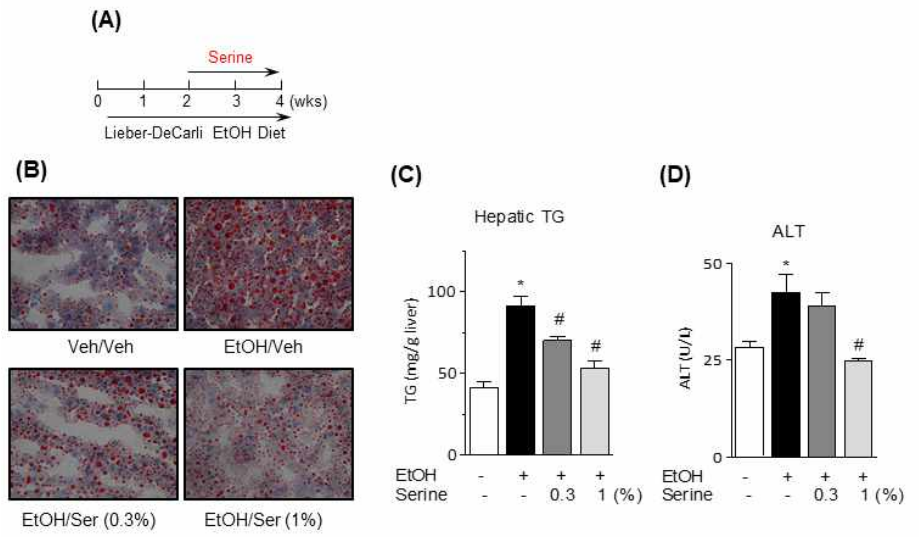

Figure 9. L-serine ameliorates chronic ethanol feeding-induced fatty liver.

Chronic ethanol feeding by Lieber-DeCarli ethanol diet was performed as described in Materials and Methods section. Graphical protocol is described in left upper panel (A). Below are Oil red O staining of the livers (B), hepatic TG (C) and serum ALT (D) in the chronic ethanol feeding study. Values in panels C-D are means ± SDs, n = 8~10 rats per group. Within each graph, * represents significance (*; $P < 0.05$) relative to the control group; # represents significance (#; $P < 0.05$) relative to the ethanol group. Statistical analysis was performed by using one-way ANOVA with Tukey's multiple-comparison procedure.

Table 3. Concentrations of sulfur amino acids and metabolites in the liver obtained from binge ethanol study and chronic ethanol feeding study.

	Binge ethanol study (mice)				Chronic ethanol study (rats)		
Variable	Con	EtOH	EtOH +Ser20	EtOH +Ser200	Con	EtOH	EtOH+Ser
Cysteine	287±52.8	277±157	404±178	408±323	584±98.9	488±92.4	494±151
SAM	59.3±29.5	25.2±23.6	45.3±22.4	50.1±15.9	54.8±3.4	28.4±3.5*	55.1±8.8#
SAH	26.2±0.5	31.1±12.9	25.4±3.4	34.7±5.2	19.5±3.9	21.8±1.1	17.1±0.7
SAM:SAH	2.31±1.1	1.0±1.1	1.9±1.1	1.5±0.7	2.9±0.6	1.3±0.1*	3.2±0.4#
Methionine	670±175	733±391	427±91.1	627±165	1380±398	924±356	812±147
Cystathionine	39.6±4.7	24.4±1.5	27.9±14.6	25.9±6.2	30.9±6.7	14.6±1.9*	18.3±3.4
GSH	6.6±1.3	6.0±3.4	8.8±0.6	8.9±0.5	7.7±0.5	6.2±0.4*	8.1±0.7#

Values are means ± SDs, n = 3 mice and rats per group. Data were analyzed by 1-way ANOVA followed by Tukey's multiple comparison procedure. Homocysteine in rat liver and cystathionine in mouse liver were analyzed by Kurskal-Wallis test because of unequal variance. * represents significance (* ; $P < 0.05$) relative to the control and # represents significance (# ; $P < 0.05$) relative to the ethanol group.

3.1.2. L-serine inhibited homocysteine by MS and CβS-dependent homocysteine metabolism

L-serine is used as a precursor of one-carbon donor. Homocysteine is known to induce fatty liver disease and trans-methylation pathway is important in metabolizing homocysteine. To identify whether the effect of L-serine on alcoholic fatty liver is associated with homocysteine metabolism, homocysteine or methionine treated in vitro model was used. When AML12 cells were treated with homocysteine or methionine, intracellular homocysteine and lipid accumulation were observed. L-serine reversed homocysteine- or methionine-induced up-regulated homocysteine and lipid levels (Figure 10).

Homocysteine metabolism is achieved by three enzymes including MS, CβS, and BHMT which convert homocysteine to methionine or cysteine via trans-methylation or trans-sulfuration pathway. To identify which enzyme is related with L-serine effect on homocysteine and lipid accumulation, siRNA knockdown experiment was performed. When each enzyme of homocysteine metabolism was blocked with siRNA, homocysteine and lipid accumulation were increased and L-serine reversed these effects only when BHMT was knockdown. When MS and CβS expression was blocked, L-serine had no effect on homocysteine and lipid accumulation. These results imply that MS and CβS use L-serine to metabolize homocysteine (Figure 11).

To confirm these in vitro effects of L-serine on in vivo, the serum and hepatic levels of homocysteine of binge ethanol treated mice and chronic Lieber-DeCarli ethanol diet treated rats were investigated. L-serine significantly and dose-dependently decreased homocysteine in the serum and livers (Figure 12).

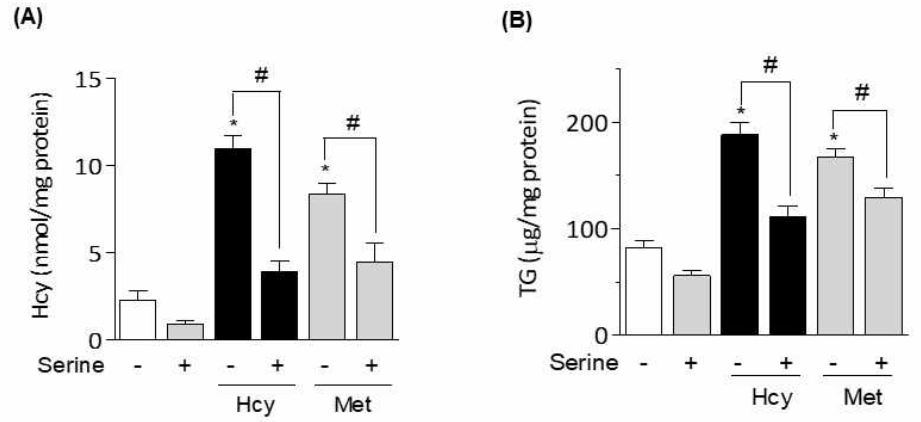

Figure 10. L-serine lowered homocysteine and lipid in AML12 cells.

Intracellular total homocysteine (A) and TG (B) concentrations in homocysteine (5 mM) or methionine (5 mM)-treated AML12 cells in the absence or presence of L-serine (1 mg/mL) for 24 hr. Homocysteine and TG concentrations were normalized by intracellular proteins. Values are means ± SDs, n = 3 (means of triplicates). Within each graph, * represents significance (*; $P < 0.05$) relative to the control group; # represents significance (#; $P < 0.05$) relative to the homocysteine or methionine group. Statistical analysis was performed by using 2-way ANOVA with Bonferroni's multiple-comparison procedure.

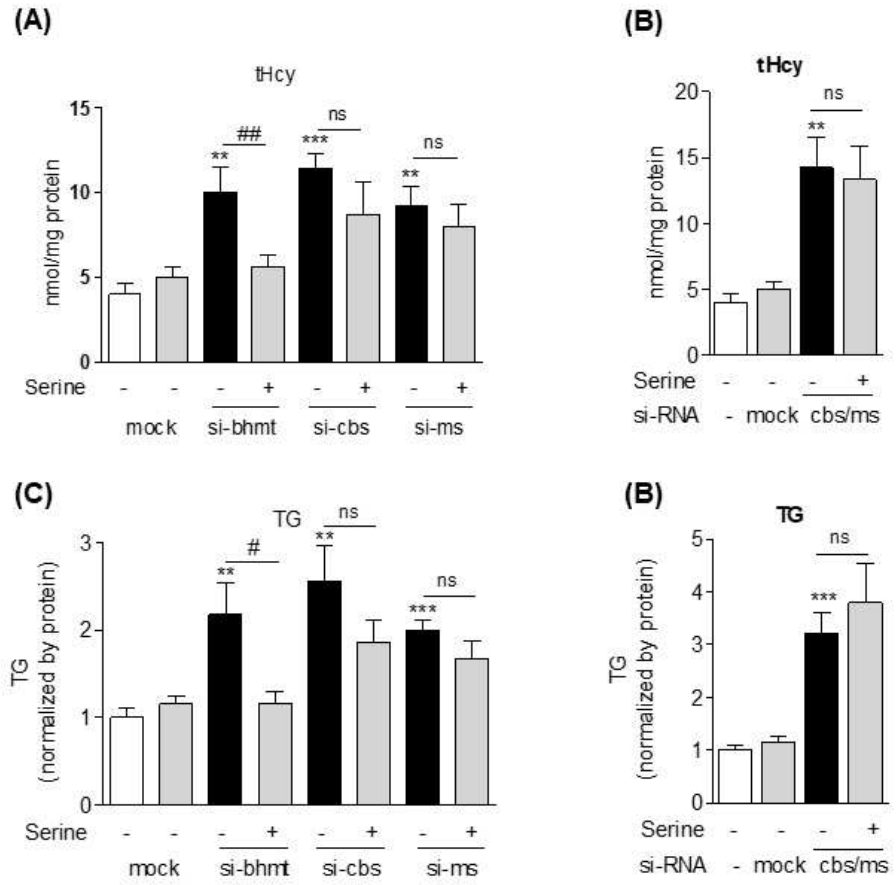

Figure 11. L-serine decreased homocysteine and TG on homocysteine only when MS and/or CβS activity are intact.

Intracellular total homocysteine and TGs in *Bhmt*-, *Cbs*-, or *Ms*-siRNA transfected AML12 cells (A, C) and *Ms*/*Cbs*-siRNA co-transfected AML12 cells (B, D) in the absence or presence of L-serine (1 mg/mL). Homocysteine and TG concentrations were normalized by intracellular proteins. Values are means ± SDs, n = 3 (means of triplicates). Within each graph, ** and *** represent significance (**; $P < 0.01$, ***; $P < 0.001$) relative to the control group; # and ## represent significance (#; $P < 0.05$, ##; $P < 0.01$). ns means 'not significant'. Statistical analysis was performed by using 2-way ANOVA with Bonferroni's multiple-comparison procedure.

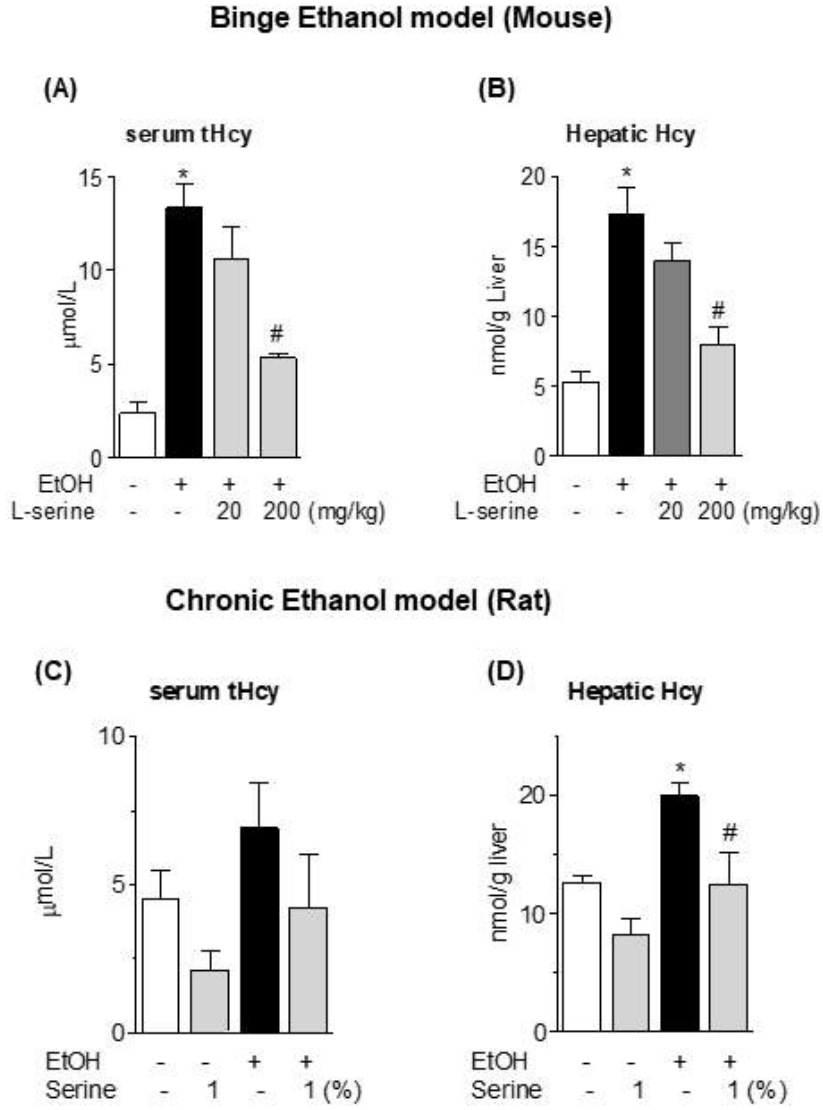

Figure 12. L-serine decreased serum and hepatic homocysteine in binge ethanol and chronic ethanol model.

Serum total homocysteine and hepatic homocysteine in the binge ethanol (A, B) and the chronic ethanol (C, D) study. Values are means ± SDs, n = 3 mice or 8~10 rats per group. Within each graph, * represents significance (*; $P < 0.05$) relative to the control group; # represents significance (#; $P < 0.05$) relative to the ethanol group. Statistical analysis was performed by using one-way ANOVA with Tukey's multiple-comparison procedure.

3.2. L-serine up-regulates SIRT1 activity

3.2.1. L-serine increases intracellular NAD^+ by lactate dehydrogenase and SIRT1 activity.

To investigate whether L-serine can increase NAD^+ and up-regulate SIRT1 activity, C2C12 myocytes which highly express SIRT1 and have active metabolic capacity were treated with L-serine. After 24 hr treatment, intracellular NAD^+ and the acetylation of PGC-1α was detected. Because PGC-1α is a substrate of SIRT1, PGC-1α can be deacetylated by the increasing activity of SIRT1. As a result, L-serine increased NAD^+ and deacetylated PGC-1α concentration-dependently which implies up-regulated SIRT1 activity (Figure 13).

To find how L-serine can increase NAD^+, lactate dehydrogenase (LDH) activity was blocked by sodium oxamate or si-*Ldh* transfection. LDH inhibition by both sodium oxamate and si-*Ldh* reversed L-serine induced increase in NAD^+ and SIRT1 activity (Figure 14).

These results showed that L-serine can increase intracellular NAD^+ by lactate dehydrogenase and SiRT1 activity.

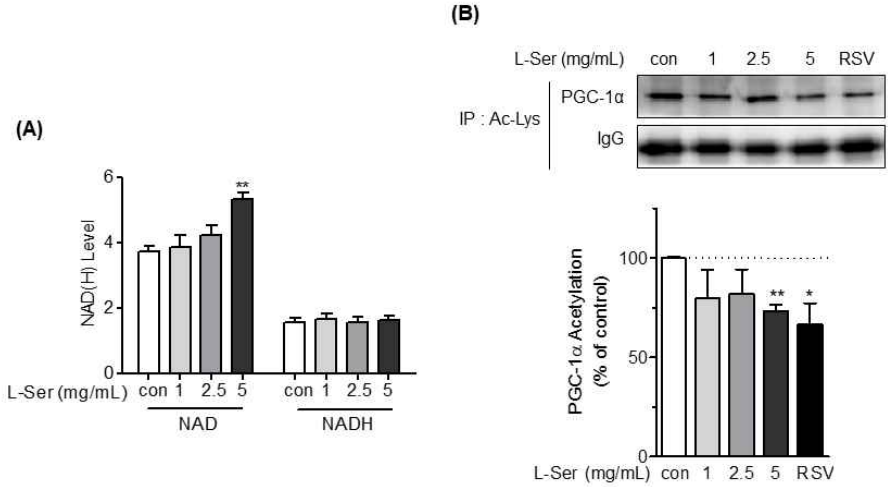

Figure 13. L-serine up-regulates intracellular NAD^+ and SIRT1 activity.

L-serine was treated at the indicated concentrations in C2C12 myotubes for 24 hr. Intracellular NAD^+ and NADH were measured (A). C2C12 myotubes were treated with L-serine (suggested concentrations) for 24 hr and 50 μM resveratrol (RSV) for 6 hr. Then, acetylation status of PGC-1α was measured using immunoprecipitation and quantification graph is suggested below (B). Values are means ± SDs, n = 3 of three independent experiments. * and ** represent significance (*; $P < 0.05$, **; $P < 0.01$) relative to the control group using one-way ANOVA with Dunnett's post tests.

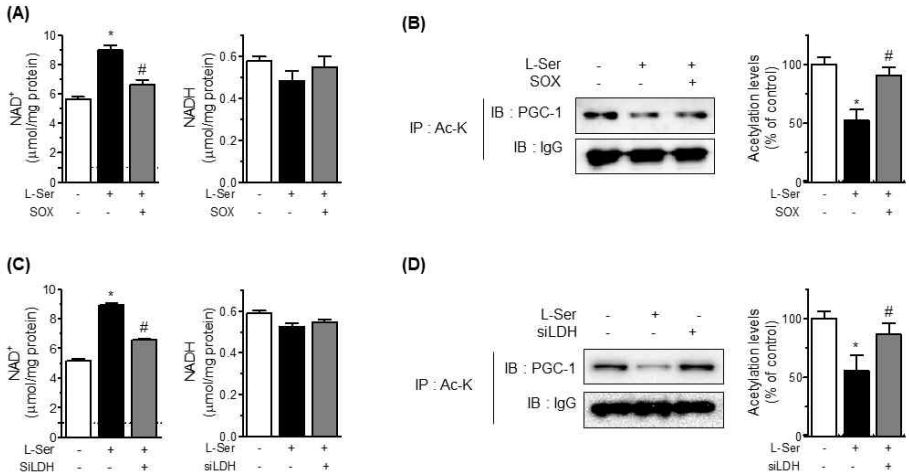

Figure 14. L-serine mediated increases in NAD$^+$ and SIRT1 activity are mediated by lactate dehydrogenase.

L-serine and sodium oxamate (SOX) were treated in C2C12 myotubes for 24 hr. Intracellular NAD$^+$ and NADH (A) and the acetylation status of PGC-1α (B) were measured. C2C12 myotubes were transfected with si-*Ldh* and 5 mg/mL L-serine was treated for 24 hr. Then, intracellular NAD$^+$ and NADH (C) and the acetylation status of PGC-1α was measured using immunoprecipitation (D). Values are means ± SDs, n = 3 of three independent experiments. * represents significance (*; $P < 0.05$) relative to the control and # represents significance (#; $P < 0.05$) relative to the L-serine treatment group using one-way ANOVA with Tukey's post tests.

3.2.2. L-serine up-regulates mitochondrial mass and function.

PGC-1α is a major regulator of mitochondrial biogenesis. Because increased deacetylation of PGC-1α by SIRT1 results in up-regulated PGC-1α activity, L-serine effect on the mitochondrial gene expression was confirmed by real-time PCR. *Cytochrome c, ATP synthase subunit β, and Tfam* gene expression were increased by L-serine and mitochondrial mass, which was detected by Mitotracker red, was also up-regulated. As a result, mitochondrial function was also improved which was detected by measuring intracellular ATP levels and oxygen consumption rate (Figure 15).

SIRT1 also has anti-steatotic effect by inhibiting fatty acid synthesis and increasing lipid β-oxidation. To find SIRT1 activating effect of L-serine on lipid β-oxidation, oleic acid-induced lipid accumulation and L-serine mediated oxygen consumption ratio were measured. As a result, L-serine concentration-dependently decreased oleic acid-induced intracellular triglyceride level and up-regulated oxygen consumption ratio (Figure 16).

SIRT1 is one of a key metabolic regulator and known to improve insulin resistance and fatty liver (Schenk et al., 2011; Colak et al., 2011). To identify whether L-serine has insulin sensitizing effect, in vitro model which uses palmitic acid as a insulin resistance inducer was used. Palmitic acid reduced the phosphorylation status of Akt and translocation of GLUT4, which is a major glucose transporter in muscle tissues. L-serine reversed the phosphorylation status of Akt and also increased GLUT4 membrane translocation (Figure 17). EX-527, which is known as a SIRT1 inhibitor, blocked L-serine induced phosphorylation of Akt.

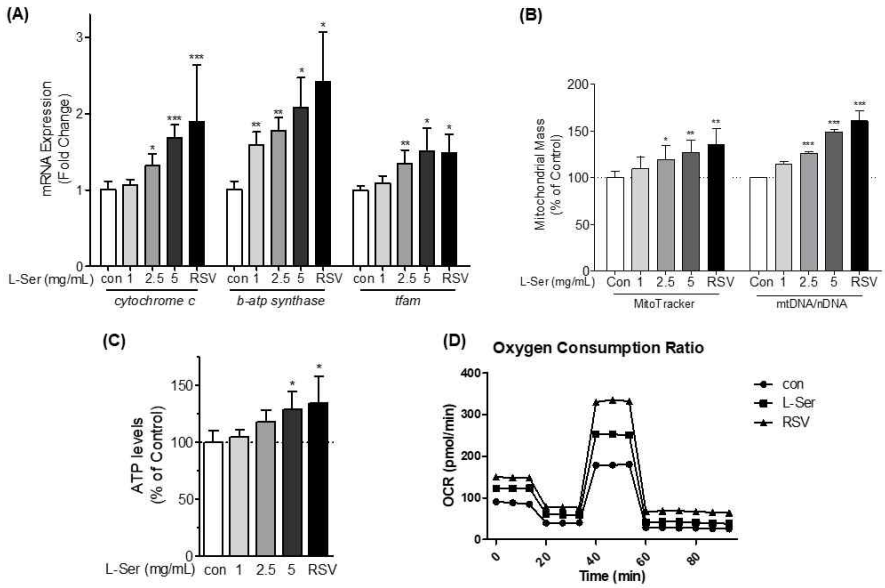

Figure 15. L-serine increases mitochondrial mass and function.

C2C12 myotubes were treated with L-serine at the indicated concentrations for 24 hr and 50 μM RSV for 6 hr. Total RNA was extracted from cells and mitochondrial gene expression was analyzed by real-time PCR (A). Mitochondrial mass was analyzed by Mitotracker red and mtDNA copy number (B). Mitochondrial function was measured by measuring intracellular ATP levels (C) and oxygen consumption ratio (OCR) (D). Values in are means ± SDs, n = 3 of three independent experiments. *, ** and *** represent significance (*; $P < 0.05$, **; $P < 0.01$, ***; $P < 0.001$) relative to the control group using one-way ANOVA with Dunnett's post tests.

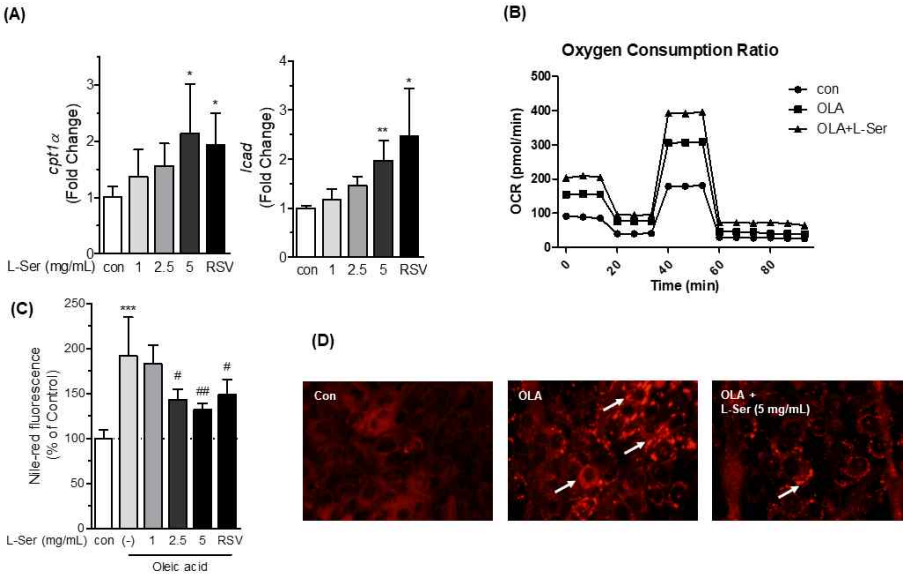

Figure 16. L-serine ameliorates oleic-acid induced lipid accumulation.

C2C12 myotubes were treated with indicated concentrations of L-serine for 24 hr and 50 uM resveratrol for 6 hr. Total RNA was extracted and *cpt1a* and *lcad* mRNA levels were measured by real-time PCR (A). C2C12 myotubes were treated with 250 uM oleic acid and 5 mg/mL L-serine and OCR was measured using Seahorse Bioscience XFp analyzer (B). C2C12 myotubes were treated with 250 uM oleic acid and indicated concentrations of L-serine and 50 uM resveratrol. Intracellular lipid droplets were quantitatively determined using nile red assay (C) and microscopic images were confirmed (D). Values in are means ± SDs, n = 3 of three independent experiments. *, ** and *** represent significance (*; $P < 0.05$, **; $P < 0.01$, ***; $P < 0.001$) relative to the control and #, and ## represent significance (#; $P < 0.05$, ##; $P < 0.01$) relative to the oleic acid group using one-way ANOVA with Tukey's post tests.

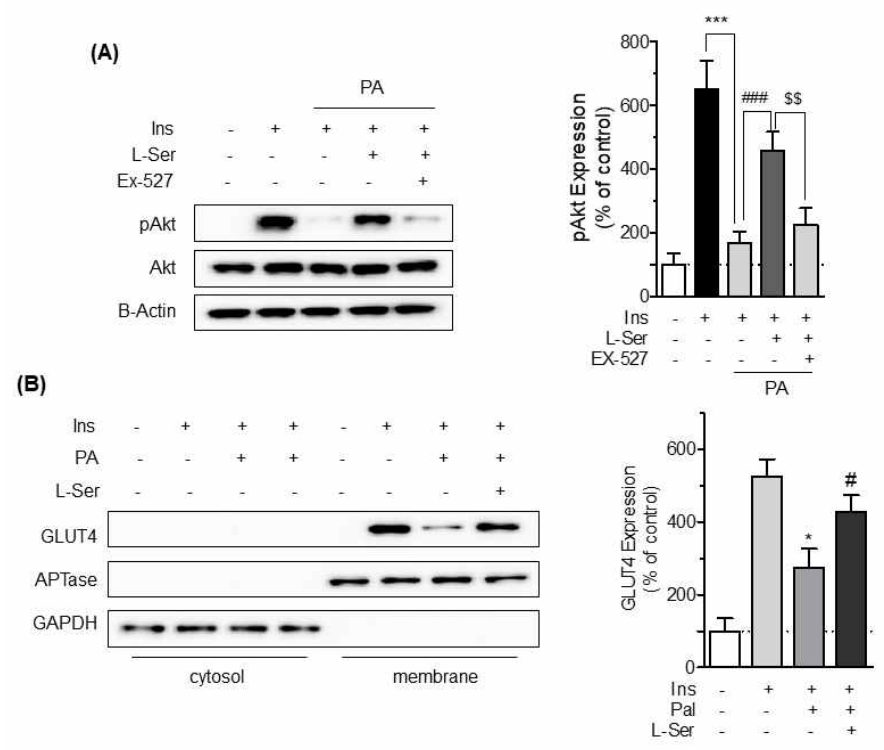

Figure 17. L-serine improved insulin resistance *in vitro*

C2C12 myoblasts were differentiated into myotubes and treated with 5 mg/mL L-serine in the absence or presence of EX-527 with 250 μM palmitic acid for 24 hr. After treatment, insulin (100 nM) was incubated for 20 minutes. Protein extracts were prepared from cell lysates and western blotting was performed to measure the levels of pAkt, Akt and B-Actin. Right panel shows the band densities determined using an image analysis system and expressed as percentages of the control (A). Total cell lysates were collected and subjected to subcellular fractionation as described in Materials and Methods. The protein levels of GLUT4, ATPase, and GAPDH were measured by western blotting. Right panel shows the band densities of GLUT4 in membrane fraction determined using an image analysis system and expressed as percentages of the control. Western blot images are representative of three independent experiments. Values are means ± SDs, n = 3 of three independent experiments. * and *** represent significance (*; $P < 0.05$, ***; $P < 0.001$) relative to the insulin group. #, and ### represent significance (#; $P < 0.05$, ###; $P < 0.001$) relative to the insulin+palmitate group. $$ represents significance ($$; P < 0.01). Statistical analysis was performed using one-way ANOVA with Tukey's post tests.

3.3. PHGDH, a rate-limiting enzyme in de novo serine synthesis, is down-regulated in fatty liver disease.

3.3.1. Hepatic L-serine synthesizing enzyme expression and L-serine level in vivo and in vitro disease model.

L-serine can be not only uptaken by dietary supply but also synthesized through de novo synthesis. To identify whether L-serine is decreased because of decreased de novo synthesizing L-serine in the liver, the expression of enzymes which are involved in de novo serine synthesis was investigated in the livers from 4 weeks of Lieber-DeCarli ethanol diet treated rats, 6 weeks of high-fat (HF) diet fed mice, and 4 weeks of methionine-choline deficient (MCD) diet fed mice. The expression of 3-phosphoglycerate dehydrogenase (PHGDH), which regulates the first step of L-serine synthesis, was significantly reduced in chronic ethanol, HF diet, and MCD diet induced fatty liver disease models (Figure 18). The down-regulated enzyme of L-serine synthesis enzyme results in the reduction of hepatic L-serine levels in Lieber-DeCarli ethanol diet-fed rats and HF diet-fed mice except MCD diet-fed mice (Figure 18).

PHGDH expression was also identified from in vitro model. Isolated hepatocytes were treated with ethanol or the mixture of free fatty acids (FFA; oleic acid:palmitic acid = 2:1). Ethanol and FFA treatment significantly decreased the mRNA and protein expression of PHGDH (Figure 19).

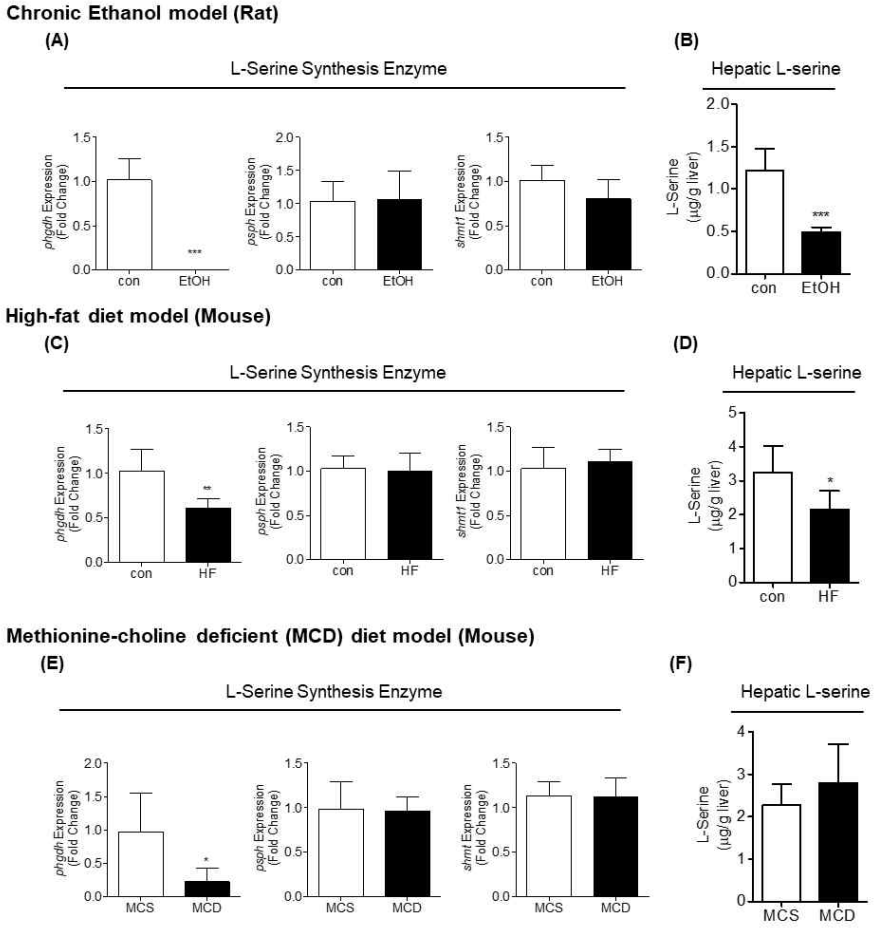

Figure 18. L-serine synthesizing enzyme, PHGDH expression and hepatic L-serine is decreased in pathological fatty liver model.

mRNA level of L-serine synthesis enzymes including *phgdh, psph, and shmt1* in the livers and hepatic L-serine were measured in the chronic ethanol study (A, B), HF diet study (C, D), and MCD diet study (E, F). Values are means ± SDs, n = 8 rats in chronic ethanol study, n = 8 mice in HF diet study, and n = 5 mice in MCD diet study per group. Within each graph, *, **, and *** represent significance (* ; $P < 0.05$, ** ; $P < 0.01$, *** ; $P < 0.001$) relative to the control group using student's *t*-test.

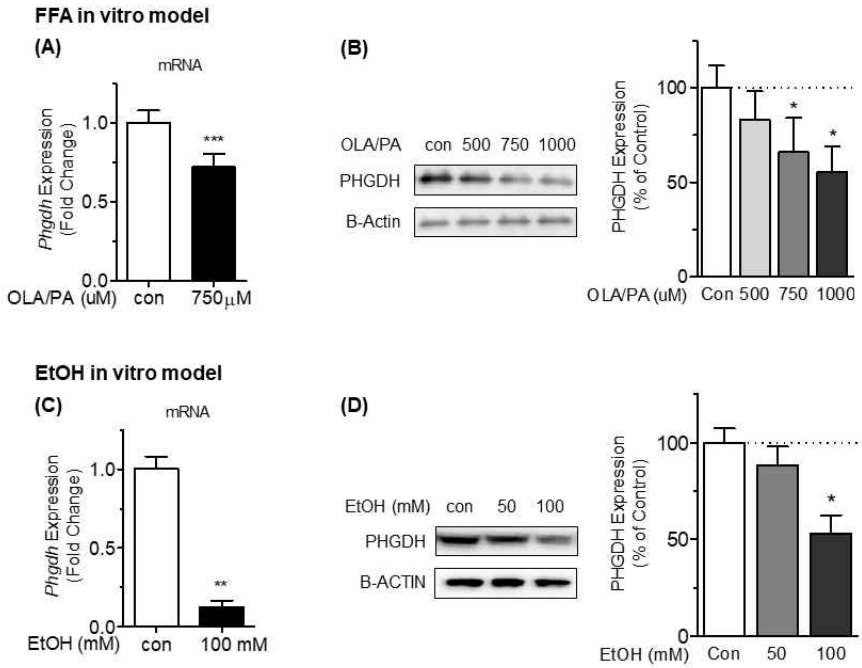

Figure 19. The expression of PHGDH was reduced by free fatty acid and ethanol treatment.

The mRNA level and protein expression of PHGDH in mouse primary hepatocytes were determined after 24 hr treatment of FFA (A, B) and ethanol (C, D). Values are means ± SDs of three independent experiments. Within each graph, *, ** and *** represent significance (* ; $P < 0.05$, ** ; $P < 0.01$, *** ; $P < 0.001$) relative to the control group using student's t-test in (A) and (C) and one-way ANOVA with Dunnett's post tests in (B) and (D).

3.3.2. Sphingolipids and ceramides level was affected in fatty liver disease.

L-Serine and palmitoyl CoA are condensed into sphinganine (SA) and L-serine deficiency was reported to elicit intracellular accumulation of cytotoxic deoxysphingolipids, including deoxysphinganine (doxSA), and deoxymethylsphinganine (doxmeSA) which are produced by palmitoyl CoA with alanine and glycine instead of L-serine (Esaki et al., 2015). To find whether L-serine deficiency in Phgdh-KO MEF cells leads to accumulate cytotoxic sphingolipids. As reported, doxSA and deoxysphingosine (doxSO) are increased by L-serine deficiency, but SA and SO (sphingosine) are decreased by L-serine deficiency (Figure 20).

These sphingolipids and ceramides are also analyzed in the livers from in vivo models. Deoxyceramide (doxCer) and deoxydihydroceramide (doxDHCer) which are abnormal form of ceramides, which are produced from doxSA, were increased in chronic ethanol model (Figure 21) implying correlation between decreased PHGDH function and increased abnormal ceramides. But in HF diet model, doxSA and doxCer level were decreased (Figure 22).

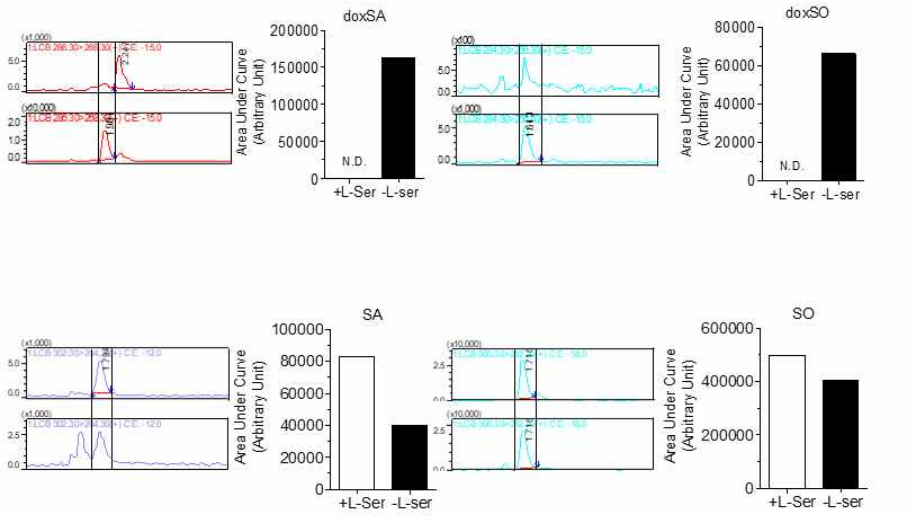

Figure 20. Deoxysphingolipids were increased in *Phgdh*-KO MEF cell.

Phgdh-KO MEF cells were incubated in L-serine sufficient control media or L-serine deficient media for 24 hr. After incubation, cell lysates were collected and doxSA (A), doxSO (B), SA (C), and SO (D) were analyzed by LC/MS. Chromatograms were presented at left side and area under the curve (AUC) were calculated on right panel.

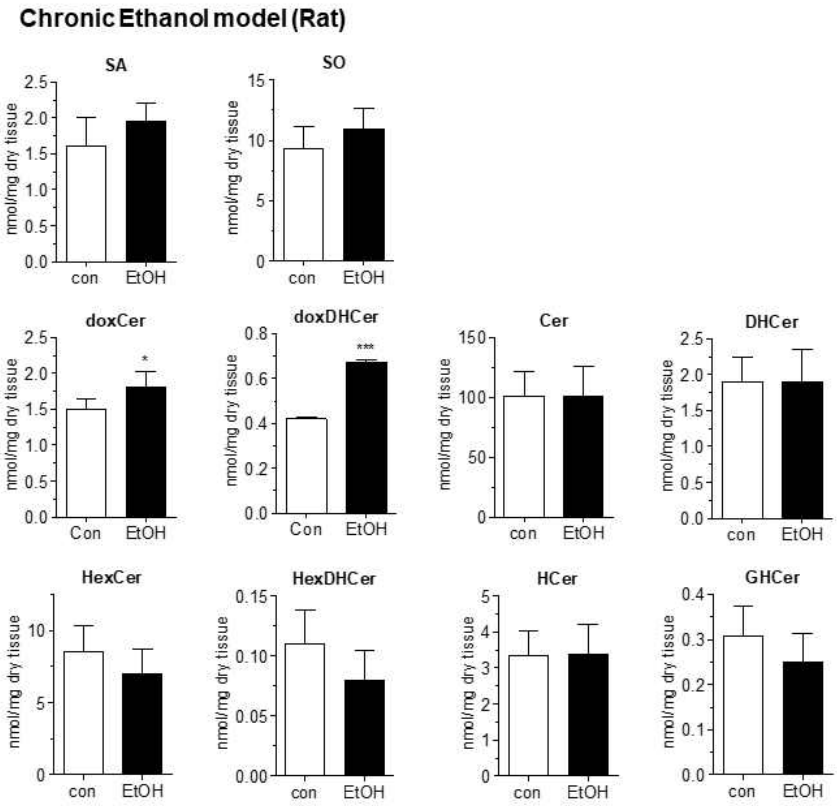

Figure 21. Chronic ethanol feeding increased deoxy-form of ceramides.

Sphingolipids (sphinganine (SA) and sphingosine (SO)) and Ceramides (deoxyceramide (doxCer), deoxydihydroceramide (doxDHCer), Ceramide (Cer), Dihydroceramide (DHCer), hexosylceramide (HexCer), hexosyldihydroceramide (HexDHCer), hydroxyceramide (HCer), and glucosylhydroxylceramide (GHCer)) were analyzed from the livers from chronic ethanol diet-fed rats. Values are means ± SDs, n = 8 rats per group. Within each graph, * and *** represent significance (* ; $P < 0.05$, *** ; $P < 0.001$) relative to the control group using student's t-test.

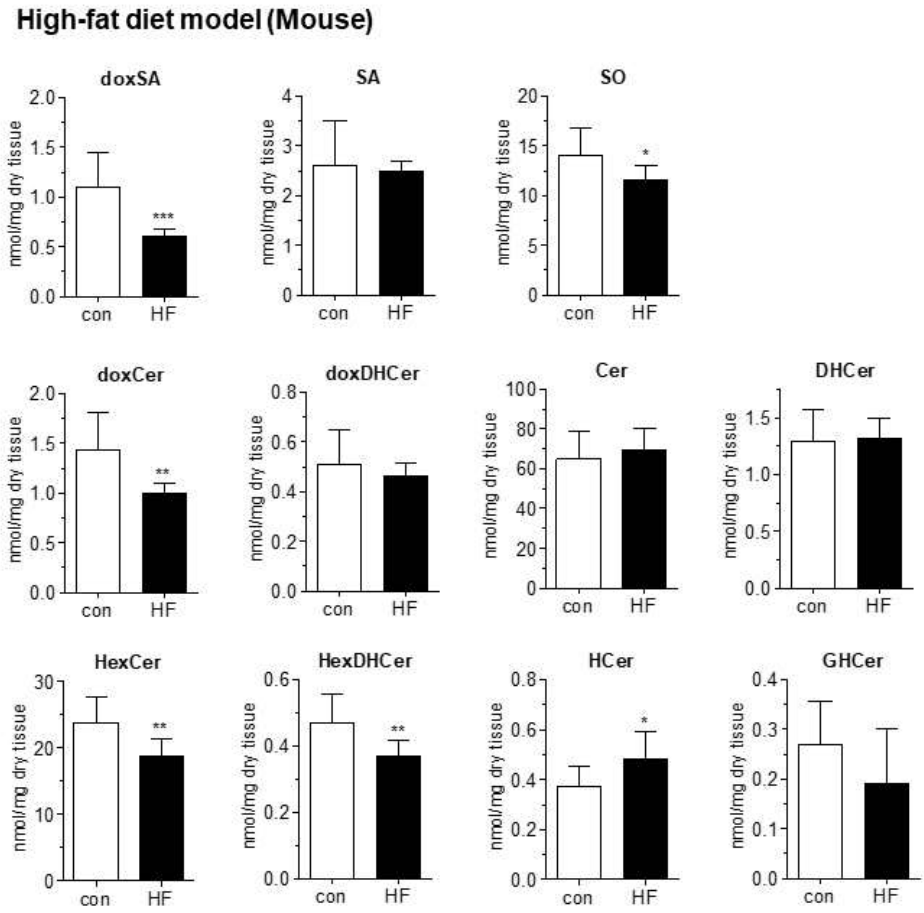

Figure 22. High-fat diet feeding decreased deoxy-form of sphingolipid and ceramide.

Sphingolipids (deoxysphinganine (doxSA), sphinganine (SA), and sphingosine (SO)) and Ceramides (deoxyceramide (doxCer), deoxydihydroceramide (doxDHCer), ceramide (Cer), dihydroceramide (DHCer), hexosylceramide (HexCer), hexosyldihydroceramide (HexDHCer), hydroxyceramide (HCer), and glucosylhydroxylceramide (GHCer)) were analyzed from the livers from HF diet-fed mice. Values are means ± SDs, n = 9-10 mice per group. Within each graph, *, **, and *** represent significance (* ; $P < 0.05$, ** ; $P < 0.01$, *** ; $P < 0.001$) relative to the control group using student's *t*-test.

3.3.3. Hepatic L-serine synthesizing enzyme expression and L-serine level in clinical patients.

To identify whether these in vitro and in vivo effects are shown clinically, first microarray data analysis was performed. GEO analysis showed that the expression of PHGDH in alcoholic steatohepatitis, non-alcoholic fatty liver patients and HBV-related non-alcoholic advanced fibrosis patients was significantly decreased (Figure 23).

And then, we measured the serum amino acid level of 20 control groups and 68 fatty liver disease patients. Serum L-serine was significantly reduced in fatty liver disease patients and the fat deposition analyzed by MRI was negatively correlated with serum L-serine level (Figure 24). The serum biomarkers of liver, kidney functions and glucose, lipid metabolism were also analyzed and some of these markers, including ALT and triglycerides are found to be negatively correlated with serum L-serine (Figure 25).

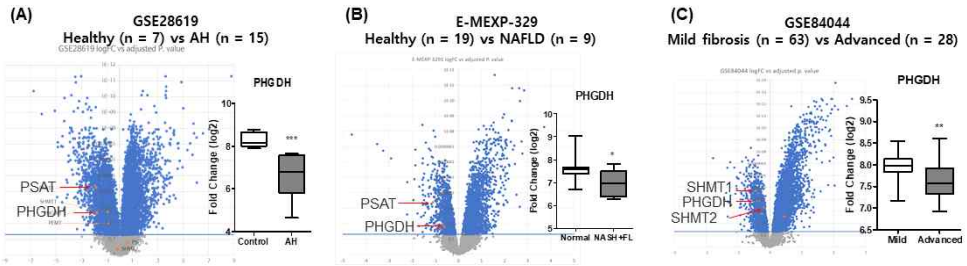

Figure 23. Microarray data analysis showed down-regulation of serine synthesis pathway in human fatty liver disease.

GEO dataset was analyzed to find statistical difference in the expression of serine synthesis pathway enzyme between healthy patients and fatty liver diseases patients. The volcano plot shows false discovery rate (FDR) adjusted P value versus log value for fold changes ($\log_2$FC) of gene enrichment. Genes associated with serine synthesis pathway are plotted in orange dots. Horizontal blue line indicates significance cut-off (Adjusted p value < 0.05). Right panel in (A), (B) and (C) shows fold change of *Phgdh* in each group. *, **, and *** represent significance (* ; P <0.05, ** ; P < 0.01, *** ; P <0.001).

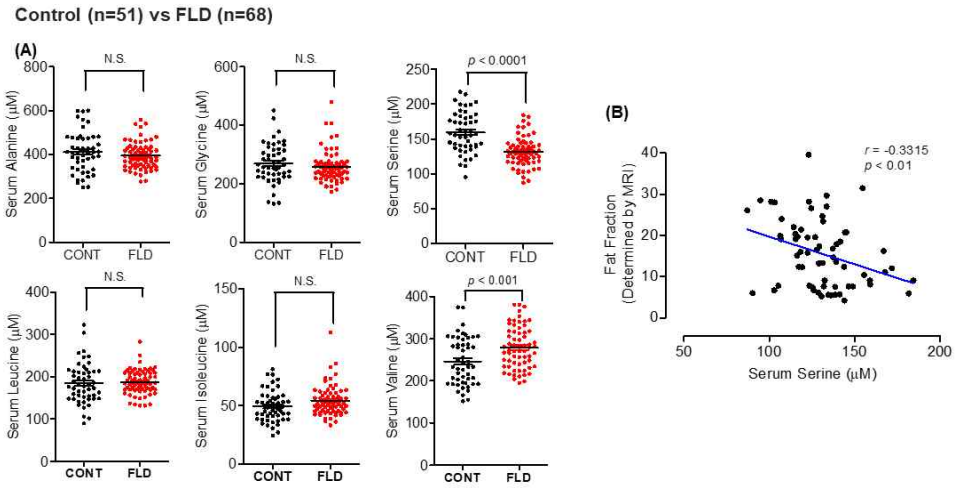

Figure 24. The serum L-serine was reduced in fatty liver disease patients and negatively correlated with fat fraction.

Serum amino acids were detected in 51 controls and 68 fatty liver disease patients (A). *P* value was suggested relative to the control group using student's *t*-test. Serum L-serine and MRI determined fat fraction were analyzed by correlation analysis (B). Pearson R value and *p* value were suggested.

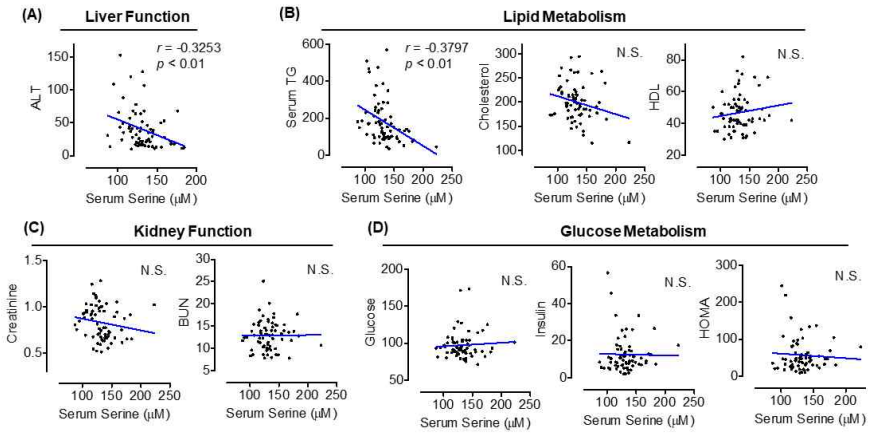

Figure 25. Serum L-serine is negatively correlated with serum ALT and TG in fatty liver disease patients.

The relationship between serum L-serine and several clinical biomarkers representing liver functions (A), lipid metabolism (B), kidney function (C) and glucose metabolism (D) was suggested by correlation analysis. Pearson R value and p value were suggested (N.S means not significant).

3.3.4. Up-regulation of L-serine and PHGDH function reverses lipid metabolism.

Because the lowered expression of PHGDH and synthesis of L-serine were confirmed in disease models and clinical patients, we assumed that FFA or L-serine deficiency may reduce L-serine level, and decreased L-serine may result in down-regulation of intracellular NAD^+. FFA and L-serine deficiency condition decreased NAD^+ and this effect was reversed by additional L-serine treatment (Figure 26). The deacetylation status of PGC-1α, implying SIRT1 activity, was decreased by L-serine deficient condition in PHGDH KO-MEF cells and the increased L-serine by transfection of PHGDH vector reversed this effect (Figure 26).

Then, the up-regulation of L-serine by amplification of PHGDH function on lipid metabolism in vitro disease models was also measured. The overexpression of PHGDH by genetic vector transfection in AML12 cells reversed the FFA-induced intracellular lipid accumulations (Figure 27). Genetic siRNA knockdown of PHGDH induced lipid accumulation and L-serine deficiency accelerated this effect. PHGDH overexpression reversed the TG accumulation in AML12 cells (Figure 27). The FFA also increased intracellular TG in primary hepatocytes and PHGDH gain of function by genetic transfection reversed that. Genetic knockout model using PHGDH knockout MEF showed that when L-serine was enough in media, there is no additional lipid accumulation, but when L-serine was depleted, PHGDH knockout induced about 2 fold TG levels. PHGDH overexpression reduced lipid accumulation to control level (Figure 27).

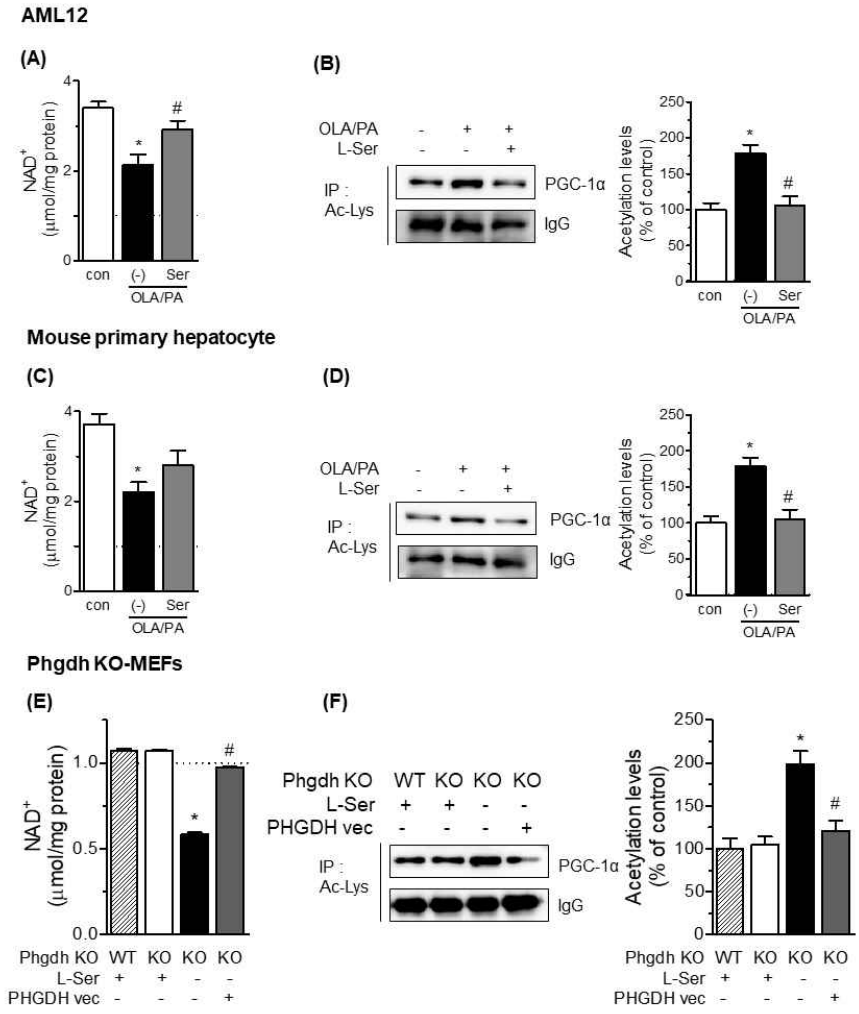

Figure 26. PHGDH loss of function or L-serine deficiency decreased intracellular NAD$^+$ and SIRT1 activity in AML12, mouse primary hepatocytes, and PHGDH-KO MEF cells.

750 uM of FFA and 5 mg/mL L-serine were treated and intracellular NAD$^+$ and acetylation status of PGC-1α were measured in AML12 (A, B) and primary hepatocytes (C, D). PHGDH WT and KO-MEF cells were cultured in L-serine sufficient or deficient media and PHGDH expression vector was transfected. After treatment, intracellular NAD$^+$ and acetylation status of PGC-1α (E, F) were measured. Values are means ± SDs, n = 3 of three independent experiments. Within each graph, labeled means without a common letter differ ($P < 0.05$). Statistical analysis was performed by using one-way ANOVA with Tukey's multiple-comparison procedure.

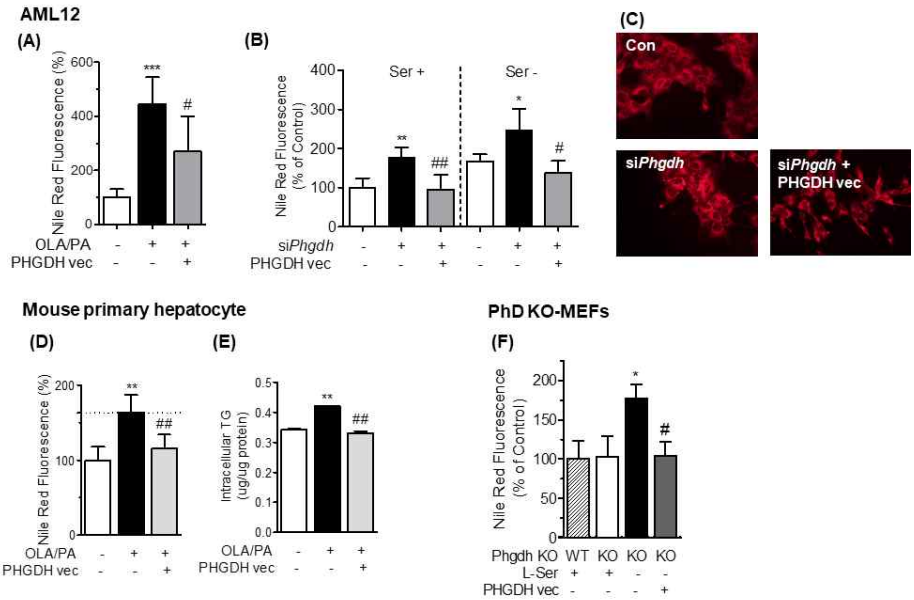

Figure 27. Increased L-serine synthesis by up-regulating PHGDH reversed lipid accumulation in FFA treatment or L-serine depleted condition.

AML12 cells were incubated with 750 uM FFA or si-*Phgdh* and transfected with PHGDH expression vector in L-serine sufficient or deficient media. Intracellular TG was measured by nile-red assay (A, B). Microscopic images of the nile red staining of AML12 cells in serine depletion condition were suggested (C). 750 uM FFA was treated in mouse primary hepatocytes and PHGDH expression vector was transfected. After treatment, intracellular TG was measured by nile red staining (D) and TG extraction and quantification (E). PHGDH wild-type (WT) MEF cells were cultured in L-serine sufficient media and knock-out (KO) MEF cells were cultured in L-serine sufficient or deficient media. PHGDH overexpression vector was transfected and nile red assay was performed (F). Values are means ± SDs, n = 3 of three independent experiments. Within each graph, *, **, and *** represent significance (*; $P < 0.05$, **; $P < 0.01$, ***; $P < 0.001$) relative to the control; # and ## represent significance (#; $P < 0.05$, ##; $P < 0.01$) relative to its left bar. Statistical analysis was performed by using one-way ANOVA with Tukey's multiple-comparison procedure.

3.4. Regulation of PHGDH is mediated by NRF2.

3.4.1. PHGDH is not regulated by epigenetic modification.

To identify the mechanism of PHGDH regulation, epigenetic assays were performed. First, PHGDH promoter methylation was assessed. Because the promoter methylation is known to repress the gene expression, the methylation status of the PHGDH promoter was measured by DNA bisulfite conversion. But in vitro FFA and ethanol treatment decreased the methylation status and there were no changes in the promoter methylation in vivo models (Figure 28).

Next, histone methylation was also investigated. The global histone H3 and H4 acetylation assay showed there were no changes in histone acetylation in vitro and in vivo disease models (Figure 29). Trichostatin A (TSA) was also used to investigate histone methylation and PHGDH expression, but TSA did not affect the mRNA and protein level of PHGDH (Figure 30).

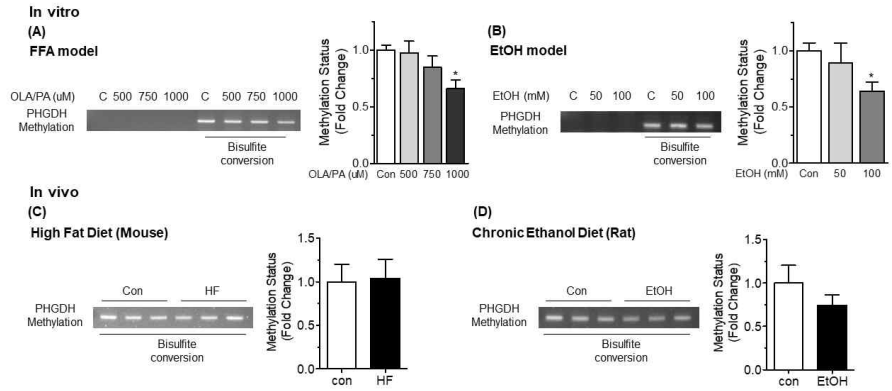

Figure 28. Promoter methylation of PHGDH is decreased by FFA and ethanol in vitro and not affected by HF diet or chronic ethanol diet.

AML12 cells were treated with indicated concentrations of FFA (A) or ethanol (B) for 24 hr and the livers from HF diet fed mice (C) and chronic Lieber-DeCarli ethanol diet fed rats (D) were prepared for DNA extraction. After bisulfite conversion, DNA was amplified by semi-quantitative PCR. Graphs show the quantification of intensities of DNA bands. Values are means ± SDs, n = 3 of three independent experiments in vitro or n = 3 of mice or rats in vivo. Within each graph, * represents significance (*; $P < 0.05$) relative to the control. Statistical analysis was performed by using one-way ANOVA with Dunnett's post-test in vitro and by using student's *t*-test in vivo.

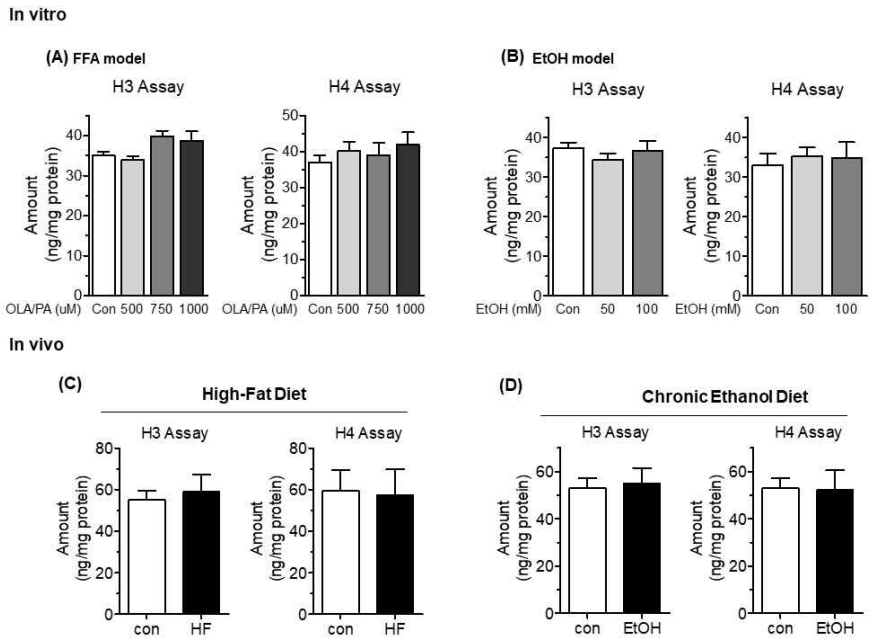

Figure 29. Global hitone H3 and H4 acetylation were not affected in pathological models.

AML12 cell pellets treated with indicated concentrations of FFA (A), ethanol (B) and the livers from HF diet fed mice (C), chronically Lieber-DeCarli ethanol diet fed rats (D) were used to measure global H3 and H4 acetylation. In each graph, values are means ± SDs, n = 3 of three independent experiments (A, B) or n = 8 mice or rats (C, D). Statistical analysis was performed by using one-way ANOVA followed by Dunnett's post-test (A, B) or by using student's *t*-test (C, D).

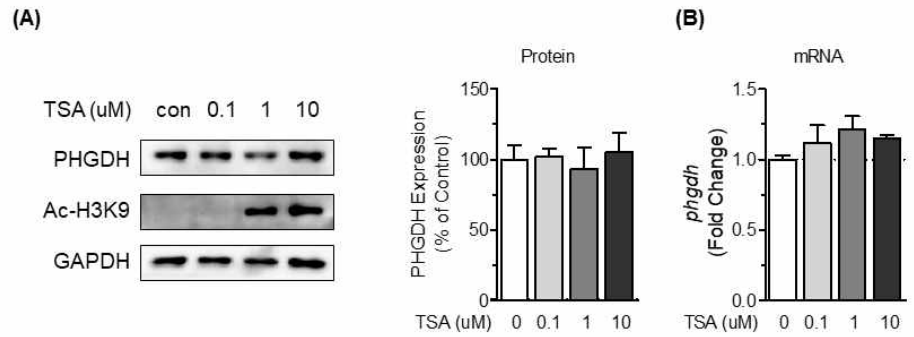

Figure 30. The expression of PHGDH is not affected by trichostatin A, HDAC inhibitor.

AML12 cells were treated with indicated concentrations of trichostatin A (TSA) for 24 hr. Protein and mRNA were extracted from cell pellets. PHGDH and H3K9 histone acetylation were detected by western blot (A) and *Phgdh* mRNA expression was measured by qRT-PCR (B). Values are means ± SDs, n = 3 of three independent experiments (A, B) or n = 8 mice or rats (C, D). Statistical analysis was performed by using one-way ANOVA followed by Dunnett's post-test.

3.4.2. PHGDH is regulated by NRF2.

DeNicola et al. reported that NRF2 positively regulates L-serine biosynthesis through the up-regulation of enzymes involved in de novo serine synthesis. Adenoviral transduction of dominant negative form of NRF2 (DN-NRF2) or overexpression of NRF2 decreased or increased PHGDH expression, respectively (Figure 31).

To find whether NRF2 is associated with down-regulated PHGDH in pathological models. The expression of NRF2 is measured in vitro FFA and ethanol model and in vivo HF diet and chronic ethanol diet model. Figure 32. showed that not only in vitro FFA and ethanol treatment decreased NRF2 protein level, but also in vivo HF diet and chronic ethanol diet reduced NRF2 expression.

As NRF2 protein stability can be regulated by ubiquitination, we confirmed NRF2 protein expression with treatment of tert-butylhydroquinone (tBHQ) which is used as a NRF2 activator or proteasome inhibitor, MG132. FFA increased the ubiquitination of NRF2 and tBHQ and MG132 teatment reversed these effects (Figure 33).

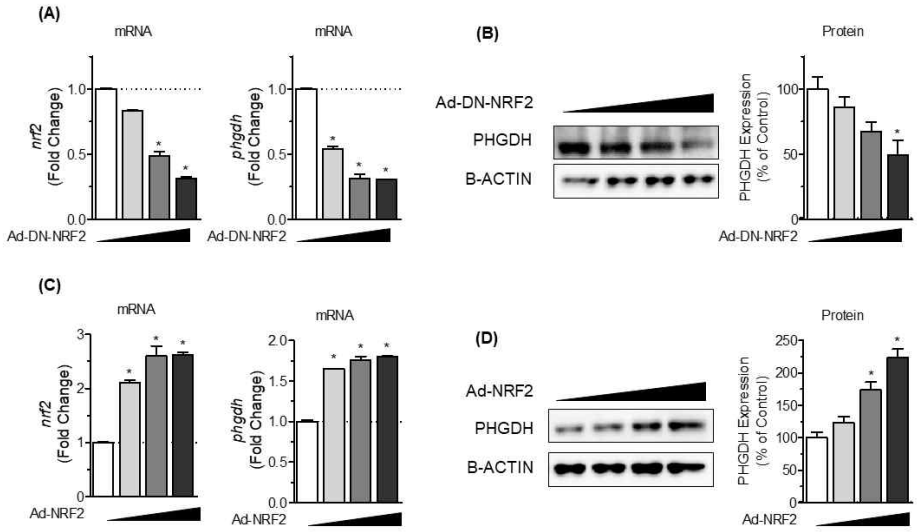

Figure 31. NRF2 positively regulates PHGDH at transcriptional and translational level.

AML12 cells were transducted with adenoviral dominant negative (DN)-NRF2 (A, B) or NRF2 (C, D) for 24 hr After transfection, cells were collected and subjected to PCR or western blot for NRF2 and PHGDH expression. Values are means ± SDs, n = 3 of three independent experiments. Within each graph, * represents significance (*; $P < 0.05$) relative to the control. Statistical analysis was performed by using one-way ANOVA followed by Dunnett's post-test.

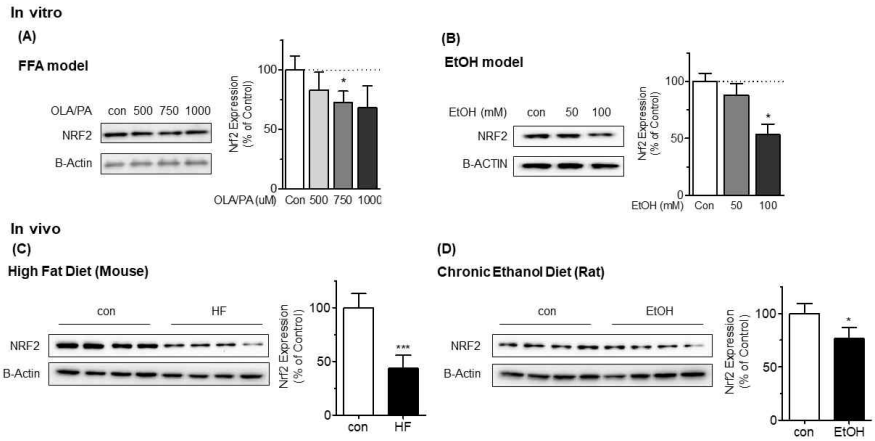

Figure 32. NRF2 protein expression is down-regulated in pathological models in vitro and in vivo.

AML12 cells treated with indicated concentrations of FFA (A), ethanol (B) and the livers from HF diet fed mice (C), chronically Lieber-DeCarli ethanol diet fed rats (D) were prepared to measure NRF2 protein expression. In each graph, values are means ± SDs, n = 3 of three independent experiments (A, B) or n = 4 mice or rats (C, D). Within each graph, * and *** represent significance (*; $P < 0.05$, ***; $P < 0.001$) relative to the control. Statistical analysis was performed by using one-way ANOVA followed by Dunnett's post-test (A, B) or by using student's *t*-test (C, D).

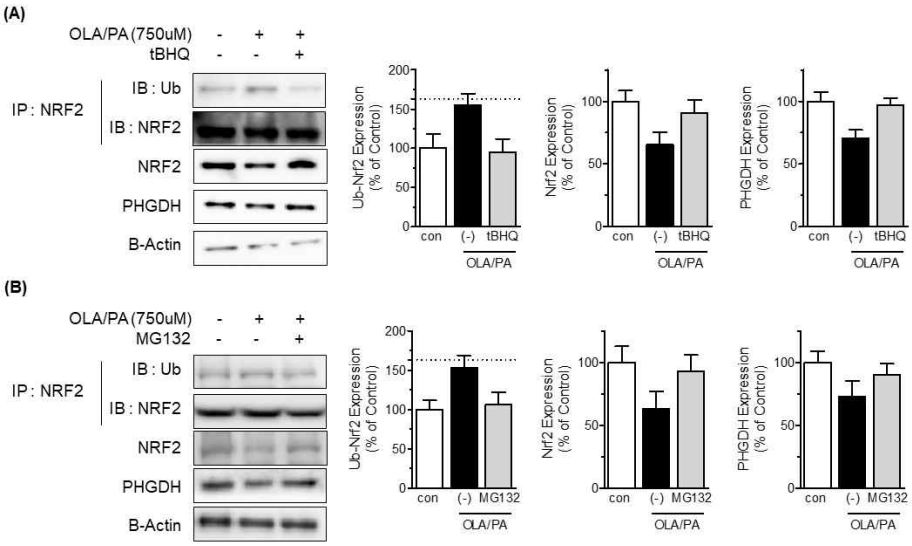

Figure 33. Increasing the stability of NRF2 reversed FFA-induced PHGDH down-regulation.

AML12 cells were treated with FFA with or without tBHQ (A) and MG132 (B). After 24 hr treatment, cells were centrifuged and subjected to immunoprecipitation for detecting ubiquitination of NRF2 and western blot for measuring NRF2 and PHGDH expression. Right panels shows the quantification of ubiquitination of NRF2, expression of NRF and PHGDH which are normalized to B-Actin. In each graph, values are means ± SDs, n = 2 of two independent experiments.

IV. Discussion

L-Serine is a non-essential amino acid which makes up dietary proteins, but plays various roles in cellular metabolism including biosynthesis of nucleotides, other amino acids, and sphingolipids.

One of the mechanisms of alcoholic fatty liver is a disturbance in hepatic sulfur-amino acid metabolism, leading to high homocysteine concentrations (Ji et al., 2003). We first demonstrated that the natural amino acid L-serine ameliorated alcoholic fatty liver by lowering homocysteine concentrations. L-Serine reduced homocysteine and lipid accumulation by acting on MS and CβS which are important homocysteine metabolizing enzymes in livers. By studying L-serine and homocysteine metabolism, we could assume that L-serine may have potential for treatment of hyperhomocysteinemia and fatty liver.

In our study, L-serine effect on serum homocysteine showed difference between mice and rats. Shinohara et al. (2010) reported species difference between rats and mice in which ethanol induces hyperhomocysteinemia. Rats were reported to more resistant to ethanol-induced increase in serum homocysteine and fatty liver. Our results also showed similar results and L-serine effect lowering serum homocysteine was observed only in mice (Sim et al., 2015). L-serine effect of improving steatosis in rats were identified by analyzing other sulfur amino acid metabolites in the liver. Our data in chronic ethanol study found that L-serine increased hepatic SAM without affecting SAH levels and GSH contents (Table 3). SAM participates into various biological reactions as a methyl donor and impaired SAM/SAH ratio leads to develop fatty liver by down-regulating VLDL secretion (Kharbanda et al., 2007 and 2012). Therefore, normalized SAM/SAH ratio by L-serine may be an important mechanism improving alcoholic

steatosis in rats.

We found that L-serine mediated homocysteine metabolism through the regulation of MS and CβS enzyme expression in binge ethanol study. Because homocysteine metabolism can not only be affected by metabolizing enzyme expression, but also the activity of the enzyme, we measured enzyme activity of MS and CβS. L-serine did not affect the enzyme activity in both binge and chronic ethanol study. The mechanism which induces the expression of the enzymes by L-serine needs to be studied.

The effect of L-serine improving fatty liver was mediated not only by homocysteine metabolism but also by regulating SIRT1 activity. L-Serine increased intracellular NAD^+ by the action of LDH. Several amino acids are reported to modulate SIRT1 activity. Leucine, which is an essential amino acid, was reported to increase SIRT1 mRNA and protein expression in C57BL/6 mice. Leucine increased nicotinamide phosphoribosyltransferase (NAMPT) and SIRT1 expression (Koning et al., 2003). Leucine also mimicked the calorie restriction effect by lowering the activation energy for NAD^+ of SIRT1 (Lei et al., 2005). Another amino acid, tryptophan is reported to be associated with SIRT1 activity. When the kynurenine pathway which is the principle route of tryptophan metabolism producing NAD^+ is inhibited, SIRT1 activity was decreased (Brady et al., 2012).

In our study, L-serine altered intracellular redox state, which can be measured by NAD^+/NADH ratio through LDH. Lactic and pyruvic acids interact through the actions of the cytosolic near-equilibrium LDH isozymes, which reflect the cytosolic NAD^+/NADH ratios in cytosol. There are reports of mitochondrial LDH activity (Brooks, 2009) and therefore potential for coupling of the NAD^+/NADH ratios trigger several intracellular responses, including expression of genes by modification of histone deacetylases, which profoundly affect the

regulation of protein synthesis. To identify L-serine mediated regulation of redox state, pyruvate and lactate levels are needed to measured and further studies about changed redox state should be performed including glycolysis.

L-Serine is also reported to be a natural ligand and allosteric activator of pyruvate kinase M2 (PKM2) (Chaneton et al., 2012). L-serine bound to and activate human PKM2 and following serine deprivation, PKM2 activity in cells is reduced. This reduction in PKM2 activity shifts cells to a fuel-efficient mode where more pyruvate is diverted to the mitochondria and more glucose derived carbon is channelled into serine biosynthesis to support cell proliferation. Although PKM2 is the predominant isoform in cancer cells (Christofk et al., 2008; Altenberg and Greulich, 2004) and has low basal enzymatic activity compared to the constitutively active splice-variant PKM1 (Mazurek et al., 2005). Therefore, down-regulated intracellular L-serine in disease models may result in PKM2 activation and L-serine effect on PKM2 activity including increased glycolysis further needs to be elucidated.

Reduced L-serine levels in alcoholic fatty liver can be explained by PHGDH, which regulates de novo L-serine synthesis, and it was found to be decreased in chronic ethanol diet, high-fat diet, and MCD diet models. Decreased PHGDH expression resulted in reduced L-serine concentrations in the livers except in MCD diet model. This may result from different diet composition, period and so on. In vitro pathological models also showed decreased PHGDH expression and PHGDH gain of function reversed this effect by up-regulating intracellular NAD^+ and SIRT1 activity by increased L-serine.

To find the correlation between L-serine level and fatty liver disease status, hepatic L-serine was investigated in animal studies and serum L-serine was measured in human studies. Although both liver and

serum L-serine levels were correlated to the fatty liver disease status, additional serum amino acid analysis in animal studies can support the correlation between L-serine and fatty liver disease.

Esaki et al., reported that deprivation of external L-serine leads to the generation of abnormal sphingolipids, 1-deoxysphingolipids (doxSLs), including doxSA in mouse embryonic fibroblasts lacking PHGDH (PHGDH KO-MEFs) (Esaki et al., 2015). Furthermore, it is reported that human diabetics show significant increases in deoxyshpinganine (Bertea et al., 2010; Othman et al., 2012). So we detected the sphingolipids in the livers from Lieber-DeCarli ethanol diet-fed rats and high-fat diet-fed mice. In ethanol study, ethanol-fed rats showed increased doxCer and doxDHCer, which are produced by palmitoyl-CoA and alanine conjugation instead of L-serine. But high-fat diet fed mice showed different patterns of sphingolipids level. DoxSA and DoxCer were decreased by high-fat diet. Although a direct causative role between ethanol diet and high-fat diet on lipid profile is unclear, we hypothesized that different composition of diet may affect SPT activity on different substrate. Because SPT exists in a complex, composed of three distinct subunits (SPTLC1, STPLC2 and SPTLC3) (Hornemann et al., 2007) and interacts with other proteins that regulated activity of the enzyme (Han et al., 2010). Further studies about sphingolipid profile of high fat diet in vivo study or human obese patients need to be elucidated.

Regulation of PHGDH is mediated by various molecules (Bollig-Fischer et al., 2011; Jun et al., 2008; Ding et al., 2013; Ou et al., 2015; DeNicola et al., 2015). One of the mediator focused in this study is nuclear factor erythroid 2-related factor 2 (NRF2). NRF2 is one of a major regulator of cytoprotective response against reactive oxygen species (ROS) (Kansanen et al., 2012). In resting state, NRF2 binds to two Kelch ECH associating protein 1 (Keap1) molecules and

is ubiquitinated by the Cul3-based E3 ligase. The ubiquitination of NRF2 leads to degradation by the proteasome (Kansanen et al., 2009). Under oxidative condition, the cysteine residue of Keap1 is modified and ubiquitination of NRF2 is inhibited by dissociation of the Cul3-based E3 ligase complex. In this study, PHGDH is down-regulated by FFA or ethanol treatment and NRF2 activator tBHQ or proteasome inhibitor MG132 reversed the down-regulation of NRF2 and PHGDH. Although FFA and ethanol are reported to induce oxidative stress (Cui et al., 2016; Shi et al., 2016), Shi et al. reported that NRF2 is reduced in total protein level and nuclear accumulation by ethanol treatment. Because NRF2-Keap1 pathway can be regulated by various mechanisms including Keap1 mutation (Mitsuishi et al., 2012), hypermethylation of Keap1 promoter (Hanada et al., 2012; Zhang et al., 2010), and accumulation of disruptor proteins including p62 and p21 (Ma and He, 2012), further study is needed to NRF2-mediated PHGDH regulation in vitro and in vivo disease models.

In conclusion, L-serine ameliorates fatty liver by participating in homocysteine metabolism and up-regulating SIRT1 activity by increasing intracellular NAD^+ pool. Reduced L-serine is mediated by down-regulated PHGDH experssion in various in vitro and in vivo disease models. PHGDH expression is regulated by NRF2 which regulates PHGDH positively at transcriptional and translational level. This study showed that L-serine has a potential developed as a fatty liver disease therapeutics and L-serine synthesizing enzyme, PHGDH can be used as a therapeutic target for fatty liver disease.

V. Conclusion

The result of the current thesis can be summarized as follows:

1. L-serine ameliorates alcoholic fatty liver in vitro and in vivo. And L-serine showed these effects through up-regulating homocysteine catabolism via MS and CβS activity.

2. L-serine increases intracellular NAD^+ by the action of lactate dehydrogenase and SIRT1 activity. L-serine mediated increase in SIRT1 activity resulted in mitochondrial mass and function by PGC-1 α. L-serine also reversed oleaic acid-induced intracellular TG accumulation by increasing lipid β-oxidation and palmitic acid-induced insulin resistance in vitro.

3. PHGDH, which is a rate-limiting step in de novo serine synthesis, expression was decreased in various in vitro and in vivo disease model. GEO analysis also showed that human fatty liver disease patients showed reduced expression of PHGDH and serum from human fatty liver disease patients showed that L-serine is negatively correlated with liver fat fraction and biomarkers of liver function and lipid metabolism, such as ALT and TG.

4. NRF2 is identified as a PHGDH regulator in vitro and in vivo model. studied by focusing its expression and protein stability. NRF2 is found to positively regulate PHGDH at transcriptional and translational level. Increasing NRF2 stability reversed free fatty

acid-induced PHGDH down-regulation.

Taken together, PHGDH plays an important role synthesizing L-serine in pathological liver state. This study showed that PHGDH can be used as a therapeutic target for hepatosteatosis and L-serine has a potential for curing fatty liver disease.

VI. Abbreviations

3-Phosphoglycerate dehydrogenase (PHGDH); 5-Methyltetrahydrofolate (5-methylTHF); Alanine aminotransferase (ALT); Alcoholic fatty liver disease (ALD); Aspartate aminotransferase (AST); Betaine homocysteine methyltransferase (BHMT);
Chemoattractant protein (MCP); Cystathionine β synthase (CβS); Deoxyceramide (DoxCer); Deoxydihydroceramide (DoxDHCer); Deoxymethylsphinganine (DoxmeSA);
Deoxysphinganine (DoxSA); Deoxysphingosine (DoxSO); Dulbacco's modified phosphate-buffered saline (DPBS); Endoplasmic reticulum (ER); Fatty acid transport protein (FATP); Free fatty acids (FFA); Glucose-regulated protein 78 (GRP78); Glutathione (GSH); High-fat (HF); Human epideral growth factor receptor 2 (HER2);
Interleukin (IL); Knock-out (KO); Lactate dehydrogenase (LDH); Methionine-choline deficient (MCD); Methionine synthase (MS); Nonalcoholic fatty liver disease (NAFLD); Non-small cell lung cancer (NSCLC); Nuclear factor like 2 (NRF2); Nuclear transcription factor Y (NF-Y); Peroxisome proliferator-activated receptor-α (PPARα); Peroxisome proliferator activated receptor ɣ coactivator-1 α (PGC-1α); Phosphatidylethanolaine methyltransferase (PEMT); Phosphoserine aminotransferase 1 (PSAT-1); Phosphoserine phosphatase (PSPH); Protein kinase RNA-like ER kinase (PERK); Quantitative Real-time Polymerase Chain Reaction (qRT-PCR); S-adenosylmethionine (SAM); S-adenosyltransferase (MAT); Serine Palmitoyltransferase (SPT); Specificity protein 1 (Sp1); Sphinganine (SA); Sphingosine (SO); Sterol regulatory element binding protein (SREBP); Transforming growth factor (TGF); Triglyceride (TG)

VII. References

Ahn J, Cho I, Kim S, Kwon D, Ha T. Dietary resveratrol alters lipid metabolism-related gene expression of mice on an atherogenic diet. *J Hepatol.* 2008;49:1019-1028.

Altenberg B, Greulich KO. Genes of glycolysis are ubiquitously overexpressed in 24 cancer classes. *Genomics*. 2004;84:1014-1020.

Baur JA, Pearson KJ, Price NL, Jamieson HA, Lerin C, Kalra A et al. Resveratrol improves health and survival of mice on a high-calorie diet. *Nature.* 2006;444:337-342.

Beroukhim R, Mermel CH, Porter D, Wei G, Raychaudhuri S, Donovan J et al. The landscape of somatic copy-number alteration across human cancers. *Nature.* 2010;463:899-905.

Bertea M, Rütti MF, Othman A, Marti-Jaun J, Hersberger M, von Eckardstein A et al. Deoxysphingoid bases as plasma markers in diabetes mellitus. *Lipids Health Dis.* 2010;9:84.

Björck J, Hellgren M, Råstam L, Lindblad U. Associations between serum insulin and homocysteine in a Swedish population-a potential link between the metabolic syndrome and hyperhomocysteinemia: the Skaraborg project. *Metabolism.* 2006;55:1007-1013.

Bollig-Fischer A, Dewey TG, Ethier SP. Oncogene activation induces metabolic transformation resulting in insulin-independence in human breast cancer cells. *PLoS One.* 2011;6(3):e17959.

Braidy N, Guillemin GJ, Grant R. Effects of Kynurenine Pathway Inhibition on NAD Metabolism and Cell Viability in Human Primary Astrocytes and Neurons. *Int J Tryptophan Res.* 2011;4:29-37.

Brooks GA. Cell-cell and intracellular lactate shuttles. *J Physiol.* 2009;587(Pt 23):5591-5600.

Chaneton B, Hillmann P, Zheng L, Martin ACL, Maddocks ODK, Chokkathukalam A et al. Serine is a natural ligand and allosteric activator of pyruvate kinase M2. *Nature.* 2012;491:458-462.

Chaudhary N, Pfluger PT. Metabolic benefits from Sirt1 and Sirt1 activators. *Curr Opin Clin Nutr Metab Care.* 2009;12:431-437.

Christofk HR, Vander Heiden MG, Harris MH, Ramanathan A, Gerszten RE, Wei R et al. The M2 splice isoform of pyruvate kinase is important for cancer metabolism and tumour growth. *Nature.* 2008;452:230-233.

Clarke R, Daly L, Robinson K, Naughten E, Cahalane S, Fowler B et al. Hyperhomocysteinemia: an independent risk factor for vascular disease. *N Engl J Med.* 1991;324:1149-1155.

Cohen HY, Miller C, Bitterman KJ, Wall NR, Hekking B, Kessler B et al. Calorie restriction promotes mammalian cell survival by inducing the SIRT1 deacetylase. *Science.* 2004;305:390-392.

Cohen JC, Horton JD, Hobbs HH. Human fatty liver disease: old questions and new insights. *Science.* 2011;332:1519-1523.

Colak Y, Ozturk O, Senates E, Tuncer I, Yorulmaz E, Adali G et al. SIRT1 as a potential therapeutic target for treatment of nonalcoholic fatty liver disease. *Med Sci Monit.* 2011;17:HY5-9.

Cui Y, Wang Q, Yi X, Zhang X. Effects of Fatty Acids on CYP2A5 and NRF2 Expression in Mouse Primary Hepatocytes. *Biochem Genet.* 2016;54:29-40.

Cylwik B, Chrostek L, Daniluk M, Supronowicz Z, Szmitkowski M. Relationship between plasma folate and homocysteine concentrations in alcoholics according to liver enzyme activity. *J Nutr Sci Vitaminol (Tokyo).* 2009;55:439-441.

Delmas D, Jannin B, Latruffe N. Resveratrol: preventing properties against vascular alterations and ageing. *Mol Nutr Food Res.* 2005;49:377-395.

DeNicola GM, Chen PH, Mullarky E, Sudderth JA, Hu Z, Wu D et al. NRF2 regulates serine biosynthesis in non-small cell lung cancer. *Nat Genet.* 2015;47:1475-1481.

Ding J, Li T, Wang X, Zhao E, Choi JH, Yang L, Zha Y, Dong Z, Huang S, Asara JM, Cui H, Ding HF. The histone H3 methyltransferase G9A epigenetically activates the serine-glycine synthesis pathway to sustain cancer cell survival and proliferation. Cell Metab. 2013;18:896-907.

Ding S, Jiang J, Zhang G, Bu Y, Zhang G, Zhao X. Resveratrol and caloric restriction prevent hepatic steatosis by regulating

SIRT1-autophagy pathway and alleviating endoplasmic reticulum stress in high-fat diet-fed rats. *PLoS One.* 2017;12:e0183541.

Esaki K, Sayano T, Sonoda C, Akagi T, Suzuki T, Ogawa T et al. L-Serine Deficiency Elicits Intracellular Accumulation of Cytotoxic Deoxysphingolipids and Lipid Body Formation. *J Biol Chem.* 2015;290:14595-14609.

Falck-Ytter Y, Younossi ZM, Marchesini G, McCullough AJ. Clinical features and natural history of nonalcoholic steatosis syndromes. *Semin Liver Dis.* 2001;21:17-26.

Feinman L, Lieber CS. Ethanol and lipid metabolism. *Am J Clin Nutr.* 1999;70:791-792.

Finkelstein JD. Methionine metabolism in mammals. *J Nutr Biochem.* 1990;1:228-237.

Guclu A, Erdur FM, Turkmen K. The Emerging Role of Sirtuin 1 in Cellular Metabolism, Diabetes Mellitus, Diabetic Kidney Disease and Hypertension. *Exp Clin Endocrinol Diabetes.* 2016;124:131-139.

Gulsen M, Yesilova Z, Bagci S, Uygun A, Ozcan A, Ercin CN et al. Elevated plasma homocysteine concentrations as a predictor of steatohepatitis in patients with non-alcoholic fatty liver disease. *J Gastroenterol Hepatol.* 2005;20:1448-1455.

Hajer GR, van der Graaf Y, Olijhoek JK, Verhaar MC, Visseren FL; SMART Study Group. Levels of homocysteine are increased in metabolic syndrome patients but are not associated with an increased

cardiovascular risk, in contrast to patients without the metabolic syndrome. *Heart.* 2007;93:216-220.

Han S, Lone MA, Schneiter R, Chang A. Orm1 and Orm2 are conserved endoplasmic reticulum membrane proteins regulating lipid homeostasis and protein quality control. *Proc Natl Acad Sci U S A.* 2010;107:5851-5856.

Hanada K. Serine palmitoyltransferase, a key enzyme of sphingolipid metabolism. *Biochim Biophys Acta.* 2003;1632:16-30.

Heilbronn LK, Civitarese AE, Bogacka I, Smith SR, Hulver M, Ravussin E. Glucose tolerance and skeletal muscle gene expression in response to alternate day fasting. *Obes Res.* 2005;13:574-581.

Hanada N, Takahata T, Zhou Q, Ye X, Sun R, Itoh J et al. Methylation of the KEAP1 gene promoter region in human colorectal cancer. *BMC Cancer.* 2012;12:66.

Hornemann T, Wei Y, von Eckardstein A. Is the mammalian serine palmitoyltransferase a high-molecular-mass complex? *Biochem J.* 2007;405:157-164.

Jacobsen DW, Catanescu O, Dibello PM, Barbato JC. Molecular targeting by homocysteine: a mechanism for vascular pathogenesis. *Clin Chem Lab Med.* 2005;43:1076-1083.

Ji C, Kaplowitz N. Betaine decreases hyperhomocysteinemia, endoplasmic reticulum stress, and liver injury in alcohol-fed mice. *Gastroenterology.* 2003;124:1488-1499.

Ji C, Shinohara M, Vance D, Than TA, Ookhtens M, Chan C et al. Effect of transgenic extrahepatic expression of betaine-homocysteine methyltransferase on alcohol or homocysteine-induced fatty liver. *Alcohol Clin Exp Res.* 2008;32:1049-1058.

Jun DY, Park HS, Lee JY, Baek JY, Park HK, Fukui K et al. Positive regulation of promoter activity of human 3-phosphoglycerate dehydrogenase (PHGDH) gene is mediated by transcription factors Sp1 and NF-Y. *Gene.* 2008;414(1-2):106-114.

Kalhan SC, Hanson RW. Resurgence of serine: an often neglected but indispensable amino Acid. *J Biol Chem.* 2012;287:19786-19791.

Kansanen E, Kivelä AM, Levonen AL. Regulation of NRF2-dependent gene expression by 15-deoxy-Delta12,14-prostaglandin J2. *Free Radic Biol Med.* 2009;47:1310-1317.

Kansanen E, Jyrkkänen HK, Levonen AL. Activation of stress signaling pathways by electrophilic oxidized and nitrated lipids. *Free Radic Biol Med.* 2012;52:973-982.

Kaufman RJ. Stress signaling from the lumen of the endoplasmic reticulum: coordination of gene transcriptional and translational controls. *Genes Dev.* 1999 ;13:1211-1233.

Kharbanda KK, Mailliard ME, Baldwin CR, Beckenhauer HC, Sorrell MF, Tuma DJ. Betaine attenuates alcoholic steatosis by restoring phosphatidylcholine generation via the phosphatidylethanolamine methyltransferase pathway. *J Hepatol.* 2007;46:314-321.

Kharbanda KK. Alcoholic liver disease and methionine metabolism. *Semin Liver Dis.* 2009;29:155-165.

Kharbanda KK, Todero SL, King AL, Osna NA, McVicker BL, Tuma DJ et al. Betaine treatment attenuates chronic ethanol-induced hepatic steatosis and alterations to the mitochondrial respiratory chain proteome. *Int J Hepatol.* 2012;962183.

de Koning TJ, Snell K, Duran M, Berger R, Poll-The BT, Surtees R. L-serine in disease and development. *Biochem J.* 2003;371(Pt 3):653-661.

Lagouge M, Argmann C, Gerhart-Hines Z, Meziane H, Lerin C, Daussin F et al. Resveratrol improves mitochondrial function and protects against metabolic disease by activating SIRT1 and PGC-1alpha. *Cell.* 2006;127:1109-1122.

Lavu S, Boss O, Elliott PJ, Lambert PD. Sirtuins--novel therapeutic targets to treat age-associated diseases. *Nat Rev Drug Discov.* 2008;7:841-853.

LeCluyse EL, Bullock PL, Parkinson A, Hochman JH. Cultured rat hepatocytes. *Pharm Biotechnol.* 1996;8:121-59.

Lei Sun, Mark Bartlam, Yiwei Liu, Hai Pang, Zihe Rao. Crystal structure of the pyridoxal-5′-phosphate-dependent serine dehydratase from human liver. *Protein Sci.* 2005;14:791 - 798.

Li HB, Yang YR, Mo ZJ, Ding Y, Jiang WJ. Silibinin improves

palmitate-induced insulin resistance in C2C12 myotubes by attenuating IRS-1/PI3K/Akt pathway inhibition. *Braz J Med Biol Res.* 2015;48:440-446.

Li X, Zhang S, Blander G, Tse JG, Krieger M, Guarente L. SIRT1 deacetylates and positively regulates the nuclear receptor LXR. *Mol Cell.* 2007;28:91-106.

Li H, Xu M, Lee J, He C, Xie Z. Leucine supplementation increases SIRT1 expression and prevents mitochondrial dysfunction and metabolic disorders in high-fat diet-induced obese mice. *Am J Physiol Endocrinol Metab.* 2012;303:E1234-1244.

Li X. SIRT1 and energy metabolism. *Acta Biochim Biophys Sin (Shanghai).* 2013;45:51-60.

Lim A, Sengupta S, McComb ME, Théberge R, Wilson WG, Costello CE et al. In vitro and in vivo interactions of homocysteine with human plasma transthyretin. *J Biol Chem.* 2003;278:49707-49713.

Locasale JW, Grassian AR, Melman T, Lyssiotis CA, Mattaini KR, Bass AJ et al. Phosphoglycerate dehydrogenase diverts glycolytic flux and contributes to oncogenesis. *Nat Genet.* 2011;43:869-874.

Ma Q, He X. Molecular basis of electrophilic and oxidative defense: promises and perils of NRF2. *Pharmacol Rev.* 2012;64:1055-1081.

Majors AK, Sengupta S, Willard B, Kinter MT, Pyeritz RE, Jacobsen DW.
Homocysteine binds to human plasma fibronectin and inhibits its

interaction with fibrin. *Arterioscler Thromb Vasc Biol.* 2002;22:1354-1359.

Marambaud P, Zhao H, Davies P. Resveratrol promotes clearance of Alzheimer's disease amyloid-beta peptides. *J Biol Chem.* 2005;280:37377-37382.

Mato JM, Alvarez L, Ortiz P, Mingorance J, Durán C, Pajares MA. S-adenosyl-L-methionine synthetase and methionine metabolism deficiencies in cirrhosis. *Adv Exp Med Biol.* 1994;368:113-117.

Matsui T, Sekiguchi M, Hashimoto A, Tomita U, Nishikawa T, Wada K. Functional comparison of D-serine and glycine in rodents: the effect on cloned NMDA receptors and the extracellular concentration. *J Neurochem.* 1995;65:454-458.

Mazurek S, Boschek CB, Hugo F, Eigenbrodt E. Pyruvate kinase type M2 and its role in tumor growth and spreading. *Semin Cancer Biol.* 2005;15:300-308.

Milne JC, Lambert PD, Schenk S, Carney DP, Smith JJ, Gagne DJ et al. Small molecule activators of SIRT1 as therapeutics for the treatment of type 2 diabetes. *Nature.* 2007;450:712-716.

Mitsuishi Y, Taguchi K, Kawatani Y, Shibata T, Nukiwa T, Aburatani H et al. NRF2 redirects glucose and glutamine into anabolic pathways in metabolic reprogramming. *Cancer Cell.* 2012;22(1):66-79.

Mudd SH, Levy HL. Plasma homocyst(e)ine or homocysteine? *N Engl J Med.* 1995;333:325.

Nigdelioglu R, Hamanaka RB, Meliton AY, O'Leary E, Witt LJ, Cho T et al. Transforming Growth Factor (TGF)-β Promotes de Novo Serine Synthesis for Collagen Production. *J Biol Chem.* 2016;291:27239-27251.

Nisoli E, Tonello C, Cardile A, Cozzi V, Bracale R, Tedesco L et al. Calorie restriction promotes mitochondrial biogenesis by inducing the expression of eNOS. *Science.* 2005 Oct 14;310(5746):314-7.

Nogueiras R, Habegger KM, Chaudhary N, Finan B, Banks AS, Dietrich MO et al. Sirtuin 1 and sirtuin 3: physiological modulators of metabolism. *Physiol Rev.* 2012;92:1479-1514.

Nonaka H, Tsujino T, Watari Y, Emoto N, Yokoyama M. Taurine prevents the decrease in expression and secretion of extracellular superoxide dismutase induced by homocysteine: amelioration of homocysteine-induced endoplasmic reticulum stress by taurine. *Circulation.* 2001;104:1165-1170.

Othman A, Rütti MF, Ernst D, Saely CH, Rein P, Drexel H et al. Plasma deoxysphingolipids: a novel class of biomarkers for the metabolic syndrome? *Diabetologia.* 2012;55:421-431.

Ou Y, Wang SJ, Jiang L, Zheng B, Gu W. p53 Protein-mediated regulation of phosphoglycerate dehydrogenase (PHGDH) is crucial for the apoptotic response upon serine starvation. *J Biol Chem.* 2015;290:457-466.

Pfluger PT, Herranz D, Velasco-Miguel S, Serrano M, Tschöp MH. Sirt1 protects against high-fat diet-induced metabolic damage. *Proc*

Natl Acad Sci U S A. 2008;105:9793-9798.

Picard F, Kurtev M, Chung N, Topark-Ngarm A, Senawong T, Machado De Oliveira R et al. Sirt1 promotes fat mobilization in white adipocytes by repressing PPAR-gamma. *Nature.* 2004;429:771-776.

Poddar R, Sivasubramanian N, DiBello PM, Robinson K, Jacobsen DW. Homocysteine induces expression and secretion of monocyte chemoattractant protein-1 and interleukin-8 in human aortic endothelial cells: implications for vascular disease. *Circulation.* 2001;103:2717-2723.

Possemato R, Marks KM, Shaul YD, Pacold ME, Kim D, Birsoy K et al. Functional genomics reveal that the serine synthesis pathway is essential in breast cancer. *Nature.* 2011;476:346-350.

Purohit V, Gao B, Song BJ. Molecular mechanisms of alcoholic fatty liver. *Alcohol Clin Exp Res.* 2009;33:191-205.

Purushotham A, Schug TT, Xu Q, Surapureddi S, Guo X, Li X. Hepatocyte-specific deletion of SIRT1 alters fatty acid metabolism and results in hepatic steatosis and inflammation. *Cell Metab.* 2009;9:327-338.

Ravez S, Spillier Q, Marteau R, Feron O, Frédérick R. Challenges and Opportunities in the Development of Serine Synthetic Pathway Inhibitors for Cancer Therapy. *J Med Chem.* 2017;60:1227-1237.

Remková A, Remko M. Homocysteine and endothelial markers are increased in patients with chronic liver diseases. *Eur J Intern Med.* 2009;20:482-486.

Roda O, Valero ML, Peiró S, Andreu D, Real FX, Navarro P. New insights into the tPA-annexin A2 interaction. Is annexin A2 CYS8 the sole requirement for this association? *J Biol Chem.* 2003;278:5702-5709.

Sass JO, Nakanishi T, Sato T, Sperl W, Shimizu A. S-homocysteinylation of transthyretin is detected in plasma and serum of humans with different types of hyperhomocysteinemia. *Biochem Biophys Res Commun.* 2003;310:242-246.

Schenk S, McCurdy CE, Philp A, Chen MZ, Holliday MJ, Bandyopadhyay GK et al. Sirt1 enhances skeletal muscle insulin sensitivity in mice during caloric restriction. *J Clin Invest.* 2011;121:4281-4288.

Selhub J. Homocysteine metabolism. *Annu Rev Nutr.* 1999;19:217-246.

Shi X, Li Y, Hu J, Yu B. Tert-butylhydroquinone attenuates the ethanol-induced apoptosis of and activates the NRF2 antioxidant defense pathway in H9c2 cardiomyocytes. *Int J Mol Med.* 2016;38:123-130.

Sim WC, Yin HQ, Choi HS, Choi YJ, Kwak HC, Kim SK et al. L-serine supplementation attenuates alcoholic fatty liver by enhancing homocysteine metabolism in mice and rats. *J Nutr.* 2015;145:260-267.

Simmons GE Jr, Pruitt WM, Pruitt K. Diverse roles of SIRT1 in cancer biology and lipid metabolism. *Int J Mol Sci.* 2015;16:950-965.

Snell K, Weber G. Enzymic imbalance in serine metabolism in rat

hepatomas. *Biochem J.* 1986;233:617-620.

Sørensen T, Orholm M, Bentsen KD, Høybye G, Eghøje K, Christoffersen P. Prospective evaluation of alcohol abuse and alcoholic liver injury in men as predictors of development of cirrhosis. *Lancet.* 1984;2:241-244.

Stipanuk MH. Sulfur amino acid metabolism: pathways for production and removal of homocysteine and cysteine. *Annu Rev Nutr.* 2004;24:539-577.

Sumiyoshi M, Sakanaka M, Kimura Y. Chronic intake of a high-cholesterol diet resulted in hepatic steatosis, focal nodular hyperplasia and fibrosis in non-obese mice. *Br J Nutr.* 2010;103:378-385.

Teli MR, Day CP, Burt AD, Bennett MK, James OF. Determinants of progression to cirrhosis or fibrosis in pure alcoholic fatty liver. *Lancet.* 1995;346:987-990.

Undas A, Williams EB, Butenas S, Orfeo T, Mann KG. Homocysteine inhibits inactivation of factor Va by activated protein C. *J Biol Chem.* 2001;276:4389-4397.

Verhoef P, Steenge GR, Boelsma E, van Vliet T, Olthof MR, Katan MB. Dietary serine and cystine attenuate the homocysteine-raising effect of dietary methionine: a randomized crossover trial in humans. *Am J Clin Nutr.* 2004;80:674-679.

Wang G, Siow YL, O K. Homocysteine stimulates nuclear factor

kappaB activity and monocyte chemoattractant protein-1 expression in vascular smooth-muscle cells: a possible role for protein kinase C. *Biochem J.* 2000;352(Pt 3):817-826.

Wang G, O K. Homocysteine stimulates the expression of monocyte chemoattractant protein-1 receptor (CCR2) in human monocytes: possible involvement of oxygen free radicals. *Biochem J.* 2001;357(Pt 1):233-240.

Wang RH, Li C, Deng CX. Liver steatosis and increased ChREBP expression in mice carrying a liver specific SIRT1 null mutation under a normal feeding condition. *Int J Biol Sci.* 2010;6:682-690.

Werstuck GH, Lentz SR, Dayal S, Hossain GS, Sood SK, Shi YY et al. Homocysteine-induced endoplasmic reticulum stress causes dysregulation of the cholesterol and triglyceride biosynthetic pathways. *J Clin Invest.* 2001;107:1263-1273.

Xie J, Zhang X, Zhang L. Negative regulation of inflammation by SIRT1. *Pharmacol Res.* 2013;67:60-67.

Zhang P, Singh A, Yegnasubramanian S, Esopi D, Kombairaju P, Bodas M et al. Loss of Kelch-like ECH-associated protein 1 function in prostate cancer cells causes chemoresistance and radioresistance and promotes tumor growth. *Mol Cancer Ther.* 2010(2):336-346.

국문초록

지방간은 초기 단계의 간질환으로서 지방이 간 무게의 5% 이상을 차지하는 상태를 의미한다. 지방간은 가역적이고 양성의 질환이지만, 적절한 치료가 진행되지 않으면 간기능 장애를 야기하게 된다. 본 연구에서는 세린 생합성 단계에서 율속단계 효소로 작용하는 3-phosphoglycerate dehydrogenase (PHGDH)가 지방간 질환에서 세린 합성을 조절하여 지질대사에 영향을 줄 것임을 제안하였다.

이전 연구에서 만성적으로 에탄올을 투여한 랫트에서 세린이 감소하는 것을 확인하였다. 이에 근거하여, 알콜성 지방간 모델에서 세린을 투여하였으며 세린의 투여는 methionine synthase와 cystathionine β synthase를 경유하여 호모시스테인을 대사시킴으로써 에탄올에 의해 유도된 지방간을 억제하였다. 또한 세린은 lactate dehydrogenase에 의해 세포내 NAD^+와 SIRT1의 활성을 증가시켰다. 세린은 미토콘드리아 유전자 발현, 양 그리고 기능을 증가시켰다. 세린에 의한 SIRT1 활성의 증가는 in vitro에서 지질 축적 및 인슐린 저항성을 억제하였다.

PHGDH와 세린은 만성 에탄올 그리고 고지방식이에 의한 지방간 질환 모델에서 유의미하게 감소하였다. 유리지방산 및 에탄올은 in vitro에서 PHGDH의 발현을 감소시켰다. 세린 생합성의 감소는 PHGDH-KO MEF 세포 및 알콜성 지방간 모델에서 비정상적인 스핑고지질 및 세라마이드의 증가를 야기하였다. 또한 간염 환자의 GEO 분석을 통해 PHGDH 유전자 발현이 감소하는 것을 확인하였다. 지방간 환자의 혈청 세린은 MRI로 확인한 지질분획, 혈청 ALT 및 중성지방과 역의 상관관계를 가지는 것을 확인하였다. PHGDH 기능회복에 의한 세린 합성의 증가는 세포내 NAD^+ 및 SIRT1의 활성을 증가시켜 지질 축적을 억제하였다.

PHGDH는 전사 및 번역 수준에서 NRF2에 의해 증가하는 것을 확인하였다. 지방간 질환 모델에서 NRF2의 발현이 감소하는 것을 확인하였으며 NRF2 활성의 증가는 유리지방산에 의해 감소하였던 PHGDH의 발현을 회복시켰다.

결론적으로 PHGDH는 간에서 세린을 생합성함으로써 지질대사를 조절하는 중요한 역할을 한다. 본 연구를 통해 PHGDH를 지방간 질환을 치료하는 타겟으로 사용할 수 있으며 이에 의해 합성되는 세린이 지방간 질환을 치료하는 가능성을 가짐을 확인하였다.

In conclusion, PHGDH plays an important role regulating lipid metabolism by synthesizing L-serine in the liver. This study showed that PHGDH can be used as a therapeutic target for hepatosteatosis and L-serine has a potential for curing fatty liver disease.

Key words : 세린, 호모시스테인, 3-Phosphoglycerate dehydrogenase, SIRT1, 지질대사, 지방간

Student Number : 2011-21733

약학박사학위논문

지방간 발생에서 3-Phosphoglycerate Dehydrogenase 발현 억제에 의한 L-Serine 대사 이상의 역할

Role of Abnormal L-Serine Metabolism by Lowered Expression of 3-Phosphoglycerate Dehydrogenase in Fatty Liver Disease

2018년 2월

서울대학교 대학원
약학과 예방약학전공
심우철

Abstract

Role of Abnormal L-Serine Metabolism by Lowered Expression of 3-Phosphoglycerate Dehydrogenase in Fatty Liver Disease

Woo-Cheol Sim
Preventive Pharmacy, College of Pharmacy
Seoul National University

Fatty liver disease is early-stage liver disease that fat makes up more than 5% of the organ's weight. Fatty liver is a reversible state and benign, but without proper treatments, it can lead to liver dysfunction. In this study, we propose that 3-phosphoglycerate dehydrogenase (PHGDH), which is a rate-limiting enzyme in serine biosynthesis, can affect lipid metabolism by regulating L-serine pool in fatty liver disease.

Previous study showed that hepatic L-serine is decreased in chronically ethanol-fed rats. Based on the result, L-serine was treated in alcoholic fatty liver model and it reversed ethanol-induced fatty liver by metabolizing homocysteine via methionine synthase (MS) and cystathionine β-synthase (CβS). L-serine also increased intracellular NAD^+ and silent information regulator 1 (SIRT1) activity via lactate dehydrogenase (LDH). L-serine increased mitochondrial gene expression, mass and function by deacetylated PGC-1α.. Increased SIRT1 activity by L-serine ameliorated lipid accumulation and insulin resistance *in vitro*.

PHGDH and L-serine were found to be significantly lowered in chronic ethanol diet and high-fat diet fatty liver model. Free fatty acids and ethanol also decreased PHGDH expression *in vitro*.

Diminished synthesis of L-serine led to increase in abnormal sphingolipids and ceramides in PHGDH-KO MEF cells and alcoholic fatty liver model. GEO analysis of hepatitis patients revealed *phgdh* gene expression was diminished. Serum L-serine of fatty liver patients was also down-regulated and negatively correlated with MRI fat fraction, serum ALT and triglyceride (TG). Increased synthesis of L-serine by PHGDH gain of function reversed lipid accumulation in various cells by increasing intracellular NAD^+ and SIRT1 activity.

PHGDH is found to be positively regulated by nuclear factor like 2 (NRF2) at both transcriptional and translational levels. Fatty liver disease model showed the decreased expression of NRF2 and increased NRF2 activity reversed free fatty acid-induced decrease in PHGDH expression.

In conclusion, PHGDH plays an important role in regulating lipid metabolism by synthesizing L-serine in the liver. This study showed that PHGDH can be used as a therapeutic target for hepatosteatosis and L-serine has a potential for curing fatty liver disease.

Key words : L-Serine, Homocysteine, 3-Phosphoglycerate dehydrogenase, SIRT1, Lipid metabolism, Fatty liver

Student Number : 2011-21733

Contents

I. Introduction

1.1. Fatty liver

Fatty liver diseases are classified into two categories. First, alcoholic fatty liver disease (ALD) is developed by heavy alcohol intake (Feinman and lieber, 1999) and secondly, nonalcoholic fatty liver disease (NAFLD) is induced by excessive calorie intake, virus, chemicals and so on (Ahn et al., 2008; Li et al., 2012). Because intracellular lipid itself is not that toxic to hepatocyte, patients have little symptoms and liver functions are mostly normal. But without proper therapy, lipid accumulation is ongoing and reversible fatty liver can develop into irreversible steatohepatitis, liver fibrosis and finally liver failure (Figure 1 and Table 1) (Sorensen et al., 1984; Teli et al., 1995; Jonathan et al., 2011; Falck-Ytter et al., 2001).

The molecular mechanisms that contribute to fatty liver include increased de novo fatty acid synthesis by sterol regulatory element binding protein (SREBP)-1, decreased fatty acid oxidation by peroxisome proliferator-activated receptor-α (PPAR-α), up-regulated fatty acid uptake by CD36 and fatty acid transport protein (FATP) and disabled VLDL lipoprotein secretion by phosphatidylethanolamine methyltransferase (PEMT) (Figure 2) (Purohit V et al., 2009; ,Jonathan et al., 2011).

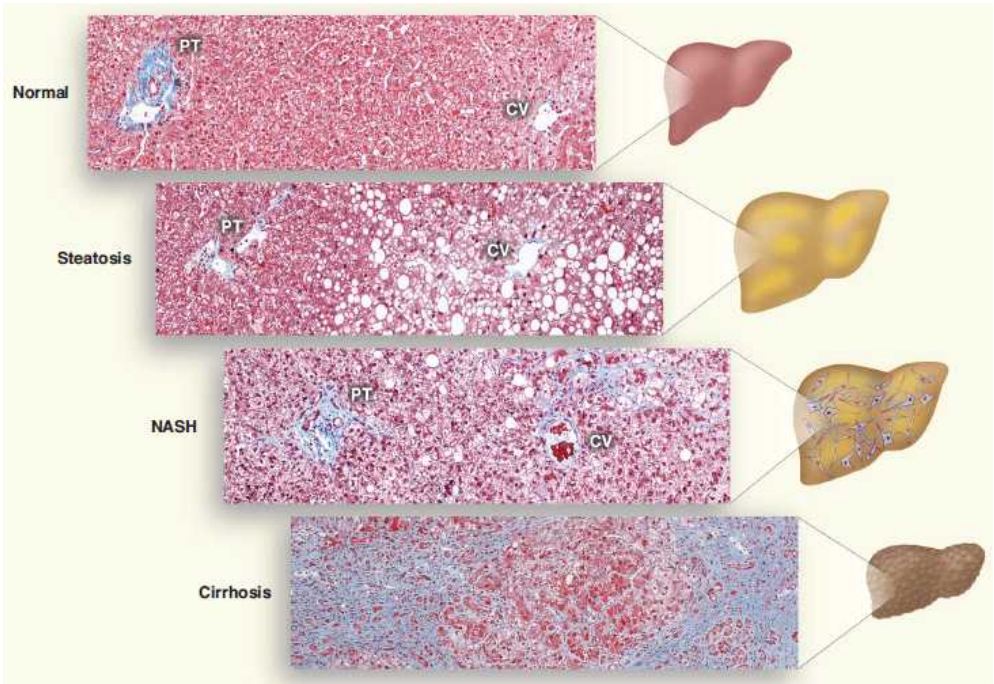

Figure 1. Histological sections illustrating normal liver, steatosis, NASH, and cirrhosis (Jonathan et al., 2011).

Table 1. NAFLD patients with sequential biopsies (Falck-Ytter et al., 2001)

	Length of Follow-up (Years)	n/Total*	Subsequent Histology			
					Progressed to	
			Improved	No Change	Fibrosis	Cirrhosis
Lee† (1989)	1.2–6.9	12/38	0/12	7/12	3/12	2/12
Powell† (1990)	1–9	12/41	1/12	5/12	4/12	2/12
Bacon (1994)	4–7	2/33	0/2	1/2	0/2	1/2
		26/112	1/26 (4%)	13/26 (50%)	7/26 (27%)	5/26 (19%)

*Represents the number of patients out of the total group who had sequential biopsies.
†In both the studies of Lee and Powell, one of the 13 patients with follow-up histology available had cirrhosis at index biopsy. Therefore, only the 12 patients without cirrhosis at index biopsy are included in this analysis.

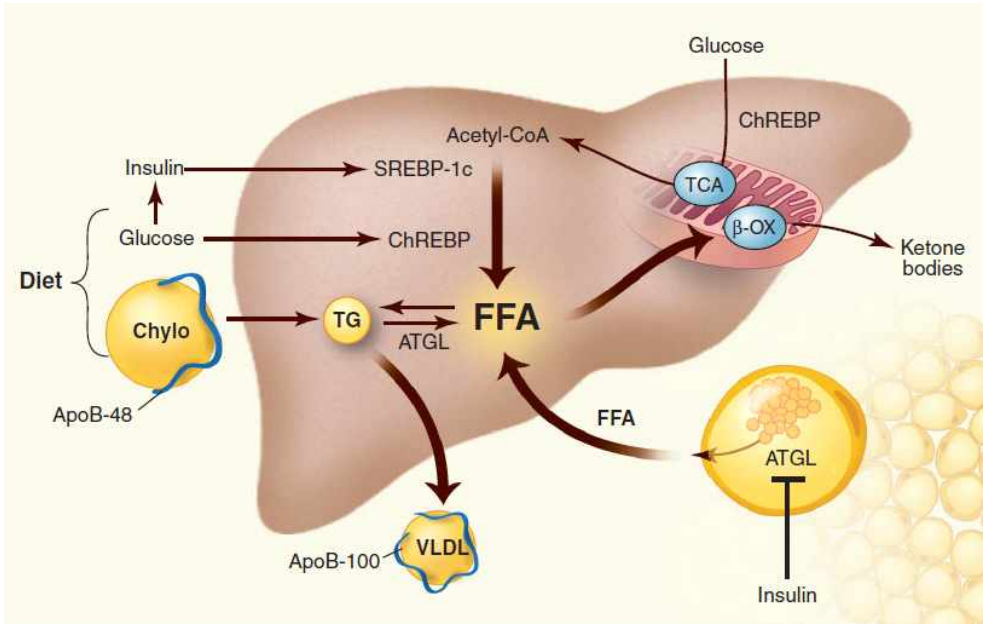

Figure 2. Metabolism of TG in the liver (Jonathan et al., 2011).

1.2. L-serine

L-serine is classified as a non-essential amino acid, but displays a diverse role in several biological processes (Figure 3) (Ming et al., 2016). L-serine is a major contributor to the one-carbon groups for the purine and pyrimidine nucleotide synthesis. L-serine is also converted to D-serine, which is a neuro-modulator acting as a N-methyl-D-aspartate (NMDA) receptor co-agonist by D/L-serine racemase (Matsui et al., 1995). L-serine also can condense with palmitoyl CoA by serine palmitoyltransferase (SPT) to produce sphinganine, which is a precursor of ceramides (Hanada, 2003). L-serine also participates in homocysteine metabolism producing glutathione by supplying glycine and cysteine which are the two products of L-serine metabolism or by reacting with homocysteine. L-serine is required either as a methyl group donor for MS or as a substrate for CβS (Sim et al., 2015).

Our previous study found that L-serine is decreased in chronic ethanol model induced by Lieber-DeCarli ethanol diet (Table 2). Based on this result, we performed further study.

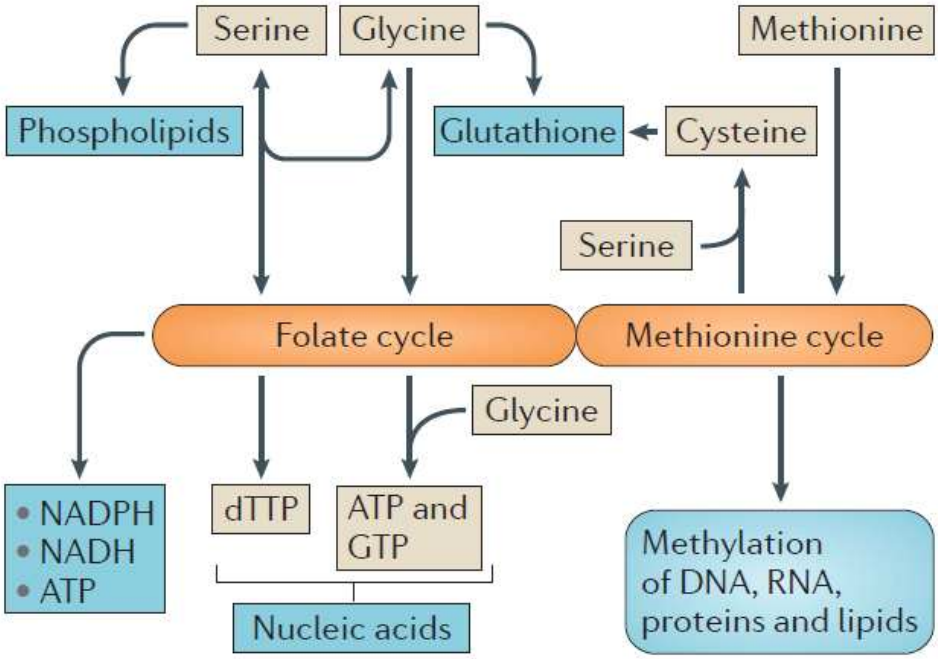

Figure 3. Overview of serine metabolism (Ming et al., 2016).

L-serine donates one-carbon units to the folate cycle while producing glycine. The folate cycle is essential for de novo synthesis of adenosine, guanosine and thymidylate, and can contribute to mitochondrial NADH, NADPH and ATP regeneration. The methionine cycle also provides precursors, such as cysteine for the synthesis of glutathione.

Table 2. Amino acid analysis in the livers from chronically ethanol fed rats.

Amino acid (μmol/g liver)	Control	Ethanol (4 week)	Change
Aspartate	26.4 ± 5.0	30.6 ± 9.6	-
Glutamate	42.3 ± 8.7	39.1 ± 10.3	-
Asparagine	1.5 ± 0.2	1.8 ± 0.3	-
Serine	8.4 ± 1.5	5.9 ± 2.1	- Δ 30%
Glutamine	88.6 ± 4.5	94.1 ± 16.9	-
Histidine	11.1 ± 1.5	11.2 ± 1.2	-
Glycine	15.8 ± 1.9	17.1 ± 3.8	-
Threonine	10.2 ± 1.3	10.9 ± 4.7	-
Alanine	29.8 ± 9.3	27.8 ± 11.4	-
Tyrosine	2.8 ± 0.4	3.7 ± 0.4	Δ 32%
Valine	4.2 ± 0.5	5.7 ± 0.8	Δ 36%
Methionine	0.39 ± 0.04	0.62 ± 0.10	Δ 59%
Tryptophan	0.69 ± 0.06	0.81 ± 0.08	Δ 17%
Phenylalanine	1.6 ± 0.2	2.1 ± 0.3	Δ 31%
Isoleucine	2.0 ± 0.2	2.5 ± 0.3	Δ 25%
Leucine	3.6 ± 0.4	5.0 ± 0.6	Δ 39%
Lysine	8.3 ± 1.9	9.5 ± 2.3	-
Proline	3.4 ± 0.9	4.5 ± 1.3	-

1.3. Homocysteine toxicity and role of homocysteine in fatty liver

Homocysteine is a sulfur-containing toxic metabolite produced by methionine metabolism and is known to be associated with the pathogenesis of the fatty liver disease (Hajer et al., 2007; Gulsen et al., 2005; Bjorck et al., 2006). Hyperhomocysteinemia has been identified as an independent risk factor for coronary artery disease (Clarke et al., 1991).

Homocysteine represents its toxicity through various mechanisms. Pathophysiological levels of homocysteine increased expression and secretion of interleukin-8 (IL-8) and monocyte chemoattractant protein-1 (MCP-1) and induced inflammatory response (Poddar et al., 2001; Wang et al., 2000; Wang and O, 2001).

Homocysteine can damage the function of proteins by making stable disulfide bonds with cysteine residues (Jacobsen et al., 2005) and homocysteine incorporation into protein via *S*-homocysteinylation may leads to impairment of protein function (Undas et al., 2001; Majors et al., 2002; Lim et al., 2003; Sass et al., 2003; Roda et al., 2003).

Homocysteine also induces endoplasmic reticulum (ER) stress, which is a consequence of unfolded protein response (Kaufman, 1999), associated gene expression including glucose-regulated protein 78 (GRP78). Homocysteine can also activate protein kinase RNA-like ER kinase (PERK) (Nonaka et al., 2001; Werstuck et al., 2001). Geoff et al. reported that homocysteine-induced ER stress can dysregulate the triglyceride synthesis pathway resulting in fatty liver (Werstuck et al., 2001).

Mice fed homocysteine or a high-methionine, and low-folate diet have increased homocysteine concentrations and increased incidence of liver

disease, characterized by hepatic steatosis (Ji et al., 2008). Chronic ethanol consumption increases homocysteine accumulation in the liver, which is closely linked to the development of various liver diseases. Moreover, patients with chronic liver disease, as well as alcoholics, develop substantially increased serum homocysteine concentrations regardless of the stage of steatosis, from mild fibrosis to severe cirrhosis (Table 2) (Remková et al., 2009; Cylwik et al., 2009).

Chronic ethanol ingestion induces a deficiency in many nutrients, including folate, choline, vitamin B, betaine and methionine (Kharbanda, 2009). Homocysteine-lowering intervention using folate, betaine, vitamin B reversed homocysteine concentrations and/or liver injuries by normalizing homocysteine metabolism (Verhoef et al., 2004; Ji et al., 2003; Sumiyoshi et al., 2010).

Table 2. Serum folate and homocysteine levels in alcoholics (Cylwik et al., 2009).

Group	Folate (nmol/L)		Homocysteine (μmol/L)	
	Median	Range	Median	Range
Healthy controls	17.9	9.7–42.4	10.58	7.58–14.96
Total alcoholic group	12.9	4.7–35.1	16.85	8.80–68.35
	p^c=0.001		p^c<0.001	
Alcoholics with normal liver enzymes	12.5	4.7–34.9	16.40	8.80–68.35
	p^c=0.002		p^c<0.001	
Alcoholics with elevated liver enzymes	14.0	5.0–35.1	17.89	10.92–48.95
	p^c=0.023		p^c<0.001	
	p^b=0.477		p^b=0.916	
Alcoholics with normal homocysteine	15.3	5.0–34.9	—	
	p^c=0.110			
Alcoholics with elevated homocysteine	11.3	4.8–35.1	—	
	p^c<0.001			
	p^b=0.058			
Alcoholics with normal folate	—		15.63	8.80–40.82
			p^c<0.001	
Alcoholics with low folate	—		17.89	9.11–68.35
			p^c<0.001	
			p^b=0.047	

The differences between alcoholic subgroups and between alcoholics and controls estimated by Mann-Whitney *U*-test. p^b, between supplementary alcoholic subgroups (i.e. alcoholics with normal homocysteine vs alcoholics with elevated homocysteine), p^c, alcoholics vs controls.
Normal liver enzymes: ALT and AST in the range 5–50 U/L, and GGT 10–75 U/L, elevated liver enzymes: ALT and AST higher than 50 U/L, and GGT than 75 U/L. Normal homocysteine: in the range 5.46–16.20 μmol/L, elevated homocysteine: above 16.20 μmol/L. Normal folate: in the range 10.92–43.03 nmol/L, low folate: below 10.92 nmol/L.

1.4. Homocysteine metabolism

The intake of dietary proteins produce various amino acids including methionine. Methionine can be metabolized into S-adenosylmethionine (SAM) by Methionine S-adenosyltransferase (MAT). SAM acts as a methyl donor which is used in amino acid, protein, phospholipids, DNA methylation (Mato et al., 1994). In this reaction, SAM is converted to SAH and metabolized SAH is metabolized into homocysteine by S-adenosylhomocysteine hydrolase.

Liver is a major organ that metabolizes homocysteine. Methionine synthase (MS), betaine homocysteine methyltransferase (BHMT) or cystathionine β-synthase (CβS) change homocysteine into methionine or cysteine (Figure 4) (Verhoef et al., 2004). First, BHMT metabolizes homocysteine into methionine by methylating homocysteine using betaine (Finkelstein, 1990). Secondly, MS metabolizes homocysteine into methionine using 5-methyltetrahydrofolate (5-methylTHF) as a methyl donor and vitamin B_{12} as a cofactor (Seljub J, 1999). Thirdly, homocysteine is metabolized by trans-sulfuration pathway. CβS converts homocysteine into cystathionine by using L-serine and vitamin B_6 as a cofactor. Cystathionine is hydrolyzed into cysteine by cystathionine γ-lyase. Cysteine is then synthesized into glutathione (GSH) or sulfate or secreted as a urea (Mudd, S.H. et al., 1995).

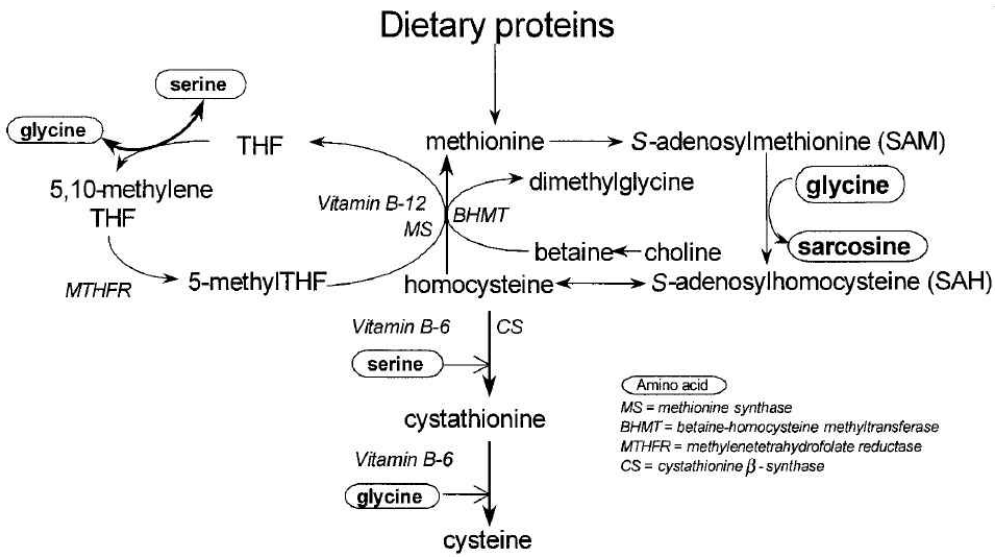

Figure 4. Schematic representation of homocysteine metabolism (Verhoef et al., 2004)

1.5. SIRT1

Mammalian silent information regulators (SIRT) have seven isoforms which belong to the SIRT family. These members have various subcellular localization and distribution in organs (Nogueiras et al., 2012). SIRT1 is most well known member of SIRT family and acts as a NAD^+-dependent deacetylase.

SIRT1 is known as one of a key metabolic sensor which regulates various proteins including transcription factors by its deacetylating activity (Li, 2013; Chaudhary and Pfluger, 2009; Xie et al., 2013; Simmons et al., 2015; Guclu et al.). SIRT1 gain of function has been known to affect vascular function, mitochondria biogenesis, neurodegenerative disease, diabetes mellitus and lipid metabolism (Delmas et al., 2005; Lagouge et al., 2006; Marambaud et al., 2005; Milne et al., 2007; Li et al., 2007).

SIRT1 is widely distributed in metabolic tissues including adipose tissue, liver, skeletal muscle, brain and kidney. In these tissues, SIRT1 expression is up-regulated by calorie restriction (Figure 5) (Cohen et al., 2004; Heilbronn et al., 2005; Nisoli et al., 2005; Picard et al., 2004).

In the muscle tissues, resveratrol improved mitochondrial function and enhanced oxidative capacity in muscle by activating SIRT1 and its target protein, PGC-1α (Lagouge et al., 2006; Milne et al., 2007).

In the liver, the role of SIRT1 in fatty liver disease was first identified by liver-specific SIRT1 knockout (KO) models (Purushotham et al., 2009; Wang et al., 2010). SIRT1 KO mice showed higher lipid deposition in liver and serum compared with control mice. SIRT1 overexpressing transgenic mouse improved high-fat diet-induced glucose tolerance, hepatic steatosis, and inflammation compared with control mouse (Pfluger et al., 2008). Resveratrol and caloric restriction

also prevented hepatic steatosis by regulating SIRT1 pathway in high-fat diet-fed animals (Ding et al., 2017; Baur et al., 2006; Lagouge et al., 2006). In this study, SIRT1 is focused as PHGDH mediated regulation of lipid metabolism.

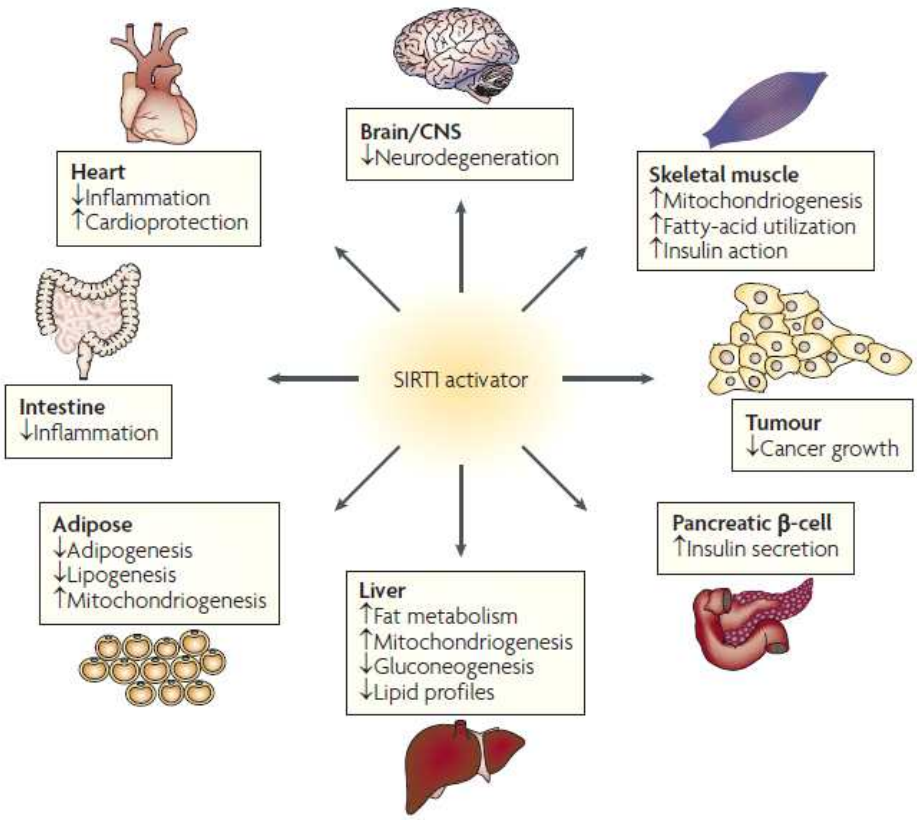

Figure 5. Multiple target organs in which SIRT1 activation can potentially have effects to treat diseases (Lavu et al., 2008).

1.6. De novo Serine Synthesis

L-serine can be synthesized by glycolytic metabolite, 3-phosphoglycerate. 3-phosphoglycerate dehydrogenase (PHGDH) catalyzes first rate-limiting step in de novo serine synthesis. PHGDH converts 3-phosphoglycerate into 3-phosphohydroxypyruvate using NAD^+ as a cofactor (Ravez et al., 2017). Then, 3-Phosphohydroxypyruvate is metabolized into phosphoserine by phosphoserine aminotransferase 1 (PSAT-1) and then L-serine is produced by phosphoserine phosphatase (PSPH). SHMT mediates serine to glycine conversion (Figure 6).

Although L-serine can be absorbed by dietary intake, L-serine from biosynthesis plays important roles in many situations. Nigdelioglu et al. reported that transforming growth factor (TGF)-β promotes de novo serine synthesis for collagen production. Whether there is serine and glycine in culture media or not, only de novo synthesis of glycine from L-serine is sufficient for the production of collagen. Snell et al, first showed that enzymic imbalance in serine metabolism in rat hepatomas (Snell et al., 1986) and several studies reported that PHGDH expression is up-regulated in melanoma and breast cancer cells (Beroukhim et al., 2010; Locasale et al., 2011; Possemato et al., 2011).

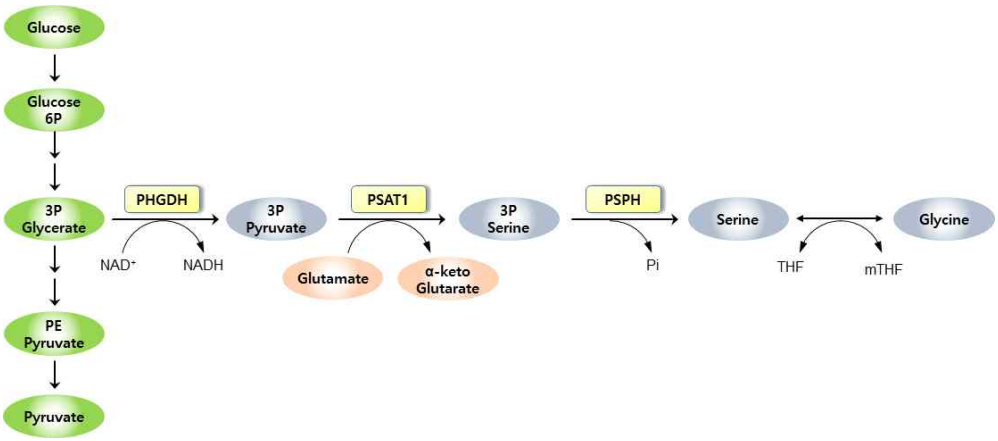

Figure 6. Schematic representation of *de novo* serine synthesis pathway and glycolysis.

1.7. Regulation of PHGDH

PHGDH expression has been known to be regulated by various molecules including human epidermal growth factor receptor 2 (HER2), specificity protein 1 (Sp1), nuclear transcription factor Y (NF-Y), G9A, p53, and erythroid 2-related factor 2 (NRF2).

First, HER2, receptor tyrosine kinase, overexpression increased PHGDH expression in MCF10A cells by using differential analysis of time series gene expression (Bollig et al., 2011).

Second, human PHGDH promoter activity was reported to be positively regulated by the action of transcription factors Sp1 and NF-Y (Jun et al., 2008). Epigenetic study showed that histone H3 lysine 9 (H3K9) methyltransferase G9A is required for maintaining the serine-glycine biosynthetic pathway enzyme genes in an active state marked by H3K9 monomethylation and for the transcriptional activation in response to serine deprivation (Ding et al., 2013).

Third, Ou et al. reported that PHGDH is a target of p53 in human melanoma cells (Ou et al., 2015). Upon serine starvation, p53 suppressed PHGDH expression and inhibited de novo serine biosynthesis and p53-mediated cell death is enhanced dramatically in response to Nutlin-3 treatment.

Fourth, the transcription factor NRF2 is a key regulator in response to oxidative stress (Kansanen et al., 2012). Frequently deregulated NRF2 in non-small cell lung cancer (NSCLC) controls the expression of the key serine/glycine biosynthetic enzyme genes PHGDH, PSAT1, and SHMT2 via activating transcription factor 4 (ATF4) to support macromolecule production (DeNicola et al., 2015).

1.8. The aim of study

The overall goal of this study is to identify the effect of the L-serine on improving fatty liver and the role of PHGDH in lipid metabolism by regulating the synthesis of L-serine.

First, L-serine was significantly reduced in Lieber-DeCarli ethanol in vivo model in previous study and it is assumed that L-serine can reverse the fatty liver. In this study, the effect of L-serine on alcoholic fatty liver disease was identified and the mechanism of L-serine on fatty liver was also studied focusing on homocysteine metabolism.

Second, L-serine mediated regulation of fatty liver disease was studied. We assumed that NAD^+ can be produced by L-serine by the action of lactate dehydrogenase and measured intracellular NAD^+ and the activity of SIRT1, NAD^+ using deacetylation enzyme.

Third, the reason why L-serine is decreased in various fatty liver diseases model was investigated. L-serine can not only be uptaken by dietary sources but also be synthesized by de novo L-serine synthesis pathway using glycolytic intermediate, 3-phosphoglycerate. The expression of enzymes involved in this pathway was measured and the rate-limiting enzyme, PHGDH, was identified as a key factor for L-serine mediated lipid metabolism.

Fourth, the regulation of PHGDH is investigated. One of the various regulators, NRF2 is studied by focusing on its expression and protein stability.

II. Materials and Methods

2.1. L-serine effect on alcoholic fatty liver

2.1.1. Cell culture

AML12 was obtained from the American Type Culture Collection (ATCC, Rockville, MD) and cultured following ATCC guidelines. Briefly, cells were cultured with growth medium which is DMEM/F12 (Gibco BRL, Grand island, NY) with 0.005 mg/mL insulin, 0.005 mg/mL transferrin, 5 ng/mL selenium (Insulin-Transferrin-Selenium, Gibco BRL), and 40 ng/mL dexamethasone (Sigma, St. Louis, MO) containing 10% heat inactivated fetal bovine serum (FBS; Gibco BRL), 50 units/mL of penicillin, and 50 units/mL of streptomycin (Antibiotic-antimycotic; Gibco BRL).

2.1.2. Nile red assay

AML12 cells were plated into black 96-well plates at a density of 10^4 cells per well and incubated overnight. Ethanol was treated for 48 hr with or without L-serine at indicated concentrations. After 48 hr, cells were fixed in paraformaldehyde containing Hoechst 33258 for 10 minutes at room temperature. Then paraformaldehyde was removed and cells were washed with Dulbacco's modified phosphate-buffered saline (DPBS) twice. DPBS containing nile red solution was added and incubated for 10 minutes and washed with DPBS. Fluorescence was measured using a microplated fluorescence reader at the excitation/emission wavelengths of 470/580 nm. Data were normalized by Hoechst 33258 determined at the excitation/emission wavelengths of

365/488 nm.

2.1.3. Animal experiments

Animals used in the study were purchased from Japan SLC, Inc., housed in an air-conditioned room (24℃) with a 12-h light/dark cycle, and acclimatized over 1 wk to a nonpurified diet. The experiments using animals were carried out in accordance with animal experiment guidelines with the approval of the Institutional Animal Care and Use Committee of Seoul National University.

2.1.3.1. Binge ethanol study

Male C57BL/6 mice (20 g) were randomly divided into 4 groups: control (C), binge ethanol + vehicle (EV), binge ethanol + 20 mg/kg L-serine (ES20), and binge ethanol + 200 mg/kg L-serine (ES200). They were fed the nonpurified diet throughout the experiments. Three mice in each group were gavaged with 5 g/kg of ethanol or isocaloric dextran-maltose 3 times every 12 h. L-Serine dissolved in tap water was administered twice by oral gavage 30 min before the last 2 ethanol doses, and the mice were killed by cardiac puncture after Zoletil (10 mg/kg tiletamine, 10 mg/kg zolazepam, ip; Virbac) anesthesia 24 h after the last dose. The binge ethanol study was performed twice independently .

2.1.3.2. Chronic ethanol feeding study

Male Wistar rats (250 g) were divided into 3 groups: C, ethanol diet (E), and ethanol diet + 1% L-serine (ES). The rats were fed a standard Lieber-DeCarli ethanol diet (36% ethanol-derived calories;

Dyets) for 4 wk ; pair-fed control rats were administered dextran-maltose to match the alcohol-derived calories in the ethanol diet. For pair-feeding, 2 rats were housed in a single cage. The food intake of each cage in the E group was determined daily between 09:00 and 10:00 h, and the same amount of the food was then given on the following day to the C and ES groups. Pair-feeding was conducted throughout the study. The ethanol diet was supplemented either with or without 1% (wt:vol) L-serine for the last 2 wk.

2.1.4. Histopathologic evaluation

For Oil Red O staining, frozen liver tissues were cut into 7-mm sections and affixed to microscope slides. Sections were stained with Oil Red O solution buffer and counter-stained with Harris hematoxylin.

2.1.5. Serum biochemistry

Serum alanine aminotransferase (ALT), aspartate aminotransferase (AST), TGs, and cholesterol were monitored by standard clinical chemistry assays on a Tokyo Boeki Prestige 24I Chemistry Analyzer (Tokyo Boeki Machinery Limited). Serum and cellular total homocysteine concentrations were quantified by using an Axis Homocysteine EIA Reagent kit (Axis-Shield) following the manufacturers' protocol with SpectraMax 340 (Molecular Devices).

2.1.6. TG analysis

Liver and cellular TGs were determined by a modified Folch method by using a Serum Triglyceride Determination kit (Sigma) following the manufacturers protocol.

2.1.7. Determination of sulfur amino acids and metabolites

Liver homogenates were diluted, and denatured protein was removed by centrifugation at 10,000 g for 10 min; the supernatant was used to measure hepatic homocysteine, SAM, SAH, cysteine and GSH. An HPLC method was used to determine SAM and SAH, and total homocysteine, total cysteine, and total GSH were quantified by the 7-benzo-2-oxa-1,3-diazole-4-sulfonic acid (SBD-F) method. For hepatic methionine and cystathionine analysis, liver homogenates were diluted in ice-cold methanol. They were then derivatized with O-phthalaldehyde/2-mercaptoethanol and quantified by using an HPLC (SCL-10A; Shimadzu) system with a fluorescence detector (RF-10AXL, Ex 385 nm and Em 515 nm; Shimadzu).

2.1.8. RNA interference

AML12 cells were seeded with 2 x 10^5 cells per well in 6-well plates in medium containing 10% FBS for 24 h. The cells were transiently transfected with *Ms*, *Cbs*, and *Bhmt* small interfering RNA (siRNA; Santa Cruz Biotechnology) by using the Fugene HD Transfection Reagent (Promega) as recommended by the manufacturers protocol. After 48 h, the cells were collected for homocysteine and TG measurement.

2.1.9. Statistical analysis

All results are presented as means ± SDs. Data were evaluated by student's t-test or one-way ANOVA followed by Tukey's multiple comparison procedure or Dunnett's post-test. All data were analyzed

by GraphPad Prism 5 (GraphPad Software).

2.2. L-serine effect on SIRT1 activity

2.2.1. Cell culture

C2C12 mouse skeletal muscle cell and AML12 was obtained from the American Type Culture Collection (ATCC) and PHGDH KO-MEF cells were kindly obtained from Dr. Furuya Shigeki from Kyushu university. Cells were cultured following ATCC guidelines. C2C12 myoblasts were maintained in DMEM (Gibco BRL) containing 10% FBS and 50and AML12 cells were cultured with DMEM/F12 containing 0.005 mg/mL insulin, 0.005 mg/mL transferrin, 5 ng/mL selenium (Insulin-Transferrin-Selenium, Gibco BRL), and 40 ng/mL dexamethasone (Sigma) containing 10% FBS and 50 units/mL of penicillin and streptomycin (Antibiotic-antimycotic; Gibco BRL). To differentiate myoblast, cells were allowed to reach 90% confluence, and the media were replaced with 2% horse serum containing DMEM for 6 days. PHGDH KO-MEF cells were cultured with DMEM (Gibco BRL) containing 10% heat inactivated fetal bovine serum (FBS) and antibiotic-antimycotic.

2.2.2. NAD^+/NADH measurement

Intracellular NAD^+ and NAD were determined using NAD+/NADH Quantitation Colorimetric Kit (Biovision, Milpitas, CA) according to the manufacturer's protocols. Briefly, cells were homogenized in 200 μL acid or alkali extraction buffer to measure NAD^+ or NADH. After extraction, samples were neutralized using the opposite buffer and the

intracellular NAD and NADH were determined by enzymatic cycling reactions. The level of nucleotides were normalized by cellular protein concentrations.

2.2.3. PGC-1α deacetylation assay

To determine PGC-1α acetylation level, immunoprecipitation (IP) was performed using specific antibodies against acetyl-lysine (Cell signaling Technology) for overnight and subjected to bind protein G agarose bead (Thermo Fisher Scientific, Waltham, MA). Immunoprecipitated beads were washed with IP buffer three times and mixed with sample buffer. After centrifugation, supernatant was used for western blot analysis and PGC-1 antibody was conjugated. After overnight incubation, HRP-conjugated secondary anti-rabbit antibody were added for 2 hr and protein level was determined.

2.2.4. RNA interference

Differentiated C2C12 myotubes were transiently transfected with *Ldh* small interfering RNA (siRNA; Cell signaling) by using Lipofectamine® RNAiMax Reagent (Thermo Fischer Scientific) as recommended by the manufacturers protocol.

2.2.5. Quantitative Real-time Polymerase Chain Reaction (qRT-PCR)

For qRT-PCR, total RNA was prepared from animal livers or C2C12 myotubes using Easy-Blue™ Total RNA Extraction Kit (Intron Biotechnology, Seoul, Korea). After RNA extraction, cDNA was produced using QuantiTect Reverse Transcription Kit (Qiagen, Hilden,

Germany). The resulting cDNA was amplified by qRT-PCR using iTaq™ Universal SYBR® Green Supermix Kit (Bio-rad, Hercules, CA) in a Stepone™ Real-Time PCR System (Applied Biosystems. Seoul, Korea).

2.2.6. Mitotracker Red staining

C2C12 myotubes differentiated in 96 black well plates are stained by MitoTracker® red dye. Cells were added warmed staining media containing MitoTracker® Red CMXRos probe (Invitrogen, Carlsbad, CA) for 30 minutes. Then, cells were washed with fresh growth media and incubated with 4% formaldehyde containing Hoechst33258 (Invitrogen) for 10 minutes. After fixation, cells were rinsed twice with DPBS and analyzed by fluorescence detection.

2.2.7. Mitochondrial DNA quantification

Genomic DNA was extracted by QIAamp® DNA Mini Kit (Qiagen) from C2C12 myocytes. To quantify mtDNA, cytochrome b primers was used and to quantify nuclear DNA, 18s rRNA primers were used.

2.2.8. ATP measurements

C2C12 myotubes differentiated in a 96 white well plate and after 24 hr L-serine treatment, the plate was incubated at room temperature for 30 minutes and added with CellTiter-Glo® in 100 μL per well. After mixing contents, luminescence was detected by Centro LB960 luminometer.

2.2.9. Oxygen consumption ratio (OCR) measurements

OCR was measured using Extracellular Flux Analyzers XFp (Agilent Technologies, Santa Clara, CA). C2C12 differentiated in XFp cell culture miniplates were treated with L-serine, fatty acids, and resveratrol were washed twice with assay media and incubated in a CO2 free incubator at 37℃ 30 minutes prior to the assay. After incubation, the culture plate and drug catridge were injected according to the XFp analyzers.

2.2.10. Nile red assay

After treatment, C2C12 myotubes were fixed in paraformaldehyde containing Hoechst 33258 for 10 minutes at room temperature. Then paraformaldehyde was removed and cells were washed with Dulbacco's modified phosphate-buffered saline (DPBS) twice. DPBS containing nile red solution was added and incubated for 10 minutes and washed with DPBS. Fluorescence was measured using a microplated fluorexcence reader at the excitation/emission wavelengths of 470/580 nm. Data was normalized by Hoechst 33258 determined at the excitation/emission wavelengths of 365/488 nm.

2.2.11. Western blot analysis

Western blotting was basically performed by established procedures using specific antibodies against pAkt, Akt, GLUT4, APTase and β-Actin (Cell signaling Technology, Beverly, MA) and HRP-conjugated secondary anti-rabbit or anti-mouse antibody (Cell Signaling Technology).

2.2.12. Membrane fraction

To confirm GLUT4 membrane translocation, subcellular fractionation was performed according to Li et al (Braz J Med Biol Res, 2015). Cells were washed with cold DPBS twice and suspended in cold sample preparation buffer, sonicated, and centrifuged at 100,000 g for 1 hr at 4 ℃. Supernatant was removed and remained pellet was resuspended in 0.5% Triton X added homogenization buffer and incubated on ice for 1 hr. After centrifuge, the supernatant was kept as the plasma membrane fraction.

2.2.13. Statistical analysis

All results are presented as means ± SDs. Data were evaluated by student's t-test or one-way ANOVA followed by Tukey's multiple comparison procedure or Dunnett's post-test. All data were analyzed by GraphPad Prism 5 (GraphPad Software).

2.3. Down-regulation of PHGDH in fatty liver disease.

2.3.1. Animal experiments

Animals used in the study were purchased from Japan SLC, Inc. housed in an air-conditioned room (24℃) with a 12-h light/dark cycle, and acclimatized over 1 wk to a nonpurified diet. The experiments using animals were carried out in accordance with animal experiment guidelines with the approval of the Institutional Animal Care and Use Committee of Seoul National University.

2.3.1.1. Chronic ethanol feeding study

Male Wistar rats (250 g) were fed a standard Lieber-DeCarli ethanol diet (36% ethanol-derived calories; Dyets) for 4 wk ; pair-fed control rats were administered dextran-maltose to match the alcohol-derived calories in the ethanol diet. For pair-feeding, 2 rats were housed in a single cage. The food intake of each cage in the ethanol group was determined daily between 09:00 and 10:00 h, and the same amount of the food was then given on the following day to the C and ES groups. Pair-feeding was conducted throughout the study.

2.3.1.2. High-fat diet study

Male C57BL/6 mice were purchased from SLC Inc. (Hamamatsu, Japan) and housed in an air-conditioned room (24 °C) with a 12 h light/dark cycle. Mice were fed with lard-based high fat diet (60% of calories derived from fat; Research Diets, Inc., NJ, USA) for 6 weeks. Pair-feeding was conducted throughout the study.

2.3.1.3. Methionine-choline deficient (MCD) diet study

Male C57BL/6 mice were purchased from SLC Inc. (Hamamatsu, Japan) and housed in an air-conditioned room (24 °C) with a 12 h light/dark cycle. Mice were fed with methionine choline deficient diet (Research Diets, Inc., NJ, USA) for 4 weeks. pair-fed control mice were administered dextran-maltose to match the alcohol-derived calories in the ethanol diet.Pair-feeding was conducted throughout the study.

2.3.2. Quantitative Real-time Polymerase Chain Reaction (qRT-PCR)

For qRT-PCR, total RNA was prepared from animal livers or C2C12 myotubes using Easy-Blue™ Total RNA Extraction Kit (Intron Biotechnology). After RNA extraction, cDNA was produced using QuantiTect Reverse Transcription Kit (Qiagen). The resulting cDNA was amplified by qRT-PCR using iTaq™ Universal SYBR® Green Supermix Kit (Bio-rad) in a Stepone™ Real-Time PCR System (Applied Biosystems. Seoul, Korea).

2.3.3. Primary hepatocyte isolation

Primary hepatocytes were isolated by a two-step collagenase perfusion as dexcribed previously (LeCluyse et al., 1996). Briefly, after anesthesia, abdominal cavitiy of mouse was opened and portal vein was cannulated with catheter and perfused with Hank's balanced salt solution (HBSS; Gibco BRL). As soon as the liver is swelling, inferior vena cava was cut. When the blood from the liver is completely removed, $CaCl_2$ solution containing collagenase was perfused. After collagen perfusion, the liver was extracted and hepatocytes were suspended in digestion media. The suspension was sieved and centrifuged and cell pellet was washed twice with culture media. Cell viability was determined by trypan blue exclusion and cells were used when 90-95% cell viability was confirmed. Cells were incubated in a 37°C incubator in an atmosphere of 5 % CO_2 in air.

2.3.4. Western blot analysis

Western blotting was basically performed by established procedures

using specific antibodies against PHGDH and β-Actin (Cell signaling Technology, Beverly, MA) and HRP-conjugated secondary anti-rabbit or anti-mouse antibody (Cell Signaling Technology).

2.3.5. Clinical data from fatty liver disease patients

Serum from twenty control group and sixty-eight fatty liver disease patients were provided by Dr. Dae Won Jun from Hanyang University college of medicine and serum amino acid analysis was performed by Sang Kyum Kim from Chungnam National University. Data were provided by nd analyzed with GraphPad Prism 5 (GraphPad Software).

2.3.6. Cell culture

AML12 was obtained from the American Type Culture Collection (ATCC) and PHGDH KO-MEF cells were kindly obtained from Dr. Furuya Shigeki from Kyushu university. Cells were cultured following ATCC guidelines. Briefly, AML12 cells were cultured with DMEM/F12 containing 0.005 mg/mL insulin, 0.005 mg/mL transferrin, 5 ng/mL selenium (Insulin-Transferrin-Selenium, Gibco BRL), and 40 ng/mL dexamethasone (Sigma) containing 10% heat inactivated fetal bovine serum (FBS; Gibco BRL), 50 units/mL of penicillin, and 50 units/mL of penicillin and streptomycin (Antibiotic-antimycotic; Gibco BRL). PHGDH KO-MEF cells were cultured with DMEM (Gibco BRL) containing 10% heat inactivated fetal bovine serum (FBS) and antibiotic-antimycotic.

2.3.7. NAD^+/NADH measurement

Intracellular NAD^+ and NAD were determined using NAD^+/NADH Quantitation Colorimetric Kit (Biovision, Milpitas, CA) according to the manufacturer's protocols. Briefly, cells were homogenized in 200 μL acid or alkali extraction buffer to measure NAD^+ or NADH. After extraction, samples were neutralized using the opposite buffer and the intracellular NAD^+ and NADH were determined by enzymatic cycling reactions. The level of nucleotides were normalized by cellular protein concentrations.

2.3.8. PGC-1α deacetylation assay

To determine PGC-1α acetylation level, immunoprecipitation (IP) was performed using specific antibodies against acetyl-lysine (Cell signaling Technology) for overnight and subjected to bind protein G agarose bead (Thermo Fisher Scientific). Immunoprecipitated beads were washed with IP buffer three times and mixed with sample buffer. After centrifugation, supernatant was used for western blot analysis and PGC-1 antibody was conjugated. After overnight incubation, HRP-conjugated secondary anti-rabbit antibody were added for 2 hr and protein level was determined.

2.3.9. Nile red assay and TG analysis

Cells were plated into black 96-well plates and after treatment, cells were fixed in paraformaldehyde containing Hoechst 33258 for 10 minutes at room temperature. Then paraformaldehyde was removed and cells were washed with DPBS twice. DPBS containing nile red solution was added and incubated for 10 minutes and washed with DPBS. Fluorescence was measured using a microplated fluorexcence

reader at the excitation/emission wavelengths of 470/580 nm. Data was normalized by Hoechst 33258 determined at the excitation/emission wavelengths of 365/488 nm.

Cellular TGs were determined by a modified Folch method by using a Serum Triglyceride Determination kit (Sigma) following the manufacturers protocol.

2.3.10. Transient transfection and RNA interference

Cells were transfected with PHGDH expression vector using Lipofectamine 2000 (Invitrogen) as recommended by the manufacturer's protocol. For RNA interference, cells were seeded with 2 x 10^5 cells per well in 6 well plates in medium containing 10% FBS for 24 h. The cells were transiently transfected with *Phgdh* siRNA (Cell signaling) by using Lipofectamine® RNAiMax Reagent (Thermo Fischer Scientific) as recommended by the manufacturers protocol.

2.3.11. Statistical analysis

All results are presented as means ± SDs. Data were evaluated by student's t-test or one-way ANOVA followed by Tukey's multiple comparison procedure or Dunnett's post-test. All data were analyzed by GraphPad Prism 5 (GraphPad Software).

2.4. The mechanism of regulating PHGDH

2.4.1. Bisulfite conversion

DNA was prepared by QIAamp® DNA Mini Kit (Qiagen) from cells

and tissues. Bisulfite conversion of DNA was performed using EpiTect Bisulfite Conversion Kit by manufacturer's protocol. Briefly, DNA was prepared with bisulfite reaction mixture through denaturation procedure. Bisulfited DNA was centrifuged and washed with washing buffer and eluted with DNA spin column and elution buffer. Eluted bisulfite converted DNA was amplified by specific primers.

2.4.2. Histone H3 and H4 acetylation assay

For the measurement of global histone H3 and H4 acetylation from cells and tissues, histone H3 and H4 acetylation assay kit (Abcam) was used by manufcaturer's protocols. Briefly, cell lysis and tissue disaggregation were performed by lysis buffer. By incubating extraction buffer/glycerol solution, extracted histone was coated onto assay wells. After washing, capture antibody and detection antibody was added. By treating developing solution, color was developed and absorbance was measured.

2.4.3. Western blot analysis

Western blotting was basically performed by established procedures using specific antibodies against PHGDH, Ace-H3K9, NRF2 and β-Actin (Cell signaling Technology, Beverly, MA) and HRP-conjugated secondary anti-rabbit or anti-mouse antibody (Cell Signaling Technology).

2.4.4. Statistical analysis

All results are presented as means ± SDs. Data were evaluated by student's t-test or one-way ANOVA followed by Tukey's multiple

comparison procedure or Dunnett's post-test. All data were analyzed by GraphPad Prism 5 (GraphPad Software).

III. Results

3.1. L-serine reverses alcoholic fatty liver

3.1.1. L-serine decreased ethanol-induced lipid accumulation

Previous study revealed that hepatic L-serine was significantly decreased in alcoholic liver disease model. First, L-serine was treated with ethanol in AML12 cells to identify the effect of L-serine on lipid accumulation. Ethanol treatment increased intracellular lipid about 2 fold and L-serine reversed lipid staining concentration-dependently (Figure 7).

To confirm the effects of L-serine in vivo, mouse ethanol binge model was used. Oil red O staining revealed that 3 times of ethanol gavage caused fatty liver and L-serine decreased lipid accumulation. 200 mg/kg of L-serine decreased ALT, which is a biomarker of liver dysfunction and hepatic TG (Figure 8). Next, the effect of L-serine was identified in chronic ethanol model. Rats were fed with Lieber-DeCarli ethanol diet to induce fatty liver and L-serine was treated last 2 weeks of ethanol diet. Lieber-DeCarli ethanol diet significantly increased lipid droplets and serum ALT. L-serine decreased these effects dose-dependently (Figure 9).

The decreased concentrations of SAM and GSH observed in the ethanol group were completely recovered in the L-serine treated rat group. As a result, the SAM:SAH ratio was also restored in the L-serine group (Table 3).

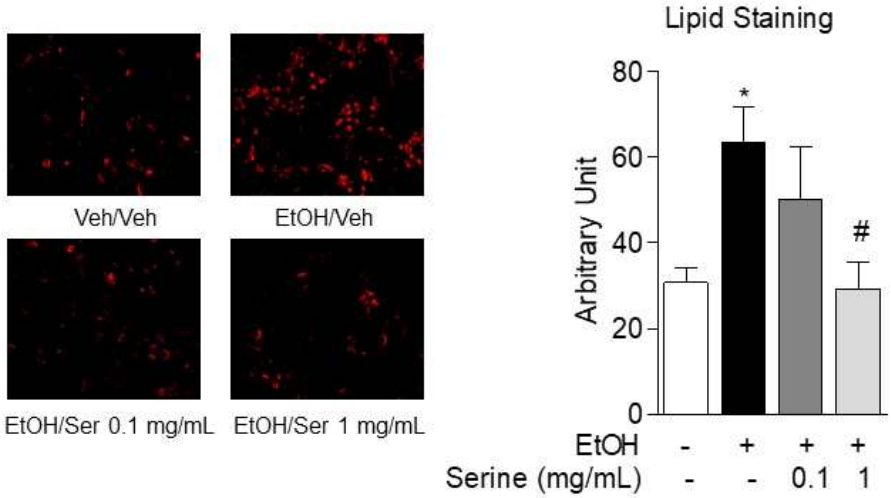

Figure 7. Nile red staining of ethanol-treated AML12 cells.

AML12 cells were treated with 100 mM ethanol with or without indicated concentrations of L-serine for 48 hr. Microscopic images of cells were shown in left panel. Right panel shows the quantification of nile red staining. Values in graph are means ± SDs, n = 3 of three independent experiments. Within each graph, * represents significance (*; $P < 0.05$) relative to the control group; # represents significance (#; $P < 0.05$) relative to the ethanol group. Statistical analysis was performed by using one-way ANOVA with Tukey's multiple-comparison procedure.

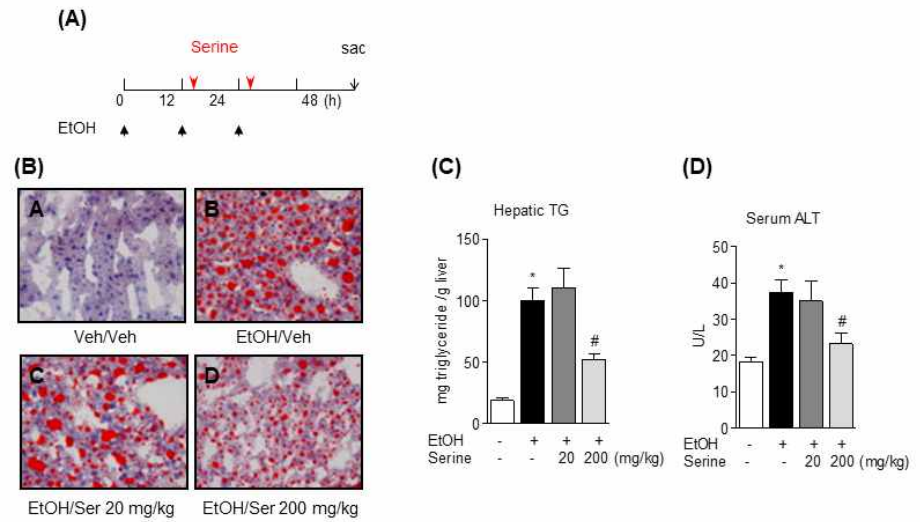

Figure 8. L-serine ameliorates binge ethanol induced fatty liver.

Binge ethanol feeding was performed as described in Materials and Methods section. Graphical protocol was described in (A). Below are Oil red O staining of the livers (B), hepatic TG (C) and serum ALT (D) in the binge ethanol study. Values in panels C-D are means ± SDs, n = 3 mice per group. Within each graph, * represents significance (*; $P < 0.05$) relative to the control group; # represents significance (#; $P < 0.05$) relative to the ethanol group. Statistical analysis was performed by using one-way ANOVA with Tukey's multiple-comparison procedure.

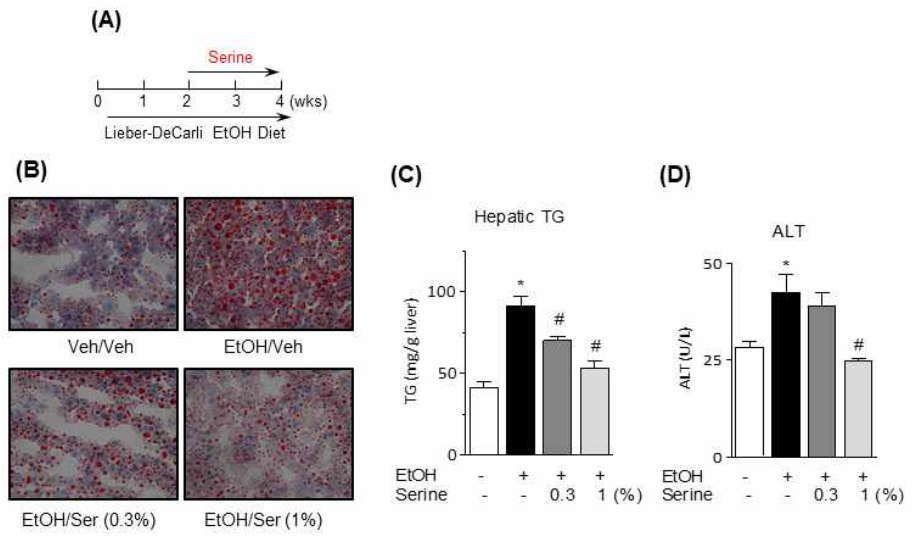

Figure 9. L-serine ameliorates chronic ethanol feeding-induced fatty liver.

Chronic ethanol feeding by Lieber-DeCarli ethanol diet was performed as described in Materials and Methods section. Graphical protocol is described in left upper panel (A). Below are Oil red O staining of the livers (B), hepatic TG (C) and serum ALT (D) in the chronic ethanol feeding study. Values in panels C-D are means ± SDs, n = 8~10 rats per group. Within each graph, * represents significance (*; $P < 0.05$) relative to the control group; # represents significance (#; $P < 0.05$) relative to the ethanol group. Statistical analysis was performed by using one-way ANOVA with Tukey's multiple-comparison procedure.

Table 3. Concentrations of sulfur amino acids and metabolites in the liver obtained from binge ethanol study and chronic ethanol feeding study.

	Binge ethanol study (mice)				Chronic ethanol study (rats)		
Variable	Con	EtOH	EtOH +Ser20	EtOH +Ser200	Con	EtOH	EtOH+Ser
Cysteine	287±52.8	277±157	404±178	408±323	584±98.9	488±92.4	494±151
SAM	59.3±29.5	25.2±23.6	45.3±22.4	50.1±15.9	54.8±3.4	28.4±3.5*	55.1±8.8#
SAH	26.2±0.5	31.1±12.9	25.4±3.4	34.7±5.2	19.5±3.9	21.8±1.1	17.1±0.7
SAM:SAH	2.31±1.1	1.0±1.1	1.9±1.1	1.5±0.7	2.9±0.6	1.3±0.1*	3.2±0.4#
Methionine	670±175	733±391	427±91.1	627±165	1380±398	924±356	812±147
Cystathionine	39.6±4.7	24.4±1.5	27.9±14.6	25.9±6.2	30.9±6.7	14.6±1.9*	18.3±3.4
GSH	6.6±1.3	6.0±3.4	8.8±0.6	8.9±0.5	7.7±0.5	6.2±0.4*	8.1±0.7#

Values are means ± SDs, n = 3 mice and rats per group. Data were analyzed by 1-way ANOVA followed by Tukey's multiple comparison procedure. Homocysteine in rat liver and cystathionine in mouse liver were analyzed by Kurskal-Wallis test because of unequal variance. * represents significance (* ; $P < 0.05$) relative to the control and # represents significance (# ; $P < 0.05$) relative to the ethanol group.

3.1.2. L-serine inhibited homocysteine by MS and CβS-dependent homocysteine metabolism

L-serine is used as a precursor of one-carbon donor. Homocysteine is known to induce fatty liver disease and trans-methylation pathway is important in metabolizing homocysteine. To identify whether the effect of L-serine on alcoholic fatty liver is associated with homocysteine metabolism, homocysteine or methionine treated in vitro model was used. When AML12 cells were treated with homocysteine or methionine, intracellular homocysteine and lipid accumulation were observed. L-serine reversed homocysteine- or methionine-induced up-regulated homocysteine and lipid levels (Figure 10).

Homocysteine metabolism is achieved by three enzymes including MS, CβS, and BHMT which convert homocysteine to methionine or cysteine via trans-methylation or trans-sulfuration pathway. To identify which enzyme is related with L-serine effect on homocysteine and lipid accumulation, siRNA knockdown experiment was performed. When each enzyme of homocysteine metabolism was blocked with siRNA, homocysteine and lipid accumulation were increased and L-serine reversed these effects only when BHMT was knockdown. When MS and CβS expression was blocked, L-serine had no effect on homocysteine and lipid accumulation. These results imply that MS and CβS use L-serine to metabolize homocysteine (Figure 11).

To confirm these in vitro effects of L-serine on in vivo, the serum and hepatic levels of homocysteine of binge ethanol treated mice and chronic Lieber-DeCarli ethanol diet treated rats were investigated. L-serine significantly and dose-dependently decreased homocysteine in the serum and livers (Figure 12).

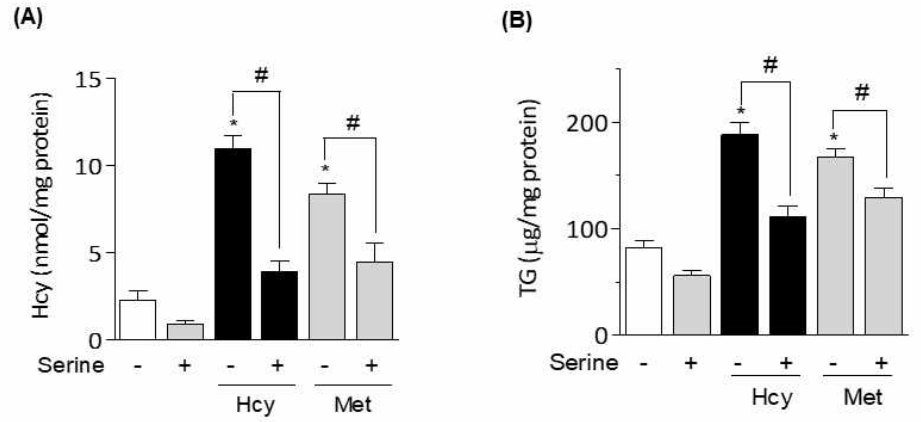

Figure 10. L-serine lowered homocysteine and lipid in AML12 cells.

Intracellular total homocysteine (A) and TG (B) concentrations in homocysteine (5 mM) or methionine (5 mM)-treated AML12 cells in the absence or presence of L-serine (1 mg/mL) for 24 hr. Homocysteine and TG concentrations were normalized by intracellular proteins. Values are means ± SDs, n = 3 (means of triplicates). Within each graph, * represents significance (*; $P < 0.05$) relative to the control group; # represents significance (#; $P < 0.05$) relative to the homocysteine or methionine group. Statistical analysis was performed by using 2-way ANOVA with Bonferroni's multiple-comparison procedure.

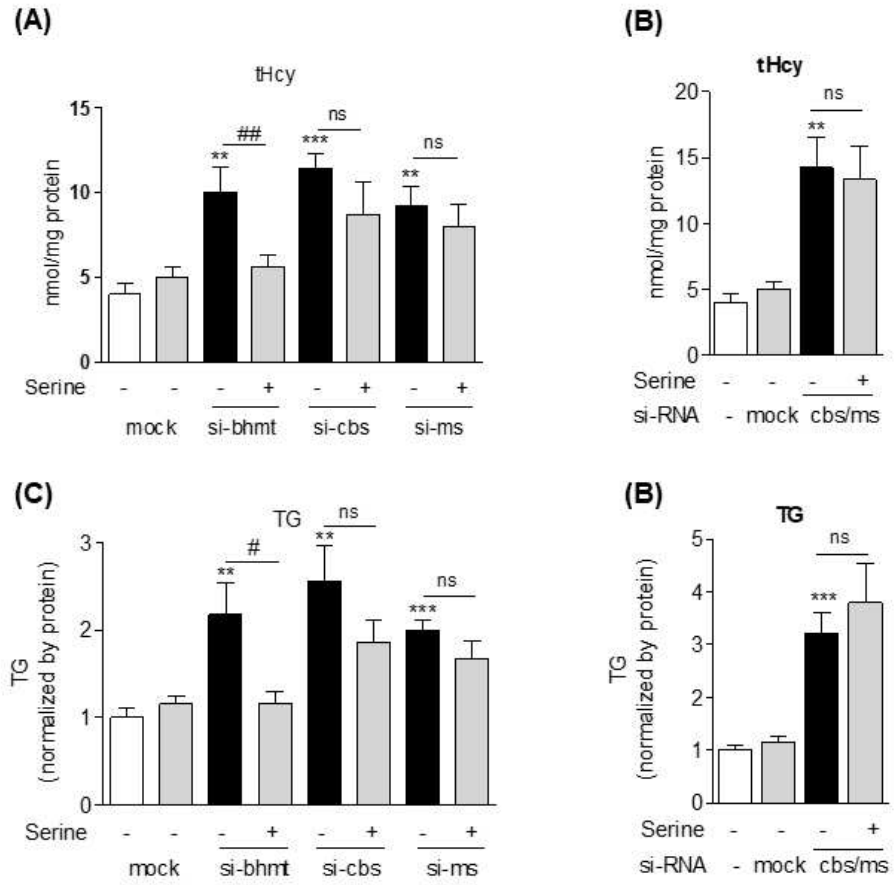

Figure 11. L-serine decreased homocysteine and TG on homocysteine only when MS and/or CβS activity are intact.

Intracellular total homocysteine and TGs in *Bhmt*-, *Cbs*-, or *Ms*-siRNA transfected AML12 cells (A, C) and *Ms*/*Cbs*-siRNA co-transfected AML12 cells (B, D) in the absence or presence of L-serine (1 mg/mL). Homocysteine and TG concentrations were normalized by intracellular proteins. Values are means ± SDs, n = 3 (means of triplicates). Within each graph, ** and *** represent significance (**; $P < 0.01$, ***; $P < 0.001$) relative to the control group; # and ## represent significance (#; $P < 0.05$, ##; $P < 0.01$). ns means 'not significant'. Statistical analysis was performed by using 2-way ANOVA with Bonferroni's multiple-comparison procedure.

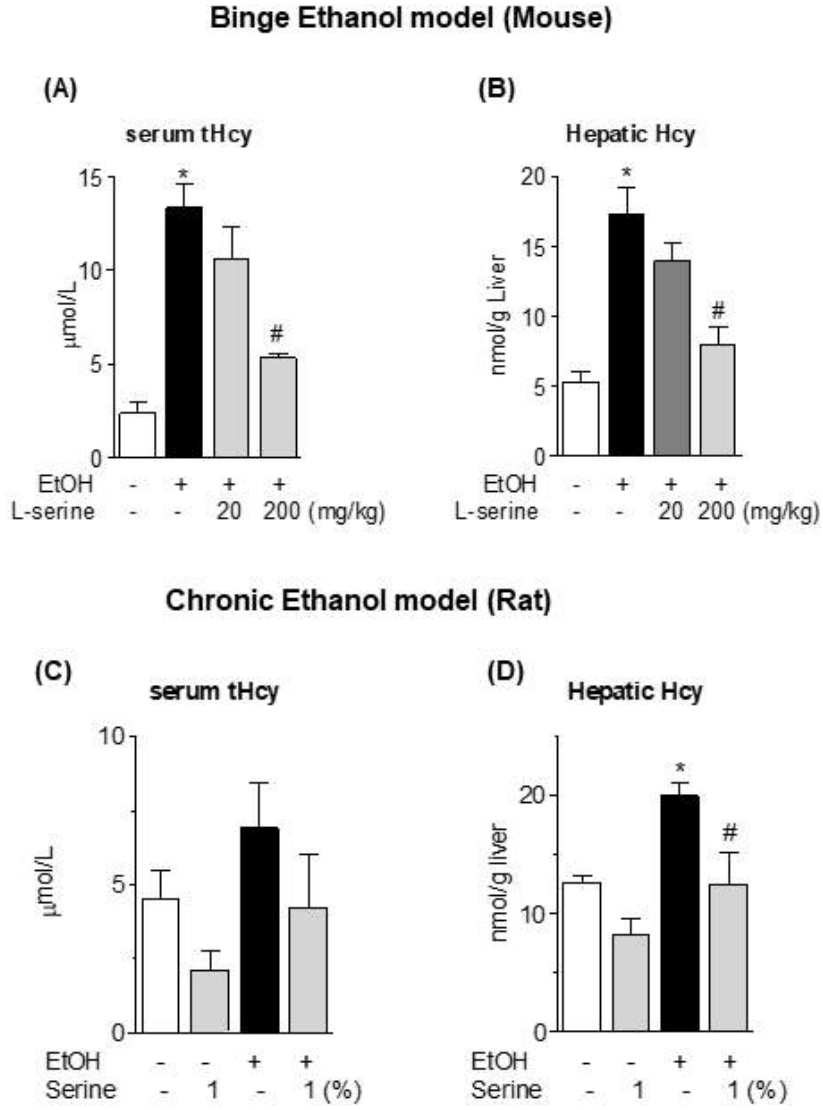

Figure 12. L-serine decreased serum and hepatic homocysteine in binge ethanol and chronic ethanol model.

Serum total homocysteine and hepatic homocysteine in the binge ethanol (A, B) and the chronic ethanol (C, D) study. Values are means ± SDs, n = 3 mice or 8~10 rats per group. Within each graph, * represents significance (*; $P < 0.05$) relative to the control group; # represents significance (#; $P < 0.05$) relative to the ethanol group. Statistical analysis was performed by using one-way ANOVA with Tukey's multiple-comparison procedure.

3.2. L-serine up-regulates SIRT1 activity

3.2.1. L-serine increases intracellular NAD^+ by lactate dehydrogenase and SIRT1 activity.

To investigate whether L-serine can increase NAD^+ and up-regulate SIRT1 activity, C2C12 myocytes which highly express SIRT1 and have active metabolic capacity were treated with L-serine. After 24 hr treatment, intracellular NAD^+ and the acetylation of PGC-1α was detected. Because PGC-1α is a substrate of SIRT1, PGC-1α can be deacetylated by the increasing activity of SIRT1. As a result, L-serine increased NAD^+ and deacetylated PGC-1α concentration-dependently which implies up-regulated SIRT1 activity (Figure 13).

To find how L-serine can increase NAD^+, lactate dehydrogenase (LDH) activity was blocked by sodium oxamate or si-*Ldh* transfection. LDH inhibition by both sodium oxamate and si-*Ldh* reversed L-serine induced increase in NAD^+ and SIRT1 activity (Figure 14).

These results showed that L-serine can increase intracellular NAD^+ by lactate dehydrogenase and SiRT1 activity.

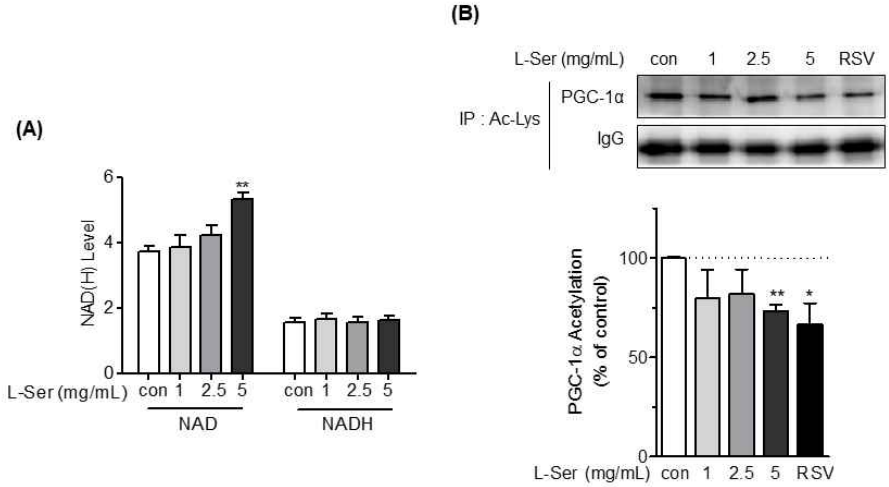

Figure 13. L-serine up-regulates intracellular NAD^+ and SIRT1 activity.

L-serine was treated at the indicated concentrations in C2C12 myotubes for 24 hr. Intracellular NAD^+ and NADH were measured (A). C2C12 myotubes were treated with L-serine (suggested concentrations) for 24 hr and 50 μM resveratrol (RSV) for 6 hr. Then, acetylation status of PGC-1α was measured using immunoprecipitation and quantification graph is suggested below (B). Values are means ± SDs, n = 3 of three independent experiments. * and ** represent significance (*; $P < 0.05$, **; $P < 0.01$) relative to the control group using one-way ANOVA with Dunnett's post tests.

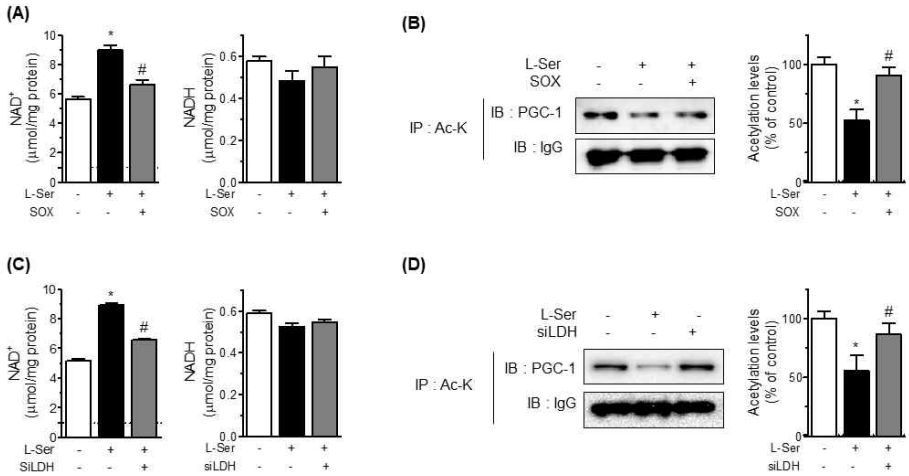

Figure 14. L-serine mediated increases in NAD$^+$ and SIRT1 activity are mediated by lactate dehydrogenase.

L-serine and sodium oxamate (SOX) were treated in C2C12 myotubes for 24 hr. Intracellular NAD$^+$ and NADH (A) and the acetylation status of PGC-1α (B) were measured. C2C12 myotubes were transfected with si-*Ldh* and 5 mg/mL L-serine was treated for 24 hr. Then, intracellular NAD$^+$ and NADH (C) and the acetylation status of PGC-1α was measured using immunoprecipitation (D). Values are means ± SDs, n = 3 of three independent experiments. * represents significance (*; $P < 0.05$) relative to the control and # represents significance (#; $P < 0.05$) relative to the L-serine treatment group using one-way ANOVA with Tukey's post tests.

3.2.2. L-serine up-regulates mitochondrial mass and function.

PGC-1α is a major regulator of mitochondrial biogenesis. Because increased deacetylation of PGC-1α by SIRT1 results in up-regulated PGC-1α activity, L-serine effect on the mitochondrial gene expression was confirmed by real-time PCR. *Cytochrome c, ATP synthase subunit β, and Tfam* gene expression were increased by L-serine and mitochondrial mass, which was detected by Mitotracker red, was also up-regulated. As a result, mitochondrial function was also improved which was detected by measuring intracellular ATP levels and oxygen consumption rate (Figure 15).

SIRT1 also has anti-steatotic effect by inhibiting fatty acid synthesis and increasing lipid β-oxidation. To find SIRT1 activating effect of L-serine on lipid β-oxidation, oleic acid-induced lipid accumulation and L-serine mediated oxygen consumption ratio were measured. As a result, L-serine concentration-dependently decreased oleic acid-induced intracellular triglyceride level and up-regulated oxygen consumption ratio (Figure 16).

SIRT1 is one of a key metabolic regulator and known to improve insulin resistance and fatty liver (Schenk et al., 2011; Colak et al., 2011). To identify whether L-serine has insulin sensitizing effect, in vitro model which uses palmitic acid as a insulin resistance inducer was used. Palmitic acid reduced the phosphorylation status of Akt and translocation of GLUT4, which is a major glucose transporter in muscle tissues. L-serine reversed the phosphorylation status of Akt and also increased GLUT4 membrane translocation (Figure 17). EX-527, which is known as a SIRT1 inhibitor, blocked L-serine induced phosphorylation of Akt.

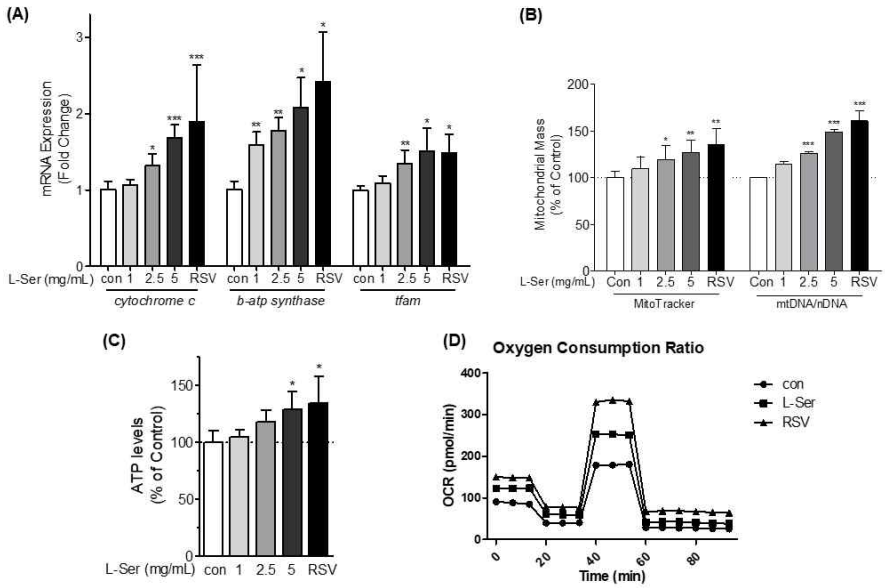

Figure 15. L-serine increases mitochondrial mass and function.

C2C12 myotubes were treated with L-serine at the indicated concentrations for 24 hr and 50 μM RSV for 6 hr. Total RNA was extracted from cells and mitochondrial gene expression was analyzed by real-time PCR (A). Mitochondrial mass was analyzed by Mitotracker red and mtDNA copy number (B). Mitochondrial function was measured by measuring intracellular ATP levels (C) and oxygen consumption ratio (OCR) (D). Values in are means ± SDs, n = 3 of three independent experiments. *, ** and *** represent significance (*; $P < 0.05$, **; $P < 0.01$, ***; $P < 0.001$) relative to the control group using one-way ANOVA with Dunnett's post tests.

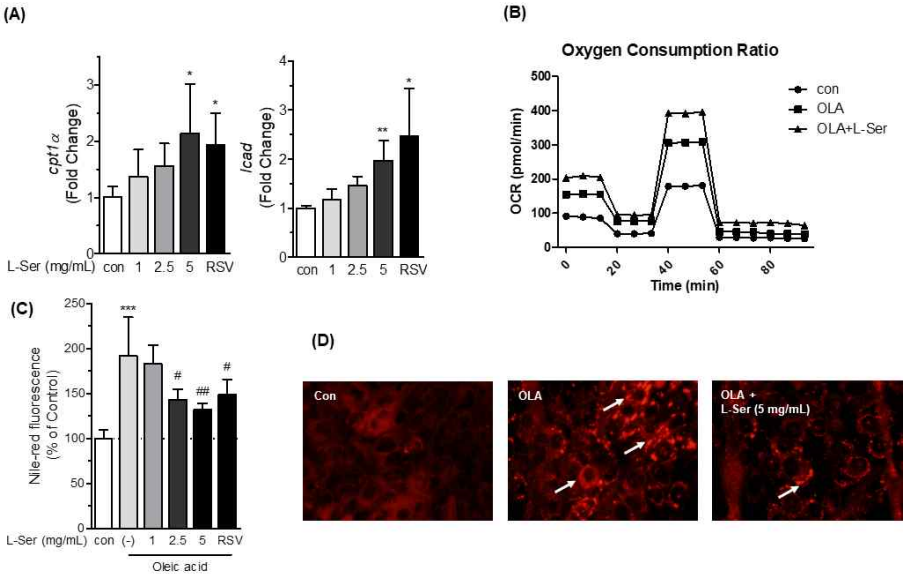

Figure 16. L-serine ameliorates oleic-acid induced lipid accumulation.

C2C12 myotubes were treated with indicated concentrations of L-serine for 24 hr and 50 uM resveratrol for 6 hr. Total RNA was extracted and *cpt1a* and *lcad* mRNA levels were measured by real-time PCR (A). C2C12 myotubes were treated with 250 uM oleic acid and 5 mg/mL L-serine and OCR was measured using Seahorse Bioscience XFp analyzer (B). C2C12 myotubes were treated with 250 uM oleic acid and indicated concentrations of L-serine and 50 uM resveratrol. Intracellular lipid droplets were quantitatively determined using nile red assay (C) and microscopic images were confirmed (D). Values in are means ± SDs, n = 3 of three independent experiments. *, ** and *** represent significance (*; $P < 0.05$, **; $P < 0.01$, ***; $P < 0.001$) relative to the control and #, and ## represent significance (#; $P < 0.05$, ##; $P < 0.01$) relative to the oleic acid group using one-way ANOVA with Tukey's post tests.

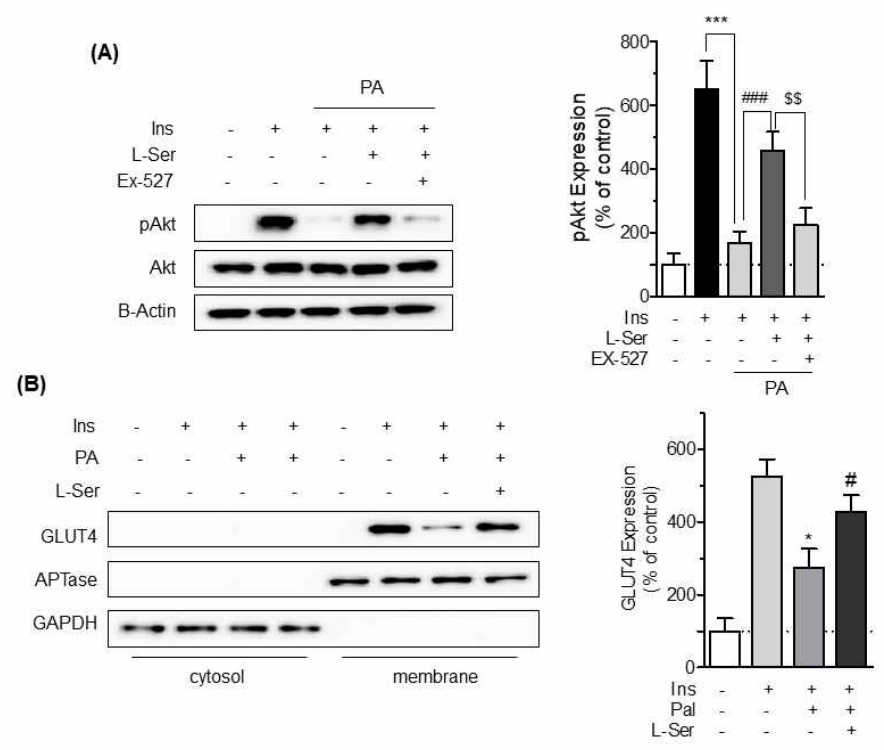

Figure 17. L-serine improved insulin resistance *in vitro*

C2C12 myoblasts were differentiated into myotubes and treated with 5 mg/mL L-serine in the absence or presence of EX-527 with 250 μM palmitic acid for 24 hr. After treatment, insulin (100 nM) was incubated for 20 minutes. Protein extracts were prepared from cell lysates and western blotting was performed to measure the levels of pAkt, Akt and B-Actin. Right panel shows the band densities determined using an image analysis system and expressed as percentages of the control (A). Total cell lysates were collected and subjected to subcellular fractionation as described in Materials and Methods. The protein levels of GLUT4, ATPase, and GAPDH were measured by western blotting. Right panel shows the band densities of GLUT4 in membrane fraction determined using an image analysis system and expressed as percentages of the control. Western blot images are representative of three independent experiments. Values are means ± SDs, n = 3 of three independent experiments. * and *** represent significance (*; $P < 0.05$, ***; $P < 0.001$) relative to the insulin group. #, and ### represent significance (#; $P < 0.05$, ###; $P < 0.001$) relative to the insulin+palmitate group. $$ represents significance ($$; P < 0.01). Statistical analysis was performed using one-way ANOVA with Tukey's post tests.

3.3. PHGDH, a rate-limiting enzyme in de novo serine synthesis, is down-regulated in fatty liver disease.

3.3.1. Hepatic L-serine synthesizing enzyme expression and L-serine level in vivo and in vitro disease model.

L-serine can be not only uptaken by dietary supply but also synthesized through de novo synthesis. To identify whether L-serine is decreased because of decreased de novo synthesizing L-serine in the liver, the expression of enzymes which are involved in de novo serine synthesis was investigated in the livers from 4 weeks of Lieber-DeCarli ethanol diet treated rats, 6 weeks of high-fat (HF) diet fed mice, and 4 weeks of methionine-choline deficient (MCD) diet fed mice. The expression of 3-phosphoglycerate dehydrogenase (PHGDH), which regulates the first step of L-serine synthesis, was significantly reduced in chronic ethanol, HF diet, and MCD diet induced fatty liver disease models (Figure 18). The down-regulated enzyme of L-serine synthesis enzyme results in the reduction of hepatic L-serine levels in Lieber-DeCarli ethanol diet-fed rats and HF diet-fed mice except MCD diet-fed mice (Figure 18).

PHGDH expression was also identified from in vitro model. Isolated hepatocytes were treated with ethanol or the mixture of free fatty acids (FFA; oleic acid:palmitic acid = 2:1). Ethanol and FFA treatment significantly decreased the mRNA and protein expression of PHGDH (Figure 19).

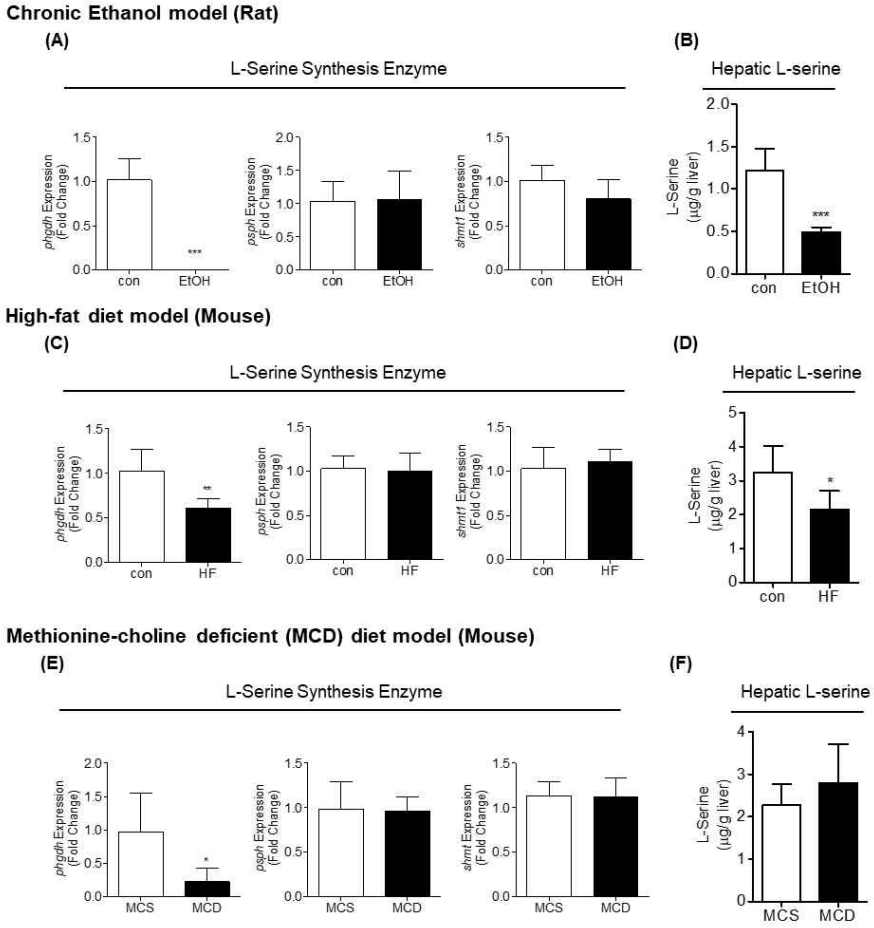

Figure 18. L-serine synthesizing enzyme, PHGDH expression and hepatic L-serine is decreased in pathological fatty liver model.

mRNA level of L-serine synthesis enzymes including *phgdh, psph, and shmt1* in the livers and hepatic L-serine were measured in the chronic ethanol study (A, B), HF diet study (C, D), and MCD diet study (E, F). Values are means ± SDs, n = 8 rats in chronic ethanol study, n = 8 mice in HF diet study, and n = 5 mice in MCD diet study per group. Within each graph, *, **, and *** represent significance (* ; $P < 0.05$, ** ; $P < 0.01$, *** ; $P < 0.001$) relative to the control group using student's *t*-test.

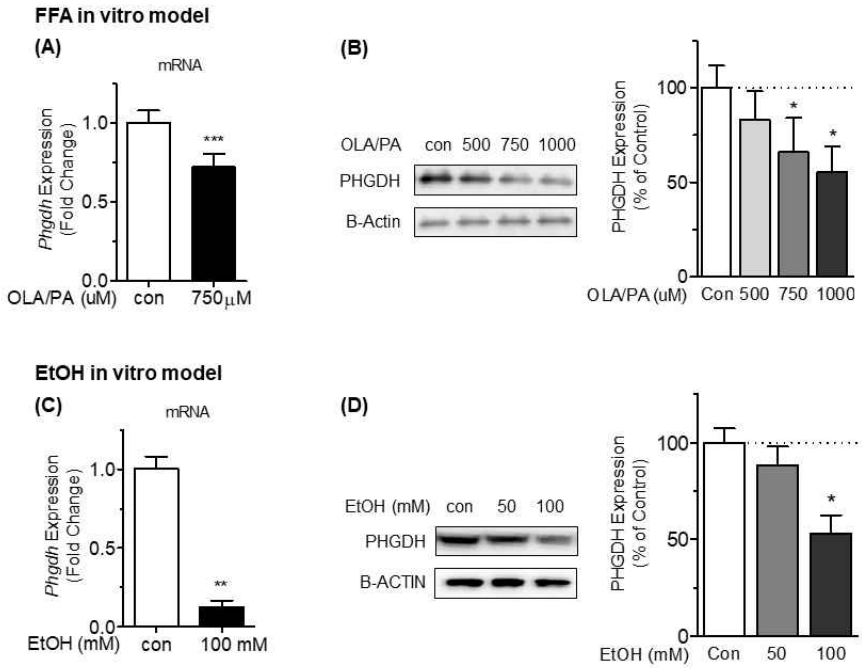

Figure 19. The expression of PHGDH was reduced by free fatty acid and ethanol treatment.

The mRNA level and protein expression of PHGDH in mouse primary hepatocytes were determined after 24 hr treatment of FFA (A, B) and ethanol (C, D). Values are means ± SDs of three independent experiments. Within each graph, *, ** and *** represent significance (* ; $P < 0.05$, ** ; $P < 0.01$, *** ; $P < 0.001$) relative to the control group using student's t-test in (A) and (C) and one-way ANOVA with Dunnett's post tests in (B) and (D).

3.3.2. Sphingolipids and ceramides level was affected in fatty liver disease.

L-Serine and palmitoyl CoA are condensed into sphinganine (SA) and L-serine deficiency was reported to elicit intracellular accumulation of cytotoxic deoxysphingolipids, including deoxysphinganine (doxSA), and deoxymethylsphinganine (doxmeSA) which are produced by palmitoyl CoA with alanine and glycine instead of L-serine (Esaki et al., 2015). To find whether L-serine deficiency in Phgdh-KO MEF cells leads to accumulate cytotoxic sphingolipids. As reported, doxSA and deoxysphingosine (doxSO) are increased by L-serine deficiency, but SA and SO (sphingosine) are decreased by L-serine deficiency (Figure 20).

These sphingolipids and ceramides are also analyzed in the livers from in vivo models. Deoxyceramide (doxCer) and deoxydihydroceramide (doxDHCer) which are abnormal form of ceramides, which are produced from doxSA, were increased in chronic ethanol model (Figure 21) implying correlation between decreased PHGDH function and increased abnormal ceramides. But in HF diet model, doxSA and doxCer level were decreased (Figure 22).

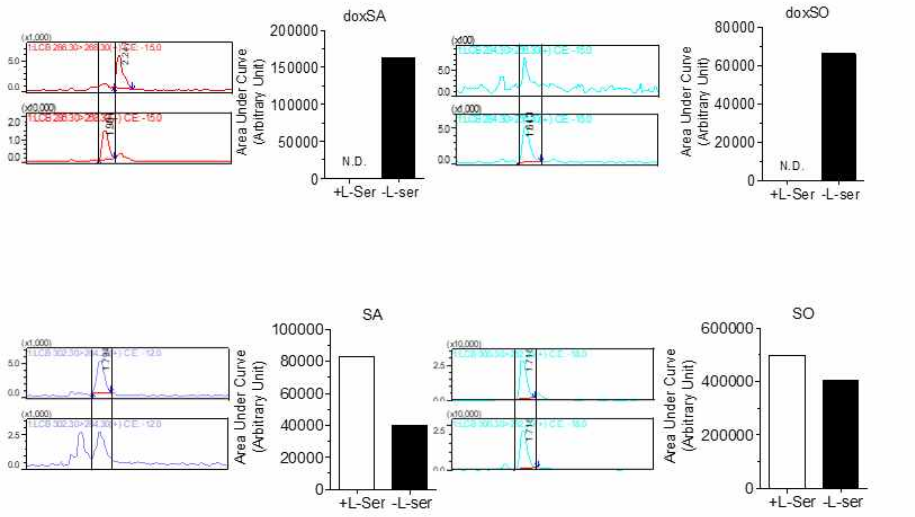

Figure 20. Deoxysphingolipids were increased in *Phgdh*-KO MEF cell.

Phgdh-KO MEF cells were incubated in L-serine sufficient control media or L-serine deficient media for 24 hr. After incubation, cell lysates were collected and doxSA (A), doxSO (B), SA (C), and SO (D) were analyzed by LC/MS. Chromatograms were presented at left side and area under the curve (AUC) were calculated on right panel.

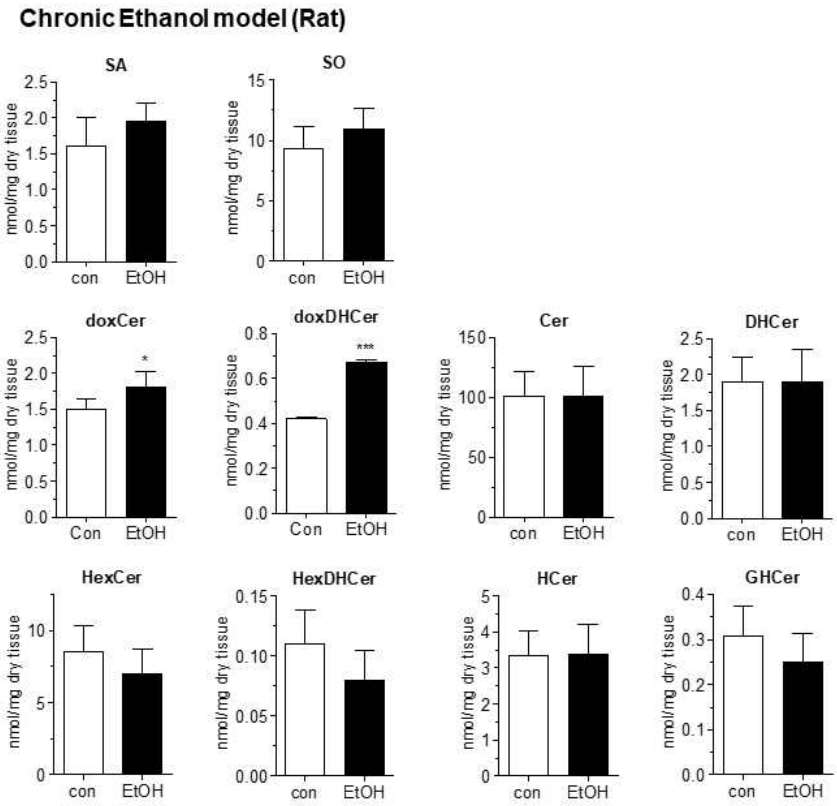

Figure 21. Chronic ethanol feeding increased deoxy-form of ceramides.

Sphingolipids (sphinganine (SA) and sphingosine (SO)) and Ceramides (deoxyceramide (doxCer), deoxydihydroceramide (doxDHCer), Ceramide (Cer), Dihydroceramide (DHCer), hexosylceramide (HexCer), hexosyldihydroceramide (HexDHCer), hydroxyceramide (HCer), and glucosylhydroxylceramide (GHCer)) were analyzed from the livers from chronic ethanol diet-fed rats. Values are means ± SDs, n = 8 rats per group. Within each graph, * and *** represent significance (* ; $P < 0.05$, *** ; $P < 0.001$) relative to the control group using student's t-test.

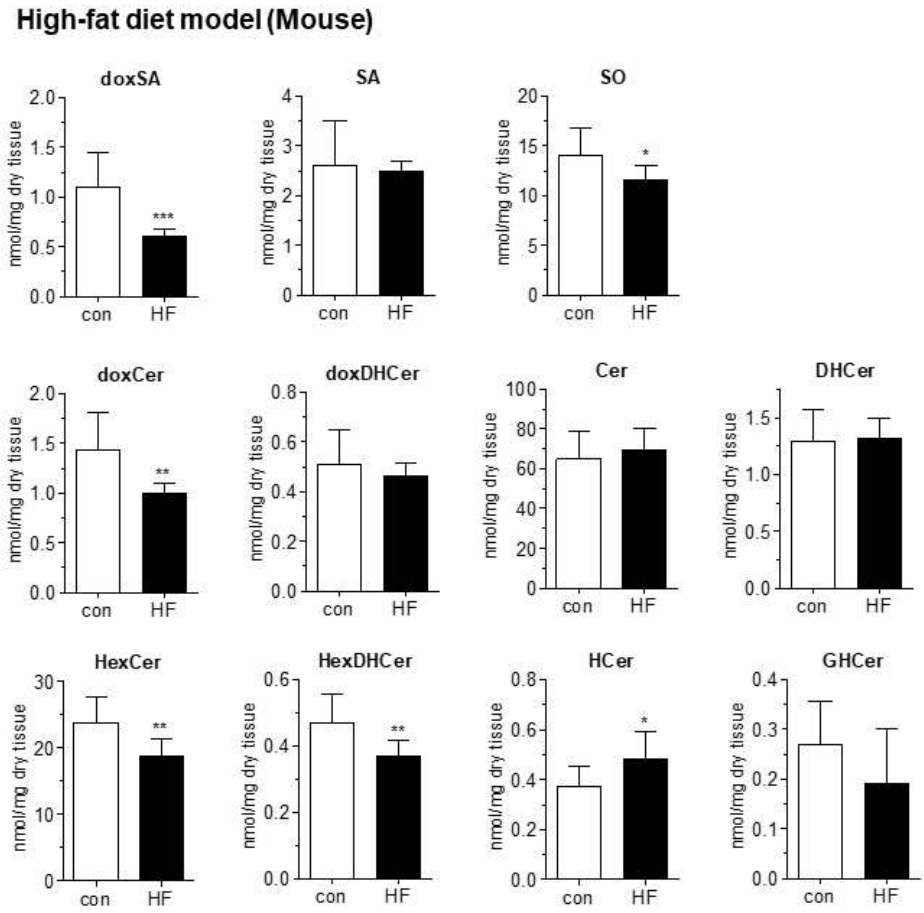

Figure 22. High-fat diet feeding decreased deoxy-form of sphingolipid and ceramide.

Sphingolipids (deoxysphinganine (doxSA), sphinganine (SA), and sphingosine (SO)) and Ceramides (deoxyceramide (doxCer), deoxydihydroceramide (doxDHCer), ceramide (Cer), dihydroceramide (DHCer), hexosylceramide (HexCer), hexosyldihydroceramide (HexDHCer), hydroxyceramide (HCer), and glucosylhydroxylceramide (GHCer)) were analyzed from the livers from HF diet-fed mice. Values are means ± SDs, n = 9-10 mice per group. Within each graph, *, **, and *** represent significance (* ; $P < 0.05$, ** ; $P < 0.01$, *** ; $P < 0.001$) relative to the control group using student's *t*-test.

3.3.3. Hepatic L-serine synthesizing enzyme expression and L-serine level in clinical patients.

To identify whether these in vitro and in vivo effects are shown clinically, first microarray data analysis was performed. GEO analysis showed that the expression of PHGDH in alcoholic steatohepatitis, non-alcoholic fatty liver patients and HBV-related non-alcoholic advanced fibrosis patients was significantly decreased (Figure 23).

And then, we measured the serum amino acid level of 20 control groups and 68 fatty liver disease patients. Serum L-serine was significantly reduced in fatty liver disease patients and the fat deposition analyzed by MRI was negatively correlated with serum L-serine level (Figure 24). The serum biomarkers of liver, kidney functions and glucose, lipid metabolism were also analyzed and some of these markers, including ALT and triglycerides are found to be negatively correlated with serum L-serine (Figure 25).

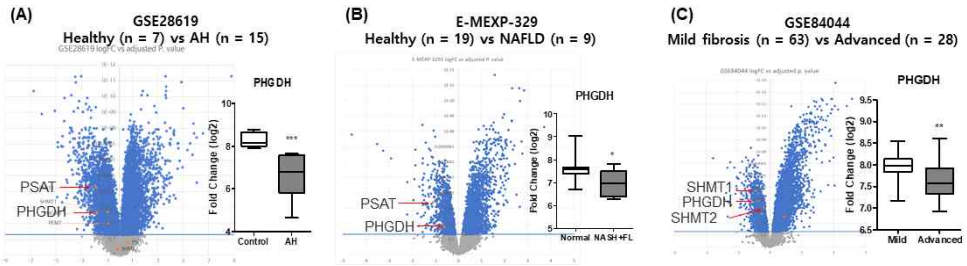

Figure 23. Microarray data analysis showed down-regulation of serine synthesis pathway in human fatty liver disease.

GEO dataset was analyzed to find statistical difference in the expression of serine synthesis pathway enzyme between healthy patients and fatty liver diseases patients. The volcano plot shows false discovery rate (FDR) adjusted P value versus log value for fold changes ($\log_2$FC) of gene enrichment. Genes associated with serine synthesis pathway are plotted in orange dots. Horizontal blue line indicates significance cut-off (Adjusted p value < 0.05). Right panel in (A), (B) and (C) shows fold change of *Phgdh* in each group. *, **, and *** represent significance (* ; P <0.05, ** ; P < 0.01, *** ; P <0.001).

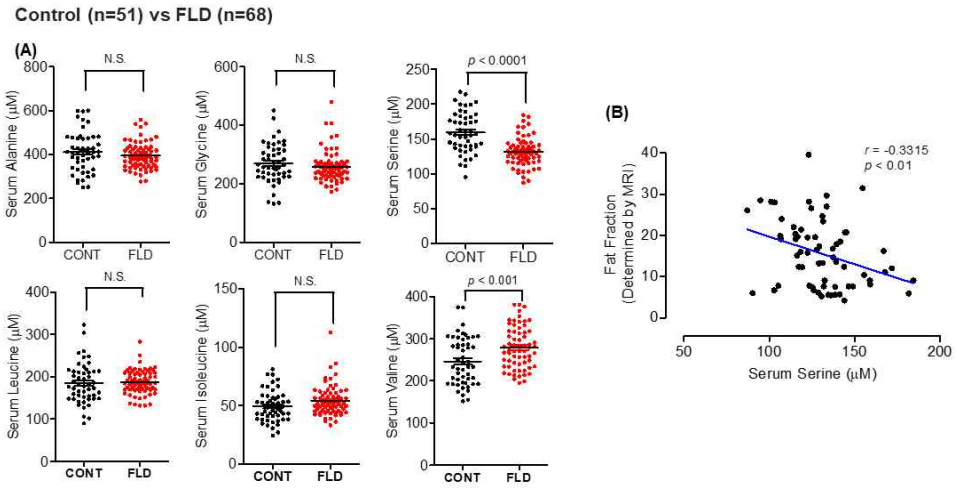

Figure 24. The serum L-serine was reduced in fatty liver disease patients and negatively correlated with fat fraction.

Serum amino acids were detected in 51 controls and 68 fatty liver disease patients (A). *P* value was suggested relative to the control group using student's *t*-test. Serum L-serine and MRI determined fat fraction were analyzed by correlation analysis (B). Pearson R value and *p* value were suggested.

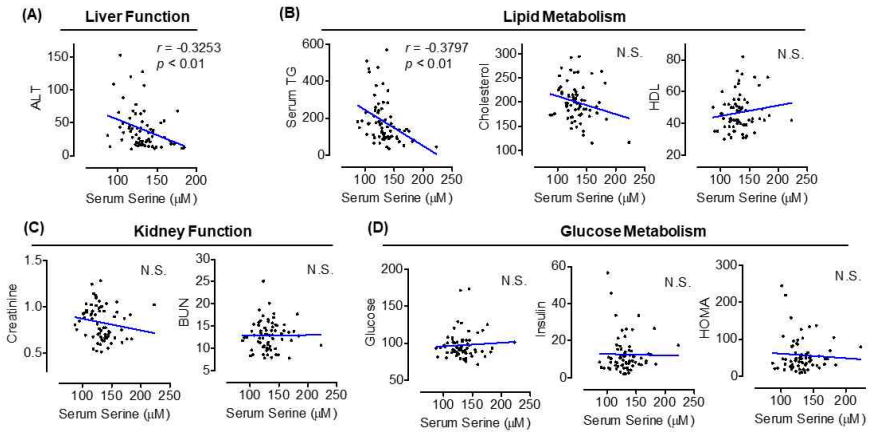

Figure 25. Serum L-serine is negatively correlated with serum ALT and TG in fatty liver disease patients.

The relationship between serum L-serine and several clinical biomarkers representing liver functions (A), lipid metabolism (B), kidney function (C) and glucose metabolism (D) was suggested by correlation analysis. Pearson R value and p value were suggested (N.S means not significant).

3.3.4. Up-regulation of L-serine and PHGDH function reverses lipid metabolism.

Because the lowered expression of PHGDH and synthesis of L-serine were confirmed in disease models and clinical patients, we assumed that FFA or L-serine deficiency may reduce L-serine level, and decreased L-serine may result in down-regulation of intracellular NAD^+. FFA and L-serine deficiency condition decreased NAD^+ and this effect was reversed by additional L-serine treatment (Figure 26). The deacetylation status of PGC-1α, implying SIRT1 activity, was decreased by L-serine deficient condition in PHGDH KO-MEF cells and the increased L-serine by transfection of PHGDH vector reversed this effect (Figure 26).

Then, the up-regulation of L-serine by amplification of PHGDH function on lipid metabolism in vitro disease models was also measured. The overexpression of PHGDH by genetic vector transfection in AML12 cells reversed the FFA-induced intracellular lipid accumulations (Figure 27). Genetic siRNA knockdown of PHGDH induced lipid accumulation and L-serine deficiency accelerated this effect. PHGDH overexpression reversed the TG accumulation in AML12 cells (Figure 27). The FFA also increased intracellular TG in primary hepatocytes and PHGDH gain of function by genetic transfection reversed that. Genetic knockout model using PHGDH knockout MEF showed that when L-serine was enough in media, there is no additional lipid accumulation, but when L-serine was depleted, PHGDH knockout induced about 2 fold TG levels. PHGDH overexpression reduced lipid accumulation to control level (Figure 27).

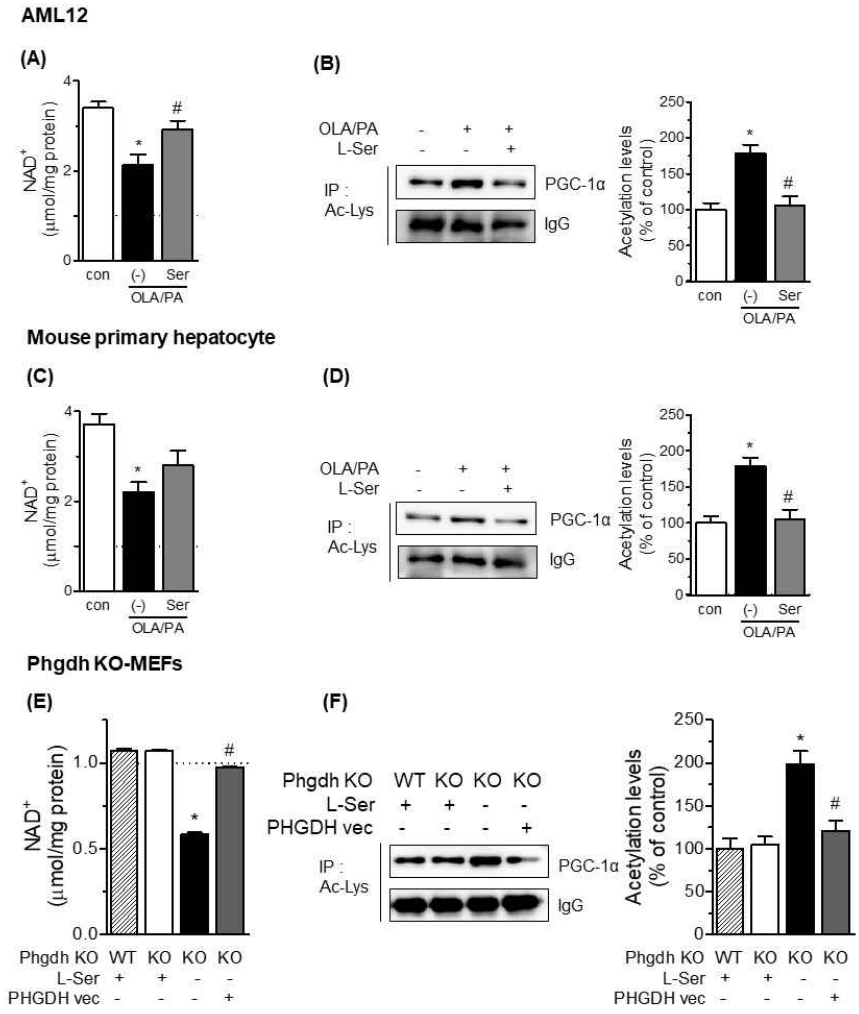

Figure 26. PHGDH loss of function or L-serine deficiency decreased intracellular NAD$^+$ and SIRT1 activity in AML12, mouse primary hepatocytes, and PHGDH-KO MEF cells.

750 uM of FFA and 5 mg/mL L-serine were treated and intracellular NAD$^+$ and acetylation status of PGC-1α were measured in AML12 (A, B) and primary hepatocytes (C, D). PHGDH WT and KO-MEF cells were cultured in L-serine sufficient or deficient media and PHGDH expression vector was transfected. After treatment, intracellular NAD$^+$ and acetylation status of PGC-1α (E, F) were measured. Values are means ± SDs, n = 3 of three independent experiments. Within each graph, labeled means without a common letter differ ($P < 0.05$). Statistical analysis was performed by using one-way ANOVA with Tukey's multiple-comparison procedure.

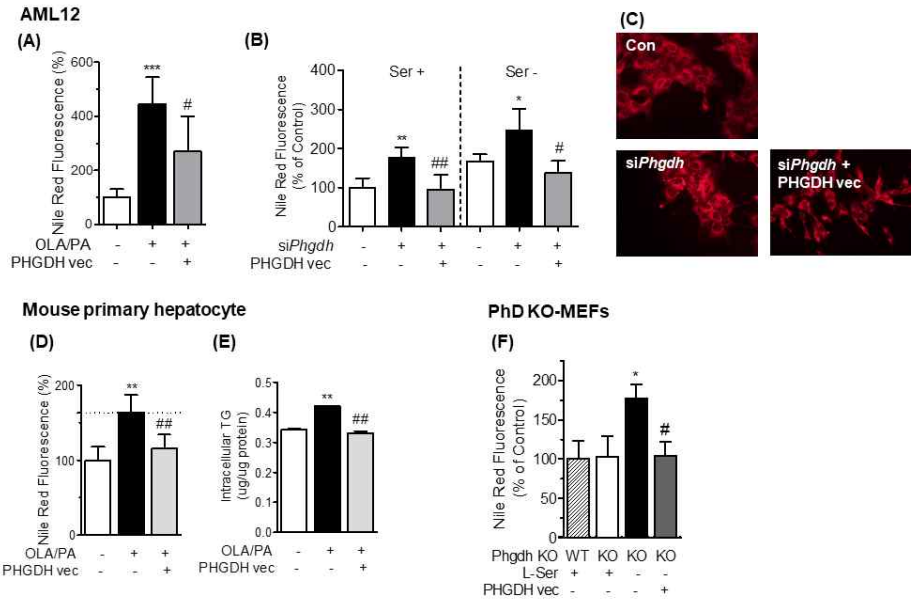

Figure 27. Increased L-serine synthesis by up-regulating PHGDH reversed lipid accumulation in FFA treatment or L-serine depleted condition.

AML12 cells were incubated with 750 uM FFA or si-*Phgdh* and transfected with PHGDH expression vector in L-serine sufficient or deficient media. Intracellular TG was measured by nile-red assay (A, B). Microscopic images of the nile red staining of AML12 cells in serine depletion condition were suggested (C). 750 uM FFA was treated in mouse primary hepatocytes and PHGDH expression vector was transfected. After treatment, intracellular TG was measured by nile red staining (D) and TG extraction and quantification (E). PHGDH wild-type (WT) MEF cells were cultured in L-serine sufficient media and knock-out (KO) MEF cells were cultured in L-serine sufficient or deficient media. PHGDH overexpression vector was transfected and nile red assay was performed (F). Values are means ± SDs, n = 3 of three independent experiments. Within each graph, *, **, and *** represent significance (*; $P < 0.05$, **; $P < 0.01$, ***; $P < 0.001$) relative to the control; # and ## represent significance (#; $P < 0.05$, ##; $P < 0.01$) relative to its left bar. Statistical analysis was performed by using one-way ANOVA with Tukey's multiple-comparison procedure.

3.4. Regulation of PHGDH is mediated by NRF2.

3.4.1. PHGDH is not regulated by epigenetic modification.

To identify the mechanism of PHGDH regulation, epigenetic assays were performed. First, PHGDH promoter methylation was assessed. Because the promoter methylation is known to repress the gene expression, the methylation status of the PHGDH promoter was measured by DNA bisulfite conversion. But in vitro FFA and ethanol treatment decreased the methylation status and there were no changes in the promoter methylation in vivo models (Figure 28).

Next, histone methylation was also investigated. The global histone H3 and H4 acetylation assay showed there were no changes in histone acetylation in vitro and in vivo disease models (Figure 29). Trichostatin A (TSA) was also used to investigate histone methylation and PHGDH expression, but TSA did not affect the mRNA and protein level of PHGDH (Figure 30).

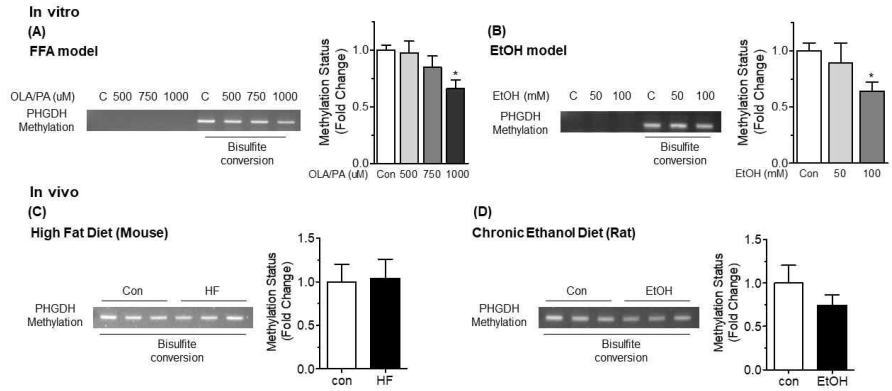

Figure 28. Promoter methylation of PHGDH is decreased by FFA and ethanol in vitro and not affected by HF diet or chronic ethanol diet.

AML12 cells were treated with indicated concentrations of FFA (A) or ethanol (B) for 24 hr and the livers from HF diet fed mice (C) and chronic Lieber-DeCarli ethanol diet fed rats (D) were prepared for DNA extraction. After bisulfite conversion, DNA was amplified by semi-quantitative PCR. Graphs show the quantification of intensities of DNA bands. Values are means ± SDs, n = 3 of three independent experiments in vitro or n = 3 of mice or rats in vivo. Within each graph, * represents significance (*; $P < 0.05$) relative to the control. Statistical analysis was performed by using one-way ANOVA with Dunnett's post-test in vitro and by using student's *t*-test in vivo.

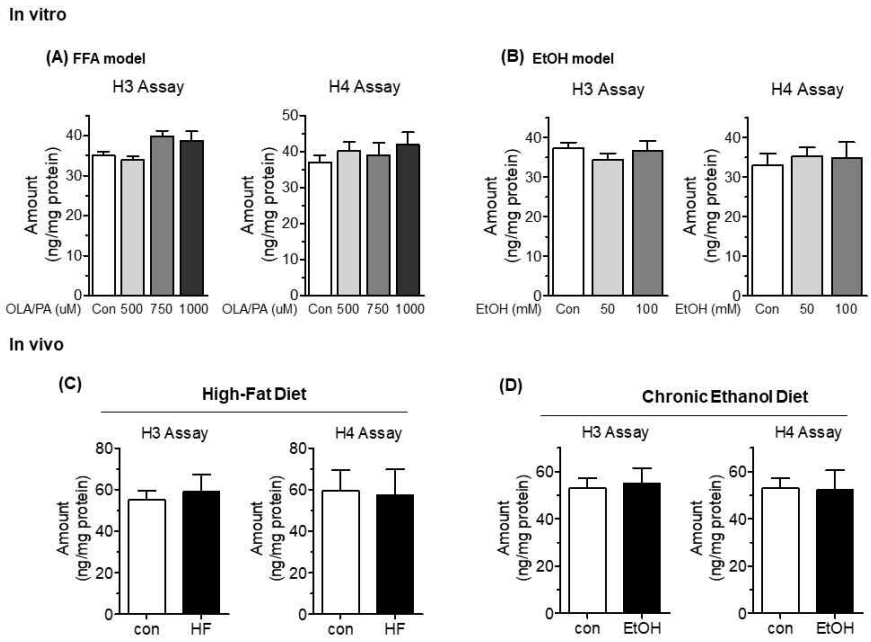

Figure 29. Global hitone H3 and H4 acetylation were not affected in pathological models.

AML12 cell pellets treated with indicated concentrations of FFA (A), ethanol (B) and the livers from HF diet fed mice (C), chronically Lieber-DeCarli ethanol diet fed rats (D) were used to measure global H3 and H4 acetylation. In each graph, values are means ± SDs, n = 3 of three independent experiments (A, B) or n = 8 mice or rats (C, D). Statistical analysis was performed by using one-way ANOVA followed by Dunnett's post-test (A, B) or by using student's *t*-test (C, D).

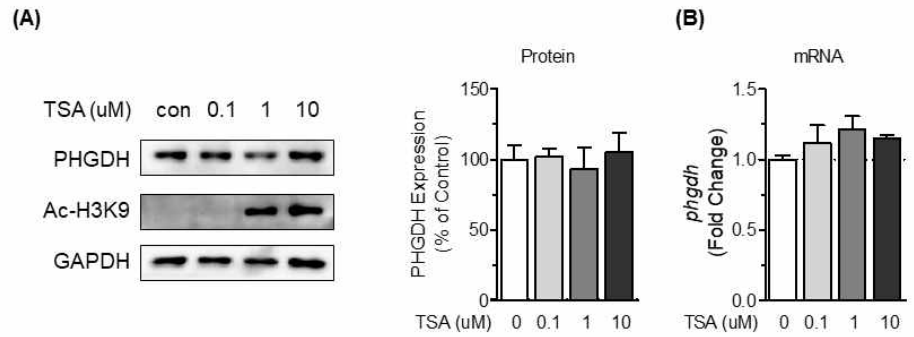

Figure 30. The expression of PHGDH is not affected by trichostatin A, HDAC inhibitor.

AML12 cells were treated with indicated concentrations of trichostatin A (TSA) for 24 hr. Protein and mRNA were extracted from cell pellets. PHGDH and H3K9 histone acetylation were detected by western blot (A) and *Phgdh* mRNA expression was measured by qRT-PCR (B). Values are means ± SDs, n = 3 of three independent experiments (A, B) or n = 8 mice or rats (C, D). Statistical analysis was performed by using one-way ANOVA followed by Dunnett's post-test.

3.4.2. PHGDH is regulated by NRF2.

DeNicola et al. reported that NRF2 positively regulates L-serine biosynthesis through the up-regulation of enzymes involved in de novo serine synthesis. Adenoviral transduction of dominant negative form of NRF2 (DN-NRF2) or overexpression of NRF2 decreased or increased PHGDH expression, respectively (Figure 31).

To find whether NRF2 is associated with down-regulated PHGDH in pathological models. The expression of NRF2 is measured in vitro FFA and ethanol model and in vivo HF diet and chronic ethanol diet model. Figure 32. showed that not only in vitro FFA and ethanol treatment decreased NRF2 protein level, but also in vivo HF diet and chronic ethanol diet reduced NRF2 expression.

As NRF2 protein stability can be regulated by ubiquitination, we confirmed NRF2 protein expression with treatment of tert-butylhydroquinone (tBHQ) which is used as a NRF2 activator or proteasome inhibitor, MG132. FFA increased the ubiquitination of NRF2 and tBHQ and MG132 teatment reversed these effects (Figure 33).

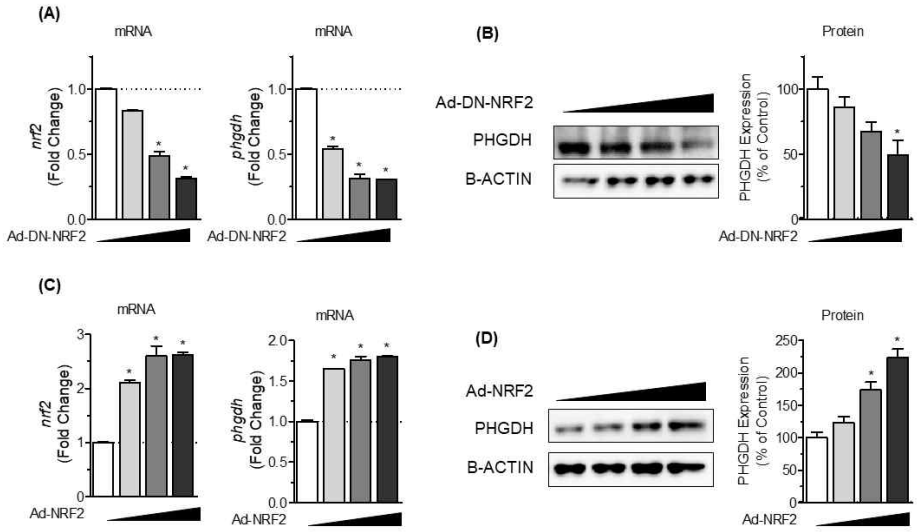

Figure 31. NRF2 positively regulates PHGDH at transcriptional and translational level.

AML12 cells were transducted with adenoviral dominant negative (DN)-NRF2 (A, B) or NRF2 (C, D) for 24 hr After transfection, cells were collected and subjected to PCR or western blot for NRF2 and PHGDH expression. Values are means ± SDs, n = 3 of three independent experiments. Within each graph, * represents significance (*; $P < 0.05$) relative to the control. Statistical analysis was performed by using one-way ANOVA followed by Dunnett's post-test.

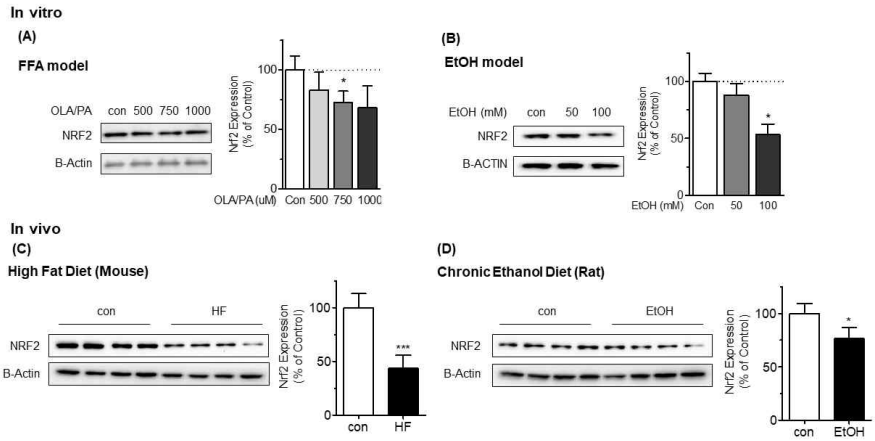

Figure 32. NRF2 protein expression is down-regulated in pathological models in vitro and in vivo.

AML12 cells treated with indicated concentrations of FFA (A), ethanol (B) and the livers from HF diet fed mice (C), chronically Lieber-DeCarli ethanol diet fed rats (D) were prepared to measure NRF2 protein expression. In each graph, values are means ± SDs, n = 3 of three independent experiments (A, B) or n = 4 mice or rats (C, D). Within each graph, * and *** represent significance (*; $P < 0.05$, ***; $P < 0.001$) relative to the control. Statistical analysis was performed by using one-way ANOVA followed by Dunnett's post-test (A, B) or by using student's *t*-test (C, D).

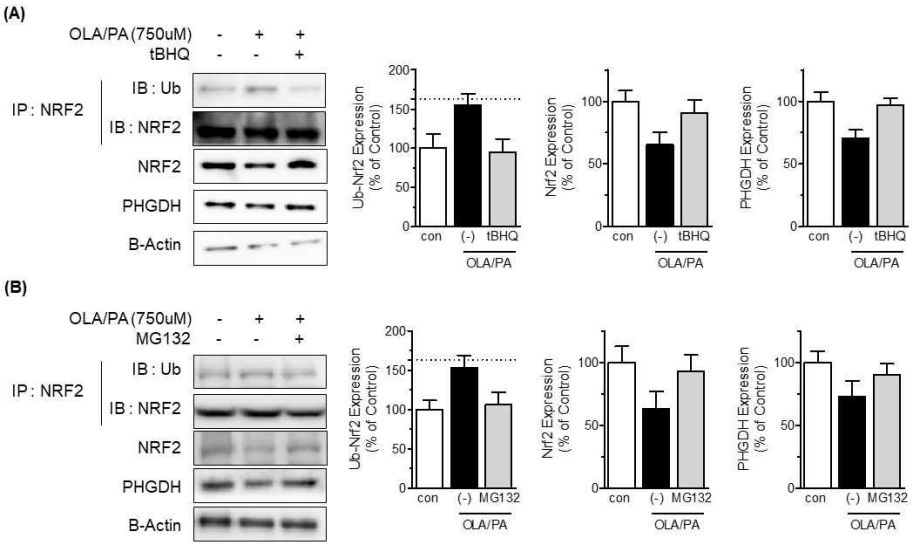

Figure 33. Increasing the stability of NRF2 reversed FFA-induced PHGDH down-regulation.

AML12 cells were treated with FFA with or without tBHQ (A) and MG132 (B). After 24 hr treatment, cells were centrifuged and subjected to immunoprecipitation for detecting ubiquitination of NRF2 and western blot for measuring NRF2 and PHGDH expression. Right panels shows the quantification of ubiquitination of NRF2, expression of NRF and PHGDH which are normalized to B-Actin. In each graph, values are means ± SDs, n = 2 of two independent experiments.

IV. Discussion

L-Serine is a non-essential amino acid which makes up dietary proteins, but plays various roles in cellular metabolism including biosynthesis of nucleotides, other amino acids, and sphingolipids.

One of the mechanisms of alcoholic fatty liver is a disturbance in hepatic sulfur-amino acid metabolism, leading to high homocysteine concentrations (Ji et al., 2003). We first demonstrated that the natural amino acid L-serine ameliorated alcoholic fatty liver by lowering homocysteine concentrations. L-Serine reduced homocysteine and lipid accumulation by acting on MS and CβS which are important homocysteine metabolizing enzymes in livers. By studying L-serine and homocysteine metabolism, we could assume that L-serine may have potential for treatment of hyperhomocysteinemia and fatty liver.

In our study, L-serine effect on serum homocysteine showed difference between mice and rats. Shinohara et al. (2010) reported species difference between rats and mice in which ethanol induces hyperhomocysteinemia. Rats were reported to more resistant to ethanol-induced increase in serum homocysteine and fatty liver. Our results also showed similar results and L-serine effect lowering serum homocysteine was observed only in mice (Sim et al., 2015). L-serine effect of improving steatosis in rats were identified by analyzing other sulfur amino acid metabolites in the liver. Our data in chronic ethanol study found that L-serine increased hepatic SAM without affecting SAH levels and GSH contents (Table 3). SAM participates into various biological reactions as a methyl donor and impaired SAM/SAH ratio leads to develop fatty liver by down-regulating VLDL secretion (Kharbanda et al., 2007 and 2012). Therefore, normalized SAM/SAH ratio by L-serine may be an important mechanism improving alcoholic

steatosis in rats.

We found that L-serine mediated homocysteine metabolism through the regulation of MS and CβS enzyme expression in binge ethanol study. Because homocysteine metabolism can not only be affected by metabolizing enzyme expression, but also the activity of the enzyme, we measured enzyme activity of MS and CβS. L-serine did not affect the enzyme activity in both binge and chronic ethanol study. The mechanism which induces the expression of the enzymes by L-serine needs to be studied.

The effect of L-serine improving fatty liver was mediated not only by homocysteine metabolism but also by regulating SIRT1 activity. L-Serine increased intracellular NAD^+ by the action of LDH. Several amino acids are reported to modulate SIRT1 activity. Leucine, which is an essential amino acid, was reported to increase SIRT1 mRNA and protein expression in C57BL/6 mice. Leucine increased nicotinamide phosphoribosyltransferase (NAMPT) and SIRT1 expression (Koning et al., 2003). Leucine also mimicked the calorie restriction effect by lowering the activation energy for NAD^+ of SIRT1 (Lei et al., 2005). Another amino acid, tryptophan is reported to be associated with SIRT1 activity. When the kynurenine pathway which is the principle route of tryptophan metabolism producing NAD^+ is inhibited, SIRT1 activity was decreased (Brady et al., 2012).

In our study, L-serine altered intracellular redox state, which can be measured by NAD^+/NADH ratio through LDH. Lactic and pyruvic acids interact through the actions of the cytosolic near-equilibrium LDH isozymes, which reflect the cytosolic NAD^+/NADH ratios in cytosol. There are reports of mitochondrial LDH activity (Brooks, 2009) and therefore potential for coupling of the NAD^+/NADH ratios trigger several intracellular responses, including expression of genes by modification of histone deacetylases, which profoundly affect the

regulation of protein synthesis. To identify L-serine mediated regulation of redox state, pyruvate and lactate levels are needed to measured and further studies about changed redox state should be performed including glycolysis.

L-Serine is also reported to be a natural ligand and allosteric activator of pyruvate kinase M2 (PKM2) (Chaneton et al., 2012). L-serine bound to and activate human PKM2 and following serine deprivation, PKM2 activity in cells is reduced. This reduction in PKM2 activity shifts cells to a fuel-efficient mode where more pyruvate is diverted to the mitochondria and more glucose derived carbon is channelled into serine biosynthesis to support cell proliferation. Although PKM2 is the predominant isoform in cancer cells (Christofk et al., 2008; Altenberg and Greulich, 2004) and has low basal enzymatic activity compared to the constitutively active splice-variant PKM1 (Mazurek et al., 2005). Therefore, down-regulated intracellular L-serine in disease models may result in PKM2 activation and L-serine effect on PKM2 activity including increased glycolysis further needs to be elucidated.

Reduced L-serine levels in alcoholic fatty liver can be explained by PHGDH, which regulates de novo L-serine synthesis, and it was found to be decreased in chronic ethanol diet, high-fat diet, and MCD diet models. Decreased PHGDH expression resulted in reduced L-serine concentrations in the livers except in MCD diet model. This may result from different diet composition, period and so on. In vitro pathological models also showed decreased PHGDH expression and PHGDH gain of function reversed this effect by up-regulating intracellular NAD^+ and SIRT1 activity by increased L-serine.

To find the correlation between L-serine level and fatty liver disease status, hepatic L-serine was investigated in animal studies and serum L-serine was measured in human studies. Although both liver and

serum L-serine levels were correlated to the fatty liver disease status, additional serum amino acid analysis in animal studies can support the correlation between L-serine and fatty liver disease.

Esaki et al., reported that deprivation of external L-serine leads to the generation of abnormal sphingolipids, 1-deoxysphingolipids (doxSLs), including doxSA in mouse embryonic fibroblasts lacking PHGDH (PHGDH KO-MEFs) (Esaki et al., 2015). Furthermore, it is reported that human diabetics show significant increases in deoxyshpinganine (Bertea et al., 2010; Othman et al., 2012). So we detected the sphingolipids in the livers from Lieber-DeCarli ethanol diet-fed rats and high-fat diet-fed mice. In ethanol study, ethanol-fed rats showed increased doxCer and doxDHCer, which are produced by palmitoyl-CoA and alanine conjugation instead of L-serine. But high-fat diet fed mice showed different patterns of sphingolipids level. DoxSA and DoxCer were decreased by high-fat diet. Although a direct causative role between ethanol diet and high-fat diet on lipid profile is unclear, we hypothesized that different composition of diet may affect SPT activity on different substrate. Because SPT exists in a complex, composed of three distinct subunits (SPTLC1, STPLC2 and SPTLC3) (Hornemann et al., 2007) and interacts with other proteins that regulated activity of the enzyme (Han et al., 2010). Further studies about sphingolipid profile of high fat diet in vivo study or human obese patients need to be elucidated.

Regulation of PHGDH is mediated by various molecules (Bollig-Fischer et al., 2011; Jun et al., 2008; Ding et al., 2013; Ou et al., 2015; DeNicola et al., 2015). One of the mediator focused in this study is nuclear factor erythroid 2-related factor 2 (NRF2). NRF2 is one of a major regulator of cytoprotective response against reactive oxygen species (ROS) (Kansanen et al., 2012). In resting state, NRF2 binds to two Kelch ECH associating protein 1 (Keap1) molecules and

is ubiquitinated by the Cul3-based E3 ligase. The ubiquitination of NRF2 leads to degradation by the proteasome (Kansanen et al., 2009). Under oxidative condition, the cysteine residue of Keap1 is modified and ubiquitination of NRF2 is inhibited by dissociation of the Cul3-based E3 ligase complex. In this study, PHGDH is down-regulated by FFA or ethanol treatment and NRF2 activator tBHQ or proteasome inhibitor MG132 reversed the down-regulation of NRF2 and PHGDH. Although FFA and ethanol are reported to induce oxidative stress (Cui et al., 2016; Shi et al., 2016), Shi et al. reported that NRF2 is reduced in total protein level and nuclear accumulation by ethanol treatment. Because NRF2-Keap1 pathway can be regulated by various mechanisms including Keap1 mutation (Mitsuishi et al., 2012), hypermethylation of Keap1 promoter (Hanada et al., 2012; Zhang et al., 2010), and accumulation of disruptor proteins including p62 and p21 (Ma and He, 2012), further study is needed to NRF2-mediated PHGDH regulation in vitro and in vivo disease models.

In conclusion, L-serine ameliorates fatty liver by participating in homocysteine metabolism and up-regulating SIRT1 activity by increasing intracellular NAD^+ pool. Reduced L-serine is mediated by down-regulated PHGDH experssion in various in vitro and in vivo disease models. PHGDH expression is regulated by NRF2 which regulates PHGDH positively at transcriptional and translational level. This study showed that L-serine has a potential developed as a fatty liver disease therapeutics and L-serine synthesizing enzyme, PHGDH can be used as a therapeutic target for fatty liver disease.

V. Conclusion

The result of the current thesis can be summarized as follows:

1. L-serine ameliorates alcoholic fatty liver in vitro and in vivo. And L-serine showed these effects through up-regulating homocysteine catabolism via MS and CβS activity.

2. L-serine increases intracellular NAD^+ by the action of lactate dehydrogenase and SIRT1 activity. L-serine mediated increase in SIRT1 activity resulted in mitochondrial mass and function by PGC-1 α. L-serine also reversed oleaic acid-induced intracellular TG accumulation by increasing lipid β-oxidation and palmitic acid-induced insulin resistance in vitro.

3. PHGDH, which is a rate-limiting step in de novo serine synthesis, expression was decreased in various in vitro and in vivo disease model. GEO analysis also showed that human fatty liver disease patients showed reduced expression of PHGDH and serum from human fatty liver disease patients showed that L-serine is negatively correlated with liver fat fraction and biomarkers of liver function and lipid metabolism, such as ALT and TG.

4. NRF2 is identified as a PHGDH regulator in vitro and in vivo model. studied by focusing its expression and protein stability. NRF2 is found to positively regulate PHGDH at transcriptional and translational level. Increasing NRF2 stability reversed free fatty

acid-induced PHGDH down-regulation.

Taken together, PHGDH plays an important role synthesizing L-serine in pathological liver state. This study showed that PHGDH can be used as a therapeutic target for hepatosteatosis and L-serine has a potential for curing fatty liver disease.

VI. Abbreviations

3-Phosphoglycerate dehydrogenase (PHGDH); 5-Methyltetrahydrofolate (5-methylTHF); Alanine aminotransferase (ALT); Alcoholic fatty liver disease (ALD); Aspartate aminotransferase (AST); Betaine homocysteine methyltransferase (BHMT);
Chemoattractant protein (MCP); Cystathionine β synthase (CβS); Deoxyceramide (DoxCer); Deoxydihydroceramide (DoxDHCer); Deoxymethylsphinganine (DoxmeSA);
Deoxysphinganine (DoxSA); Deoxysphingosine (DoxSO); Dulbacco's modified phosphate-buffered saline (DPBS); Endoplasmic reticulum (ER); Fatty acid transport protein (FATP); Free fatty acids (FFA); Glucose-regulated protein 78 (GRP78); Glutathione (GSH); High-fat (HF); Human epideral growth factor receptor 2 (HER2);
Interleukin (IL); Knock-out (KO); Lactate dehydrogenase (LDH); Methionine-choline deficient (MCD); Methionine synthase (MS); Nonalcoholic fatty liver disease (NAFLD); Non-small cell lung cancer (NSCLC); Nuclear factor like 2 (NRF2); Nuclear transcription factor Y (NF-Y); Peroxisome proliferator-activated receptor-α (PPARα); Peroxisome proliferator activated receptor ɣ coactivator-1 α (PGC-1α); Phosphatidylethanolaine methyltransferase (PEMT); Phosphoserine aminotransferase 1 (PSAT-1); Phosphoserine phosphatase (PSPH); Protein kinase RNA-like ER kinase (PERK); Quantitative Real-time Polymerase Chain Reaction (qRT-PCR); S-adenosylmethionine (SAM); S-adenosyltransferase (MAT); Serine Palmitoyltransferase (SPT); Specificity protein 1 (Sp1); Sphinganine (SA); Sphingosine (SO); Sterol regulatory element binding protein (SREBP); Transforming growth factor (TGF); Triglyceride (TG)

VII. References

Ahn J, Cho I, Kim S, Kwon D, Ha T. Dietary resveratrol alters lipid metabolism-related gene expression of mice on an atherogenic diet. *J Hepatol.* 2008;49:1019-1028.

Altenberg B, Greulich KO. Genes of glycolysis are ubiquitously overexpressed in 24 cancer classes. *Genomics*. 2004;84:1014-1020.

Baur JA, Pearson KJ, Price NL, Jamieson HA, Lerin C, Kalra A et al. Resveratrol improves health and survival of mice on a high-calorie diet. *Nature.* 2006;444:337-342.

Beroukhim R, Mermel CH, Porter D, Wei G, Raychaudhuri S, Donovan J et al. The landscape of somatic copy-number alteration across human cancers. *Nature.* 2010;463:899-905.

Bertea M, Rütti MF, Othman A, Marti-Jaun J, Hersberger M, von Eckardstein A et al. Deoxysphingoid bases as plasma markers in diabetes mellitus. *Lipids Health Dis.* 2010;9:84.

Björck J, Hellgren M, Råstam L, Lindblad U. Associations between serum insulin and homocysteine in a Swedish population-a potential link between the metabolic syndrome and hyperhomocysteinemia: the Skaraborg project. *Metabolism.* 2006;55:1007-1013.

Bollig-Fischer A, Dewey TG, Ethier SP. Oncogene activation induces metabolic transformation resulting in insulin-independence in human breast cancer cells. *PLoS One.* 2011;6(3):e17959.

Braidy N, Guillemin GJ, Grant R. Effects of Kynurenine Pathway Inhibition on NAD Metabolism and Cell Viability in Human Primary Astrocytes and Neurons. *Int J Tryptophan Res.* 2011;4:29-37.

Brooks GA. Cell-cell and intracellular lactate shuttles. *J Physiol.* 2009;587(Pt 23):5591-5600.

Chaneton B, Hillmann P, Zheng L, Martin ACL, Maddocks ODK, Chokkathukalam A et al. Serine is a natural ligand and allosteric activator of pyruvate kinase M2. *Nature.* 2012;491:458-462.

Chaudhary N, Pfluger PT. Metabolic benefits from Sirt1 and Sirt1 activators. *Curr Opin Clin Nutr Metab Care.* 2009;12:431-437.

Christofk HR, Vander Heiden MG, Harris MH, Ramanathan A, Gerszten RE, Wei R et al. The M2 splice isoform of pyruvate kinase is important for cancer metabolism and tumour growth. *Nature.* 2008;452:230-233.

Clarke R, Daly L, Robinson K, Naughten E, Cahalane S, Fowler B et al. Hyperhomocysteinemia: an independent risk factor for vascular disease. *N Engl J Med.* 1991;324:1149-1155.

Cohen HY, Miller C, Bitterman KJ, Wall NR, Hekking B, Kessler B et al. Calorie restriction promotes mammalian cell survival by inducing the SIRT1 deacetylase. *Science.* 2004;305:390-392.

Cohen JC, Horton JD, Hobbs HH. Human fatty liver disease: old questions and new insights. *Science.* 2011;332:1519-1523.

Colak Y, Ozturk O, Senates E, Tuncer I, Yorulmaz E, Adali G et al. SIRT1 as a potential therapeutic target for treatment of nonalcoholic fatty liver disease. *Med Sci Monit.* 2011;17:HY5-9.

Cui Y, Wang Q, Yi X, Zhang X. Effects of Fatty Acids on CYP2A5 and NRF2 Expression in Mouse Primary Hepatocytes. *Biochem Genet.* 2016;54:29-40.

Cylwik B, Chrostek L, Daniluk M, Supronowicz Z, Szmitkowski M. Relationship between plasma folate and homocysteine concentrations in alcoholics according to liver enzyme activity. *J Nutr Sci Vitaminol (Tokyo).* 2009;55:439-441.

Delmas D, Jannin B, Latruffe N. Resveratrol: preventing properties against vascular alterations and ageing. *Mol Nutr Food Res.* 2005;49:377-395.

DeNicola GM, Chen PH, Mullarky E, Sudderth JA, Hu Z, Wu D et al. NRF2 regulates serine biosynthesis in non-small cell lung cancer. *Nat Genet.* 2015;47:1475-1481.

Ding J, Li T, Wang X, Zhao E, Choi JH, Yang L, Zha Y, Dong Z, Huang S, Asara JM, Cui H, Ding HF. The histone H3 methyltransferase G9A epigenetically activates the serine-glycine synthesis pathway to sustain cancer cell survival and proliferation. Cell Metab. 2013;18:896-907.

Ding S, Jiang J, Zhang G, Bu Y, Zhang G, Zhao X. Resveratrol and caloric restriction prevent hepatic steatosis by regulating

SIRT1-autophagy pathway and alleviating endoplasmic reticulum stress in high-fat diet-fed rats. *PLoS One.* 2017;12:e0183541.

Esaki K, Sayano T, Sonoda C, Akagi T, Suzuki T, Ogawa T et al. L-Serine Deficiency Elicits Intracellular Accumulation of Cytotoxic Deoxysphingolipids and Lipid Body Formation. *J Biol Chem.* 2015;290:14595-14609.

Falck-Ytter Y, Younossi ZM, Marchesini G, McCullough AJ. Clinical features and natural history of nonalcoholic steatosis syndromes. *Semin Liver Dis.* 2001;21:17-26.

Feinman L, Lieber CS. Ethanol and lipid metabolism. *Am J Clin Nutr.* 1999;70:791-792.

Finkelstein JD. Methionine metabolism in mammals. *J Nutr Biochem.* 1990;1:228-237.

Guclu A, Erdur FM, Turkmen K. The Emerging Role of Sirtuin 1 in Cellular Metabolism, Diabetes Mellitus, Diabetic Kidney Disease and Hypertension. *Exp Clin Endocrinol Diabetes.* 2016;124:131-139.

Gulsen M, Yesilova Z, Bagci S, Uygun A, Ozcan A, Ercin CN et al. Elevated plasma homocysteine concentrations as a predictor of steatohepatitis in patients with non-alcoholic fatty liver disease. *J Gastroenterol Hepatol.* 2005;20:1448-1455.

Hajer GR, van der Graaf Y, Olijhoek JK, Verhaar MC, Visseren FL; SMART Study Group. Levels of homocysteine are increased in metabolic syndrome patients but are not associated with an increased

cardiovascular risk, in contrast to patients without the metabolic syndrome. *Heart.* 2007;93:216-220.

Han S, Lone MA, Schneiter R, Chang A. Orm1 and Orm2 are conserved endoplasmic reticulum membrane proteins regulating lipid homeostasis and protein quality control. *Proc Natl Acad Sci U S A.* 2010;107:5851-5856.

Hanada K. Serine palmitoyltransferase, a key enzyme of sphingolipid metabolism. *Biochim Biophys Acta.* 2003;1632:16-30.

Heilbronn LK, Civitarese AE, Bogacka I, Smith SR, Hulver M, Ravussin E. Glucose tolerance and skeletal muscle gene expression in response to alternate day fasting. *Obes Res.* 2005;13:574-581.

Hanada N, Takahata T, Zhou Q, Ye X, Sun R, Itoh J et al. Methylation of the KEAP1 gene promoter region in human colorectal cancer. *BMC Cancer.* 2012;12:66.

Hornemann T, Wei Y, von Eckardstein A. Is the mammalian serine palmitoyltransferase a high-molecular-mass complex? *Biochem J.* 2007;405:157-164.

Jacobsen DW, Catanescu O, Dibello PM, Barbato JC. Molecular targeting by homocysteine: a mechanism for vascular pathogenesis. *Clin Chem Lab Med.* 2005;43:1076-1083.

Ji C, Kaplowitz N. Betaine decreases hyperhomocysteinemia, endoplasmic reticulum stress, and liver injury in alcohol-fed mice. *Gastroenterology.* 2003;124:1488-1499.

Ji C, Shinohara M, Vance D, Than TA, Ookhtens M, Chan C et al. Effect of transgenic extrahepatic expression of betaine-homocysteine methyltransferase on alcohol or homocysteine-induced fatty liver. *Alcohol Clin Exp Res.* 2008;32:1049-1058.

Jun DY, Park HS, Lee JY, Baek JY, Park HK, Fukui K et al. Positive regulation of promoter activity of human 3-phosphoglycerate dehydrogenase (PHGDH) gene is mediated by transcription factors Sp1 and NF-Y. *Gene.* 2008;414(1-2):106-114.

Kalhan SC, Hanson RW. Resurgence of serine: an often neglected but indispensable amino Acid. *J Biol Chem.* 2012;287:19786-19791.

Kansanen E, Kivelä AM, Levonen AL. Regulation of NRF2-dependent gene expression by 15-deoxy-Delta12,14-prostaglandin J2. *Free Radic Biol Med.* 2009;47:1310-1317.

Kansanen E, Jyrkkänen HK, Levonen AL. Activation of stress signaling pathways by electrophilic oxidized and nitrated lipids. *Free Radic Biol Med.* 2012;52:973-982.

Kaufman RJ. Stress signaling from the lumen of the endoplasmic reticulum: coordination of gene transcriptional and translational controls. *Genes Dev.* 1999 ;13:1211-1233.

Kharbanda KK, Mailliard ME, Baldwin CR, Beckenhauer HC, Sorrell MF, Tuma DJ. Betaine attenuates alcoholic steatosis by restoring phosphatidylcholine generation via the phosphatidylethanolamine methyltransferase pathway. *J Hepatol.* 2007;46:314-321.

Kharbanda KK. Alcoholic liver disease and methionine metabolism. *Semin Liver Dis.* 2009;29:155-165.

Kharbanda KK, Todero SL, King AL, Osna NA, McVicker BL, Tuma DJ et al. Betaine treatment attenuates chronic ethanol-induced hepatic steatosis and alterations to the mitochondrial respiratory chain proteome. *Int J Hepatol.* 2012;962183.

de Koning TJ, Snell K, Duran M, Berger R, Poll-The BT, Surtees R. L-serine in disease and development. *Biochem J.* 2003;371(Pt 3):653-661.

Lagouge M, Argmann C, Gerhart-Hines Z, Meziane H, Lerin C, Daussin F et al. Resveratrol improves mitochondrial function and protects against metabolic disease by activating SIRT1 and PGC-1alpha. *Cell.* 2006;127:1109-1122.

Lavu S, Boss O, Elliott PJ, Lambert PD. Sirtuins--novel therapeutic targets to treat age-associated diseases. *Nat Rev Drug Discov.* 2008;7:841-853.

LeCluyse EL, Bullock PL, Parkinson A, Hochman JH. Cultured rat hepatocytes. *Pharm Biotechnol.* 1996;8:121-59.

Lei Sun, Mark Bartlam, Yiwei Liu, Hai Pang, Zihe Rao. Crystal structure of the pyridoxal-5′-phosphate-dependent serine dehydratase from human liver. *Protein Sci.* 2005;14:791 - 798.

Li HB, Yang YR, Mo ZJ, Ding Y, Jiang WJ. Silibinin improves

palmitate-induced insulin resistance in C2C12 myotubes by attenuating IRS-1/PI3K/Akt pathway inhibition. *Braz J Med Biol Res.* 2015;48:440-446.

Li X, Zhang S, Blander G, Tse JG, Krieger M, Guarente L. SIRT1 deacetylates and positively regulates the nuclear receptor LXR. *Mol Cell.* 2007;28:91-106.

Li H, Xu M, Lee J, He C, Xie Z. Leucine supplementation increases SIRT1 expression and prevents mitochondrial dysfunction and metabolic disorders in high-fat diet-induced obese mice. *Am J Physiol Endocrinol Metab.* 2012;303:E1234-1244.

Li X. SIRT1 and energy metabolism. *Acta Biochim Biophys Sin (Shanghai).* 2013;45:51-60.

Lim A, Sengupta S, McComb ME, Théberge R, Wilson WG, Costello CE et al. In vitro and in vivo interactions of homocysteine with human plasma transthyretin. *J Biol Chem.* 2003;278:49707-49713.

Locasale JW, Grassian AR, Melman T, Lyssiotis CA, Mattaini KR, Bass AJ et al. Phosphoglycerate dehydrogenase diverts glycolytic flux and contributes to oncogenesis. *Nat Genet.* 2011;43:869-874.

Ma Q, He X. Molecular basis of electrophilic and oxidative defense: promises and perils of NRF2. *Pharmacol Rev.* 2012;64:1055-1081.

Majors AK, Sengupta S, Willard B, Kinter MT, Pyeritz RE, Jacobsen DW.
Homocysteine binds to human plasma fibronectin and inhibits its

interaction with fibrin. *Arterioscler Thromb Vasc Biol.* 2002;22:1354-1359.

Marambaud P, Zhao H, Davies P. Resveratrol promotes clearance of Alzheimer's disease amyloid-beta peptides. *J Biol Chem.* 2005;280:37377-37382.

Mato JM, Alvarez L, Ortiz P, Mingorance J, Durán C, Pajares MA. S-adenosyl-L-methionine synthetase and methionine metabolism deficiencies in cirrhosis. *Adv Exp Med Biol.* 1994;368:113-117.

Matsui T, Sekiguchi M, Hashimoto A, Tomita U, Nishikawa T, Wada K. Functional comparison of D-serine and glycine in rodents: the effect on cloned NMDA receptors and the extracellular concentration. *J Neurochem.* 1995;65:454-458.

Mazurek S, Boschek CB, Hugo F, Eigenbrodt E. Pyruvate kinase type M2 and its role in tumor growth and spreading. *Semin Cancer Biol.* 2005;15:300-308.

Milne JC, Lambert PD, Schenk S, Carney DP, Smith JJ, Gagne DJ et al. Small molecule activators of SIRT1 as therapeutics for the treatment of type 2 diabetes. *Nature.* 2007;450:712-716.

Mitsuishi Y, Taguchi K, Kawatani Y, Shibata T, Nukiwa T, Aburatani H et al. NRF2 redirects glucose and glutamine into anabolic pathways in metabolic reprogramming. *Cancer Cell.* 2012;22(1):66-79.

Mudd SH, Levy HL. Plasma homocyst(e)ine or homocysteine? *N Engl J Med.* 1995;333:325.

Nigdelioglu R, Hamanaka RB, Meliton AY, O'Leary E, Witt LJ, Cho T et al. Transforming Growth Factor (TGF)-β Promotes de Novo Serine Synthesis for Collagen Production. *J Biol Chem.* 2016;291:27239-27251.

Nisoli E, Tonello C, Cardile A, Cozzi V, Bracale R, Tedesco L et al. Calorie restriction promotes mitochondrial biogenesis by inducing the expression of eNOS. *Science.* 2005 Oct 14;310(5746):314-7.

Nogueiras R, Habegger KM, Chaudhary N, Finan B, Banks AS, Dietrich MO et al. Sirtuin 1 and sirtuin 3: physiological modulators of metabolism. *Physiol Rev.* 2012;92:1479-1514.

Nonaka H, Tsujino T, Watari Y, Emoto N, Yokoyama M. Taurine prevents the decrease in expression and secretion of extracellular superoxide dismutase induced by homocysteine: amelioration of homocysteine-induced endoplasmic reticulum stress by taurine. *Circulation.* 2001;104:1165-1170.

Othman A, Rütti MF, Ernst D, Saely CH, Rein P, Drexel H et al. Plasma deoxysphingolipids: a novel class of biomarkers for the metabolic syndrome? *Diabetologia.* 2012;55:421-431.

Ou Y, Wang SJ, Jiang L, Zheng B, Gu W. p53 Protein-mediated regulation of phosphoglycerate dehydrogenase (PHGDH) is crucial for the apoptotic response upon serine starvation. *J Biol Chem.* 2015;290:457-466.

Pfluger PT, Herranz D, Velasco-Miguel S, Serrano M, Tschöp MH. Sirt1 protects against high-fat diet-induced metabolic damage. *Proc*

Natl Acad Sci U S A. 2008;105:9793-9798.

Picard F, Kurtev M, Chung N, Topark-Ngarm A, Senawong T, Machado De Oliveira R et al. Sirt1 promotes fat mobilization in white adipocytes by repressing PPAR-gamma. *Nature.* 2004;429:771-776.

Poddar R, Sivasubramanian N, DiBello PM, Robinson K, Jacobsen DW. Homocysteine induces expression and secretion of monocyte chemoattractant protein-1 and interleukin-8 in human aortic endothelial cells: implications for vascular disease. *Circulation.* 2001;103:2717-2723.

Possemato R, Marks KM, Shaul YD, Pacold ME, Kim D, Birsoy K et al. Functional genomics reveal that the serine synthesis pathway is essential in breast cancer. *Nature.* 2011;476:346-350.

Purohit V, Gao B, Song BJ. Molecular mechanisms of alcoholic fatty liver. *Alcohol Clin Exp Res.* 2009;33:191-205.

Purushotham A, Schug TT, Xu Q, Surapureddi S, Guo X, Li X. Hepatocyte-specific deletion of SIRT1 alters fatty acid metabolism and results in hepatic steatosis and inflammation. *Cell Metab.* 2009;9:327-338.

Ravez S, Spillier Q, Marteau R, Feron O, Frédérick R. Challenges and Opportunities in the Development of Serine Synthetic Pathway Inhibitors for Cancer Therapy. *J Med Chem.* 2017;60:1227-1237.

Remková A, Remko M. Homocysteine and endothelial markers are increased in patients with chronic liver diseases. *Eur J Intern Med.* 2009;20:482-486.

Roda O, Valero ML, Peiró S, Andreu D, Real FX, Navarro P. New insights into the tPA-annexin A2 interaction. Is annexin A2 CYS8 the sole requirement for this association? *J Biol Chem.* 2003;278:5702-5709.

Sass JO, Nakanishi T, Sato T, Sperl W, Shimizu A. S-homocysteinylation of transthyretin is detected in plasma and serum of humans with different types of hyperhomocysteinemia. *Biochem Biophys Res Commun.* 2003;310:242-246.

Schenk S, McCurdy CE, Philp A, Chen MZ, Holliday MJ, Bandyopadhyay GK et al. Sirt1 enhances skeletal muscle insulin sensitivity in mice during caloric restriction. *J Clin Invest.* 2011;121:4281-4288.

Selhub J. Homocysteine metabolism. *Annu Rev Nutr.* 1999;19:217-246.

Shi X, Li Y, Hu J, Yu B. Tert-butylhydroquinone attenuates the ethanol-induced apoptosis of and activates the NRF2 antioxidant defense pathway in H9c2 cardiomyocytes. *Int J Mol Med.* 2016;38:123-130.

Sim WC, Yin HQ, Choi HS, Choi YJ, Kwak HC, Kim SK et al. L-serine supplementation attenuates alcoholic fatty liver by enhancing homocysteine metabolism in mice and rats. *J Nutr.* 2015;145:260-267.

Simmons GE Jr, Pruitt WM, Pruitt K. Diverse roles of SIRT1 in cancer biology and lipid metabolism. *Int J Mol Sci.* 2015;16:950-965.

Snell K, Weber G. Enzymic imbalance in serine metabolism in rat

hepatomas. *Biochem J.* 1986;233:617-620.

Sørensen T, Orholm M, Bentsen KD, Høybye G, Eghøje K, Christoffersen P. Prospective evaluation of alcohol abuse and alcoholic liver injury in men as predictors of development of cirrhosis. *Lancet.* 1984;2:241-244.

Stipanuk MH. Sulfur amino acid metabolism: pathways for production and removal of homocysteine and cysteine. *Annu Rev Nutr.* 2004;24:539-577.

Sumiyoshi M, Sakanaka M, Kimura Y. Chronic intake of a high-cholesterol diet resulted in hepatic steatosis, focal nodular hyperplasia and fibrosis in non-obese mice. *Br J Nutr.* 2010;103:378-385.

Teli MR, Day CP, Burt AD, Bennett MK, James OF. Determinants of progression to cirrhosis or fibrosis in pure alcoholic fatty liver. *Lancet.* 1995;346:987-990.

Undas A, Williams EB, Butenas S, Orfeo T, Mann KG. Homocysteine inhibits inactivation of factor Va by activated protein C. *J Biol Chem.* 2001;276:4389-4397.

Verhoef P, Steenge GR, Boelsma E, van Vliet T, Olthof MR, Katan MB. Dietary serine and cystine attenuate the homocysteine-raising effect of dietary methionine: a randomized crossover trial in humans. *Am J Clin Nutr.* 2004;80:674-679.

Wang G, Siow YL, O K. Homocysteine stimulates nuclear factor

kappaB activity and monocyte chemoattractant protein-1 expression in vascular smooth-muscle cells: a possible role for protein kinase C. *Biochem J.* 2000;352(Pt 3):817-826.

Wang G, O K. Homocysteine stimulates the expression of monocyte chemoattractant protein-1 receptor (CCR2) in human monocytes: possible involvement of oxygen free radicals. *Biochem J.* 2001;357(Pt 1):233-240.

Wang RH, Li C, Deng CX. Liver steatosis and increased ChREBP expression in mice carrying a liver specific SIRT1 null mutation under a normal feeding condition. *Int J Biol Sci.* 2010;6:682-690.

Werstuck GH, Lentz SR, Dayal S, Hossain GS, Sood SK, Shi YY et al. Homocysteine-induced endoplasmic reticulum stress causes dysregulation of the cholesterol and triglyceride biosynthetic pathways. *J Clin Invest.* 2001;107:1263-1273.

Xie J, Zhang X, Zhang L. Negative regulation of inflammation by SIRT1. *Pharmacol Res.* 2013;67:60-67.

Zhang P, Singh A, Yegnasubramanian S, Esopi D, Kombairaju P, Bodas M et al. Loss of Kelch-like ECH-associated protein 1 function in prostate cancer cells causes chemoresistance and radioresistance and promotes tumor growth. *Mol Cancer Ther.* 2010(2):336-346.

국문초록

지방간은 초기 단계의 간질환으로서 지방이 간 무게의 5% 이상을 차지하는 상태를 의미한다. 지방간은 가역적이고 양성의 질환이지만, 적절한 치료가 진행되지 않으면 간기능 장애를 야기하게 된다. 본 연구에서는 세린 생합성 단계에서 율속단계 효소로 작용하는 3-phosphoglycerate dehydrogenase (PHGDH)가 지방간 질환에서 세린 합성을 조절하여 지질대사에 영향을 줄 것임을 제안하였다.

이전 연구에서 만성적으로 에탄올을 투여한 랫트에서 세린이 감소하는 것을 확인하였다. 이에 근거하여, 알콜성 지방간 모델에서 세린을 투여하였으며 세린의 투여는 methionine synthase와 cystathionine β synthase를 경유하여 호모시스테인을 대사시킴으로써 에탄올에 의해 유도된 지방간을 억제하였다. 또한 세린은 lactate dehydrogenase에 의해 세포내 NAD^+와 SIRT1의 활성을 증가시켰다. 세린은 미토콘드리아 유전자 발현, 양 그리고 기능을 증가시켰다. 세린에 의한 SIRT1 활성의 증가는 in vitro에서 지질 축적 및 인슐린 저항성을 억제하였다.

PHGDH와 세린은 만성 에탄올 그리고 고지방식이에 의한 지방간 질환 모델에서 유의미하게 감소하였다. 유리지방산 및 에탄올은 in vitro에서 PHGDH의 발현을 감소시켰다. 세린 생합성의 감소는 PHGDH-KO MEF 세포 및 알콜성 지방간 모델에서 비정상적인 스핑고지질 및 세라마이드의 증가를 야기하였다. 또한 간염 환자의 GEO 분석을 통해 PHGDH 유전자 발현이 감소하는 것을 확인하였다. 지방간 환자의 혈청 세린은 MRI로 확인한 지질분획, 혈청 ALT 및 중성지방과 역의 상관관계를 가지는 것을 확인하였다. PHGDH 기능회복에 의한 세린 합성의 증가는 세포내 NAD^+ 및 SIRT1의 활성을 증가시켜 지질 축적을 억제하였다.

PHGDH는 전사 및 번역 수준에서 NRF2에 의해 증가하는 것을 확인하였다. 지방간 질환 모델에서 NRF2의 발현이 감소하는 것을 확인하였으며 NRF2 활성의 증가는 유리지방산에 의해 감소하였던 PHGDH의 발현을 회복시켰다.

결론적으로 PHGDH는 간에서 세린을 생합성함으로써 지질대사를 조절하는 중요한 역할을 한다. 본 연구를 통해 PHGDH를 지방간 질환을 치료하는 타겟으로 사용할 수 있으며 이에 의해 합성되는 세린이 지방간 질환을 치료하는 가능성을 가짐을 확인하였다.

In conclusion, PHGDH plays an important role regulating lipid metabolism by synthesizing L-serine in the liver. This study showed that PHGDH can be used as a therapeutic target for hepatosteatosis and L-serine has a potential for curing fatty liver disease.

Key words : 세린, 호모시스테인, 3-Phosphoglycerate dehydrogenase, SIRT1, 지질대사, 지방간

Student Number : 2011-21733